Institute of Thermoelectricity, Academy of Sciences and Ministry of Education and Science of Ukraine

Journal of THERMOELECTRICITY

International Research

Founded in December, 1993

published 6 times a year

No. 3 *2015*

Editorial Board

International Editorial Board

Founders – National Academy of Sciences, Ukraine
Institute of Thermoelectricity of National Academy of Sciences and Ministry of Education and Science of Ukraine

Certificate of state registration № КВ 15496-4068 ПР

Editorial office manager O. Pugantseva

Approved for printing by the Academic Council of Institute of Thermoelectricity of the National Academy of Sciences and Ministry of Education and Science, Ukraine

Address of editorial office:
Ukraine, 58002, Chernivtsi, General Post Office, P.O. Box 86.
Phone: +(380-372) 90 31 65.
Fax: +(380-3722) 4 19 17.
E-mail: jt@inst.cv.ua
http://www.jt.inst.cv.ua

Signed for publication 25.07.15. Format 70×108/16. Offset paper №1. Offset printing.
Printer's sheet 11.5. Publisher's signature 9.2. Circulation 400 copies. Order 5.

Printed from the layout original made by "Journal of Thermoelectricity" editorial board in the printing house of "Bukrek" publishers,
10, Radischev Str., Chernivtsi, 58000, Ukraine

CONTENTS

P. V. Gorskyi

P. V. Gorskyi

Institute of Thermoelectricity of the NAS and MES of Ukraine,
1, Nauky Str., Chernivtsi, 58000, Ukraine

ON THE CONDITIONS OF HIGH FIGURE OF MERIT AND METHODS OF SEARCH FOR PROMISING SUPERLATTICE THERMOELECTRIC MATERIALS

This paper presents a rigorous calculation of the figure of merit of superlattice thermoelectric material (SL TEM) with regard to real three-dimensionality and nonparabolicity of its energy spectrum with the arbitrary level of openness of its Fermi surface (FS). In this case, the quantitative characteristic of the level of openness of FS is the ratio of the Fermi energy of ideal two-dimensional Fermi gas with a square law of dispersion at absolute zero temperature to half-width of a narrow miniband defining charge carrier motion between SL TEM layers. In so doing, the law of dispersion of charge carriers in a narrow miniband is assumed to be corresponding to the Fivaz model, i.e. cosine. In the calculation of the figure of merit it is also assumed that the mean free path of charge carriers is inversely proportional to temperature and does not depend on their energy, hence on quantum numbers, and the lattice component of thermal conductivity obeys the law of Leibfried and Shlemann, i.e. it is also inversely proportional to temperature. It is shown that the figure of merit of SL TEM and the respective generator efficiency in the temperature range of 300-500K is drastically increased with increasing level of openness of FS. However, due to the presence of lattice component of thermal conductivity, the figure of merit of SL TEM is rather responsive to the distance between the layers and drastically drops with its increase. The same tendencies are characteristic of the respective dependences of coefficient of performance in the temperature range of 300-230K. From these dependences the optimal parameters of high-figure-of-merit SL TEM are determined.

Using the obtained criteria as the base, four methods of search for promising SL TEM with the use of quantizing magnetic fields are proposed.

Key words: superlattice, nonparabolicity, Fivaz model, Fermi surface, level of openness, thermoelectric figure of merit, efficiency, coefficient of performance, de Haas-Shubnikov oscillations, negative longitudinal magnetoresistance.

Introduction

Thermoelectric figure of merit of material is one of the key parameters defining the advisability of its application for creation of thermoelectric energy converters. The figure of merit of thermoelectric materials is mainly improved in two ways. The first way is to improve conventional materials, for instance, solid solutions of $Bi(Sb) - Te(Se)$ system due to their optimization for concentration of doping impurities [1] or due to the use of classical and (or) quantum dimensional effects in passing from single crystals to thin films, wires or powder based materials [2 – 5]. The second way lies in devising (creation) of "nonconventional" materials, where the specific features of band spectrum of charge carriers give grounds for expecting high values of thermoelectric figure of merit. As such materials, the so-called "superlattice" materials with pronounced layered structure and carrier band spectrum anisotropy [6 – 8], for instance, materials on the basis of $Al - Ga - As$ or $Si - Ge$ system, widely used in electronics and optics [9], have been much investigated. The expectations for

high thermoelectric figure of merit of such materials are due to the fact that charge carriers in these materials are strongly localized in the layers, by virtue of which charge carrier band spectrum is "nearly" two-dimensional. And this, at least due to a drastic increase in the density of states and, hence, thermopower, should have resulted in considerable improvement of thermoelectric figure of merit of SL TEM. However, abundant evidence [10 – 15] shows that in reality the thermoelectric figure of merit of these materials does not exceed that of conventional materials or even is much lower. Relatively high ZT values of the order of 2 – 4 at 300 K in the existing or investigated SL TEM are rare in occurrence.

In view of the foregoing, the purpose of the present paper is a sound estimate of the thermoelectric figure of merit of SL TEM, analysis of factors contributing to its improvement or reduction, and development of methods of search for promising SL TEM with the use of quantizing magnetic fields.

General formula for the figure of merit of SL TEM and its analysis

In the framework of the Fivaz model [16] the band spectrum of charge carriers in SL TEM is of the form:

$$\varepsilon\left(\vec{k}\right)=\frac{\hbar^2 k_{\|}^2}{2m^*}+\Delta\left(1-\cos ak_{\perp}\right), \tag{1}$$

where $k_{\|},k_{\perp}-$ quasi pulse components in layers plane and normal to it, respectively, m^*-effective mass of charge carriers in the direction normal to layers, $\Delta-$miniband half-width in the direction normal to layers, $a-$ the distance between translation equivalent layers.

In our calculations we will assume temperature gradient and electric field to be parallel to each other and to layers plane. With this configuration, on the assumption of energy independence of charge carrier means free path, the dimensional thermoelectric figure of merit of SL TEM in the impurity region at temperature T with regard to the contribution of lattice thermal conductivity is determined as follows:

$$ZT=8\pi^3\frac{A_0}{B_0+c_l\left(2k_B\varkappa_{02D}^2 l\right)^{-1}ah^2\sqrt{m^{*-1}\varkappa_{02D}}}. \tag{2}$$

Dimensionless functions A_0 and B_0 are given by:

$$A_0=\left\{\int_0^{\infty}\int_0^{\pi}\frac{y\left[y+K^{-1}\left(1-\cos x\right)-\gamma^*\right]\exp\left\{\left[y+K^{-1}\left(1-\cos x\right)-\gamma^*\right]/t_{2D}\right\}}{\left\{\exp\left\{\left[y+K^{-1}\left(1-\cos x\right)-\gamma^*\right]/t_{2D}\right\}+1\right\}^2\sqrt{2y+4\pi K^{-2}n_0a^3\sin^2 x}}\mathrm{d}x\mathrm{d}y\right\}^2\times$$
$$\left\{\int_0^{\infty}\int_0^{\pi}\frac{y\exp\left\{\left[y+K^{-1}\left(1-\cos x\right)-\gamma^*\right]/t_{2D}\right\}}{\left\{\exp\left\{\left[y+K^{-1}\left(1-\cos x\right)-\gamma^*\right]/t_{2D}\right\}+1\right\}^2\sqrt{2y+4\pi K^{-2}n_0a^3\sin^2 x}}\mathrm{d}x\mathrm{d}y\right\}^{-1}. \tag{3}$$

In formulae (2) – (4) we introduce the following notation: c_l-lattice thermal conductivity of SL TEM inversely proportional to temperature, $l-$mean free path of charge carriers in SL TEM inversely proportional to temperature, $\zeta_{02D}=n_0ah^2/4\pi m^*$, n_0- bulk concentration of charge carriers in SL TEM, $K=\varkappa_{02D}/\Delta$, k_B-Boltzmann constant, $t_{2D}=kT/\varkappa_{02D}$.

$$B_0 = \int_0^{\infty}\int_0^{\pi} \frac{K^{-1}(1-\cos x)+y-\gamma^*}{t_{2D}^2}\cdot\frac{\exp\left\{\left[y+K^{-1}(1-\cos x)-\gamma^*\right]/t_{2D}\right\}}{\left\{\exp\left\{\left[y+K^{-1}(1-\cos x)-\gamma^*\right]/t_{2D}\right\}+1\right\}^2}\times$$
$$\times\frac{y\left[y+K^{-1}(1-\cos x)\right]}{\sqrt{2y+4\pi K^{-2}n_0a^3\sin^2 x}}\,dx\,dy+$$
$$+\left\{\int_0^{\infty}\int_0^{\pi}\frac{y\left[y+K^{-1}(1-\cos x)-\gamma^*\right]\exp\left\{\left[y+K^{-1}(1-\cos x)-\gamma^*\right]/t_{2D}\right\}}{\left\{\exp\left\{\left[y+K^{-1}(1-\cos x)-\gamma^*\right]/t_{2D}\right\}+1\right\}^2\sqrt{2y+4\pi K^{-2}n_0a^3\sin^2 x}}\,dx\,dy\right\}\times$$
$$\times\left\{\int_0^{\infty}\int_0^{\pi}\frac{y\exp\left\{\left[y+K^{-1}(1-\cos x)-\gamma^*\right]/t_{2D}\right\}}{\left\{\exp\left\{\left[y+K^{-1}(1-\cos x)-\gamma^*\right]/t_{2D}\right\}+1\right\}^2\sqrt{2y+4\pi K^{-2}n_0a^3\sin^2 x}}\,dx\,dy\right\}^{-1}\times$$
$$\times\int_0^{\infty}\int_0^{\pi}\frac{K^{-1}(1-\cos x)+y-\gamma^*}{t_{2D}}\cdot\frac{\exp\left\{\left[y+K^{-1}(1-\cos x)-\gamma^*\right]/t_{2D}\right\}}{\left\{\exp\left\{\left[y+K^{-1}(1-\cos x)-\gamma^*\right]/t_{2D}\right\}+1\right\}^2}\times$$
$$\times\frac{y\left[y+K^{-1}(1-\cos x)\right]}{\sqrt{2y+4\pi K^{-2}n_0a^3\sin^2 x}}\,dx\,dy. \qquad (4)$$

Normalized to the value ζ_{02D}, chemical potential γ^* of the subsystem of free charge carriers in SL TEM is found from the equation of constancy of their concentration:

$$\frac{t_{2D}}{\pi}\int_0^{\pi}\ln\left[1+\exp\left(\frac{\gamma^*-K^{-1}(1-\cos x)}{t_{2D}}\right)\right]-1=0. \qquad (5)$$

Note that the thermal conductivity was determined on condition of the absence of current. However, in this case the Peltier heat was disregarded, as long as from our point of view we had one type of conductivity, for instance electron [17].

The results of calculations of dimensional thermoelectric figure of merit of "model" SL TEM with electron effective mass $m^* = m_0$, bulk concentration of free charge carriers $n_0 = 3\cdot10^{19}$ cm^{-3} with different levels of openness of FS $0.01 \le K \le 1$ and two different values of a for temperatures $T = T_c = 300$ K, $T = T_h = 500$ K, as well as generator efficiency based on this SL TEM are given in Fig. 1.

Note that the values $K < 1$ correspond to closed FS, $K = 1$ – to transient FS, and $K > 1$ – to open FS. To the so-called "two-dimensional" case correspond the values $K >> 1$.

The generator efficiency in the construction of plots was calculated by the formula:

$$\eta = \frac{1}{1+2\sqrt{0.5\left(Z_cT_c+Z_hT_h\right)}\left(Z_hT_h\right)^{-1}}\cdot\frac{T_h-T_c}{T_h}. \qquad (6)$$

From the figure it is seen that the figure of merit of SL TEM and the respective generator efficiency increase sufficiently fast with increasing level of openness of FS. For the considered model SL TEM the dimensionless thermoelectric figure of merit at $K = 1$ and $a = 3$ nm can reach 30 - 70, but already at $a = 15$ nm it drops to the values not exceeding 0.25 even at 500 K. The respective generator efficiency at $a = 3$ nm and $K = 1$ reaches 34%, or 0.85 of the Carnot cycle efficiency, but at $a = 15$ nm it drops to 4%, or 0.1 of the Carnot cycle efficiency. Thus, both the level of openness of FS and the distance between the layers are important parameters defining the expedience and prospects of practical application of particular SL TEM.

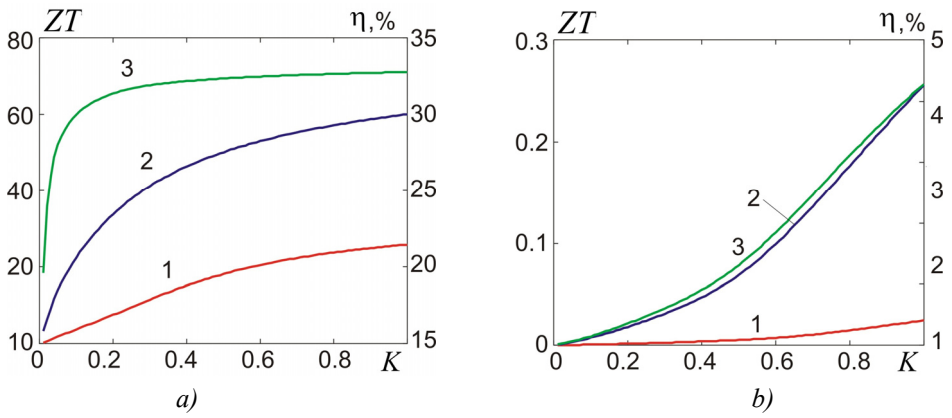

Fig. 1. Dependences of dimensionless thermoelectric figure of merit of SL TEM at T=300 K (curves 1) and T=500 K (curves 2), as well as generator efficiency at corresponding extreme temperatures (curves 3) with the distance between the layers of SL TEM 3nm (a) and 15nm (b), respectively.

Quite similarly the refrigerator coefficient of performance was found between temperatures $T_c = 230\,\text{K},\ T_h = 300\,\text{K}$. In this case the following formula was used:

$$\varepsilon = \frac{\sqrt{1+0.5\left(Z_c T_c + Z_h T_h\right)} - T_h/T_c}{\sqrt{1+0.5\left(Z_c T_c + Z_h T_h\right)}+1} \cdot \frac{T_c}{T_c - T_h}. \tag{7}$$

The results of these calculations are given in Fig. 2.

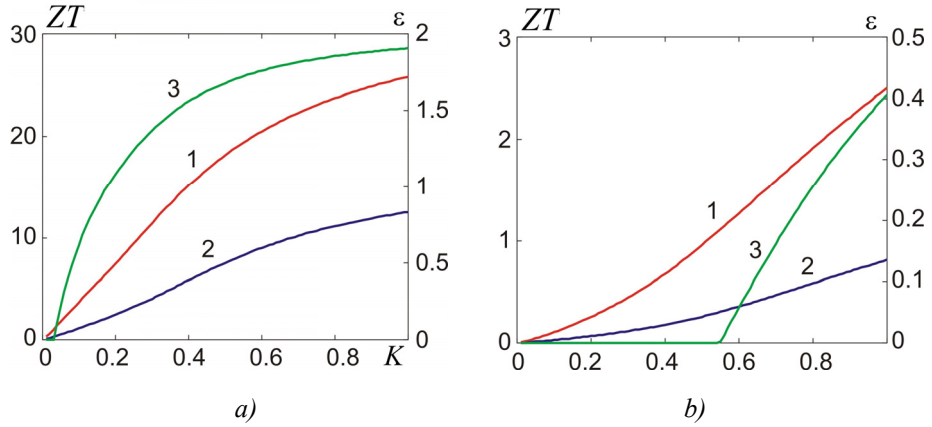

Fig.2. Dependences of dimensional thermoelectric figure of merit of SL TEM at T = 300 K (curves 1) and T = 230 K (curves 2), as well as coefficient of performance of a refrigerator at the respective extreme temperatures (curves 3) with the distance between the layers of SL TEM 3nm (a) and 6 nm (b), respectively.

From Fig. 2 it is seen that with the optimal combination of SL TEM parameters, coefficient of performance of a refrigerator at the hot side temperature 300 K and temperature difference 70 K rises sharply with increase in quasi-two-dimensionality degree of SL TEM, and with the optimal combination of parameters in case of a transient FS it can reach 1.9. However, with increasing distance between the layers beyond the optimum by a factor of 2, i.e. to 6 nm, coefficient of performance for the case of a transient FS drops to 0.4. In both considered cases for given temperature difference there exists a threshold value of the level of openness of SL TEM FS below which the coefficient of performance is zero. With increasing the distance between the layers of SL TEM, this threshold value increases dramatically.

On the reasons for low efficiency of the existing or investigated SL TEM and possible parameters of promising SL TEM

From the foregoing calculation data we see that to achieve high figure of merit of SL TEM, there must be some optimal combination of its parameters whereby the level of openness of its FS is at least close or equal to unity, and the distance between the layers is relatively small. However, the existing most popular layered and superlattice materials based on $Al-Ga-As$, $Si-Ge$ or $Bi(Sb)-Te(Se)$ systems, including those described by the Fivaz model, possess the opposite property: the distance between their layers is sufficiently large, and the level of openness of FS is low. This property is well suited for special electronics [9], including materials described by the Fivaz model, used in specific components, devices and systems, e.g. UHF-amplifiers and generators of electromagnetic waves, optical systems with self-induced transparence, soliton and breather generators, filters and delay lines, etc. However, such materials, as we can see, are not always fit for thermoelectric applications, at least as far as generators and coolers are concerned. Thus, a correct approach in this case should consist not in simple transfer of *existing* superlattice materials from electronics to thermoelectricity, but in a search for or creation of *special SL TEM,* particularly tellurium-free. This is the more relevant that the resources of tellurium-containing ores and minerals on the Earth are limited, and tellurium is just a *by-product* of their treatment, whereas the scope of application of thermoelectricity, hence production of thermoelectric modules in the world is constantly expanding. Moreover, the main consumer of tellurium today (more than 50% of available quantity) is metallurgy, rather than thermoelectricity. This raises the question of whether, at least conceptually, there can exist high-figure-of-merit SL TEM with large distances between the layers. Our analysis have shown that if free carrier concentration in the model SL TEM under study is reduced to $n_0 = 3\cdot10^{16}$ cm^{-3}, then at $a = 30$ nm, $m^* = m_0$, $K = 1$ (it corresponds to miniband half-width $\Delta = 2.16\cdot10^{-4}$ eV and the ratio of longitudinal effective mass of charge carriers to transverse one, equal to 0.393) between the temperatures of 300 and 500 K one can get generator efficiency 37.5%, which is very close to the Carnot cycle efficiency. As for coefficient of performance between the temperatures of 230 and 300 K, it can be increased to 2.92. However, the FS of such highly efficient general-purpose SL TEM should be of the form shown in Fig. 3, and its band parameters – possess high temperature stability.

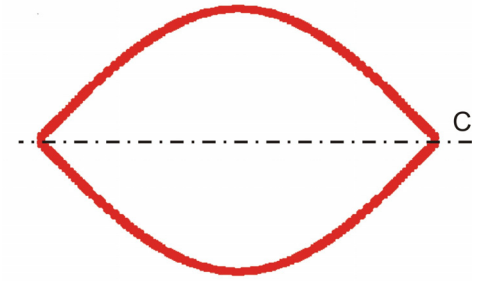

Fig. 3. The Fermi surface of possible promising high-figure-of-merit SL TEM. Cross-section of such FS by a plane parallel to SL TEM layers is a circle, the C axis is normal to the layers.

Calculations also show that such SL TEM, if only it was created, could be also applied for the subsequent deeper cooling, for instance, from 230 to 100 K, but in this case coefficient of performance would be 0.61.

In order to compare the proposed (even though hypothetical) SL TEM to the existing ones, let us note that in the overwhelming majority their miniband half-width is of the order of 0.06 – 0.1 eV, which exceeds by a factor of 300 – 500 the proposed calculated value of this half-width. Moreover, for the operation of electronic devices basically using the specific nonparabolicity of band spectrum

described by the Fivaz model, there is no need for complete occupancy of a narrow miniband at absolute zero temperature. The point is that for the operation of said devices it is important to have comparability of miniband half-width not to the Fermi energy, but to the energy gained by charge carrier from the electric field during superlattice period, i.e. at the distance between the neighbouring identical layers.

It can be shown that creation of high-efficiency SL TEM based, for instance, on silicon, is impossible in principle. Indeed, for this to be possible, the distance between the layers of SL TEM should satisfy the condition $a = 4\pi m^* \Delta / n_0 h^2$. In so doing, Δ , at any rate, is a value of the order of forbidden energy band E_g , and even higher, since in traditional calculations Δ is assumed to be infinite, and FS appears to consist of equal ellipsoids. Therefore, substituting known parameters for silicon, namely $m^* = 1.26 m_0$, $E_g = 1.21$ eV, at $n_0 = 10^{15}$ cm^{-3} we obtain $a = 6.3$ mm (!!!). It is clear that such SL TEM cannot exist. The situation will not change much even if, for instance, $n_0 = 10^{19}$ cm^{-3}. In this case there must be $a = 210$ nm, while SL TEM based on $Si - Ge$ have the highest a about 30 nm, and their highest dimensionless thermoelectric figure of merit does not exceed 0.75 at $a = 7$ nm and concentration $n_0 = 3 \cdot 10^{19}$ cm^{-3}, which is considered to be an order higher than the dimensionless thermoelectric figure of merit of the bulk samples. In the former case the level openness of FS is 0.16, and in the latter – 0.011. Naturally, this is very far from the required value of Q2D of high-efficiency SL TEM equal to unity.

Exactly as if at $n_0 = 3 \cdot 10^{19}$ cm^{-3}, $a = 3$ nm, $m^* = m_0$ bismuth telluride was a one-valley SL TEM obeying the Fivaz model, the level of openness of its FS would be $K = 0.81\pi$ and the value of dimensionless thermoelectric figure of merit at 300 K would be equal to 30.9. However, in reality, taking into account that forbidden energy band of this material is 0.13 eV, and, consequently, the allowed energy band is of the order of 1.3 eV (this is necessary for the validity of conventional approaches based on the parabolic band spectrum), we have $K = 0.017$, and, hence, the value of dimensionless thermoelectric figure of merit at 300K, equal to 0.531, which is quite correlated with the experimental data [18] for generator materials. For cooling materials of $Bi(Sb) - Te(Se)$ system this value is equal to 0.78 [19], which is matched by $K = 0.024$. Thus, nonparabolicity in cooling materials is somewhat more pronounced than in generator materials. But these values are almost 40 – 60 times lower than the thermoelectric figure of merit of "genuine" high-efficiency SL TEM. It appears that conventional generator and cooling materials are also SL TEM, but with a rather low level of openness of FS, hence nonparabolicity.

Thus, we can see that the relatively low efficiency of the existing SL TEM is attributable to the fact that they do not possess a combination of parameters necessary for high figure of merit, and their FS are considerably different from that shown in Fig. 3. High-efficiency SL TEM must differ from the existing in that their minibands should be so narrow that nonparabolicity described by the Fivaz model be well-expressed at low concentrations of free charge carriers. On the contrary, forbidden gaps must be sufficiently wide, in order not to "get" into intrinsic region in generation mode, since it can reduce the thermoelectric figure of merit of material. The author understands that this requirement is apparently difficult to realize technologically, but he is unaware of some fundamental physical law or principle on the basis of which this requirement might be claimed to unrealizable.

On the methods of search for promising SL TEM with the use of quantizing magnetic fields

In view of the foregoing, one can recommend the following four methods of search for promising SL TEM, including those described by the Fivaz model, with the use of quantizing magnetic fields:

1) investigation of de Haas-Shubnikov oscillations in quasi-classical magnetic fields at helium temperatures [20 – 22], including analysis of the field dependence of oscillation amplitude;

2) selection of materials according the presence of negative longitudinal magnetoresistance area and its pronounced minimum in ultra-quantum magnetic fields, if such are attainable [20, 22, 23];

3) selection of materials according to the degree of roundness of power factor peak in ultra-quantum magnetic fields [20, 21, 24, 25];

4) selection of materials according to the extent of negative longitudinal magnetoresistance at higher temperatures [20, 21, 26].

The above methods should be supplemented with measurement of free carrier concentration with the aid of the Hall effect and X-ray structural control of interlayer distance.

Conclusions

1. High-figure-of-merit SL TEM, intended for creation of thermoelectric energy converters must have FS of special form.

2. Such SL TEM must have optimal combination of parameters, in particular, free carrier concentration and the distance between the layers, and possess rather narrow conduction minibands, so that nonparaboicity described by the Fivaz model be well expressed at low charge carrier concentrations.

3. At creation or in the search for such SL TEM, for the identification of their FS one can employ methods based on the investigation of longitudinal electric conductivity and power factor in quantizing magnetic fields with inductions up to several T both at helium and nitrogen or room temperatures. In so doing, quantizing magnetic field, electric field and temperature gradient must be normal to SL TEM layers.

The Author is grateful to chief research scientist L. N. Vikhor for the helpful constructive discussion of the results of the work.

References

1. L. I. Anatychuk, L. N. Vikhor, *Functionally Graded Materials. Thermoelectricity, Vol. IV*.
2. N. S. Lidorenko, V. A. Andriyako, L. D. Dudkin, E. L. Nagayev, and O. M. Narva, On the Effect of Tunneling on the Efficiency of Thermoelectric Devices, *Doklady AN SSSR* **186**, 1295 (1969).
3. A. Casian, V. Dusciak, and Iu. Coropceanu, Huge Carrier Mobilities Expected in Quasi-One-Dimensional Organic Crystals, *Phys. Rev.* B, **66,** 165404, 1 – 5 (2002).
4. A. I. Casian, I. I. Balmush, and V. G. Duschak, Reduction of the Lorentz Number as a New Direction of *ZT* Increase in Quasi-One-Dimensional Organic Crystals, *J.Thermoelectricity* **3**, 19 (2011).
5. L. P. Bulat, I. A. Drabkin, V. V. Karatayev, V. B. Osvensky, and D.A.Pshenai-Severin, Effect of Interface Scattering on the Thermal Conductivity of $Bi_xSb_{2-x}Te_3$ Nanostructured Semiconductor Material, *Physics of the Solid State* **52**, 1712 (2010).
6. L. I. Anatychuk, *Thermoelectricity, Vol.1, Physics of Thermoelectricity* (Chernivtsi: Institute of Thermoelectricity, 2008), 404 p.
7. J. P. Heremans, Low Dimensional Thermoelectricity. Proceedings of XXXIV International School of Semiconducting Compounds. Jaszowiec-2005, *Acta Physica Polonica* **108**(4), 609 –634 (2005).
8. M. S. Dresselhaus, G. Dresselhaus, X. Sun, Z. Zhang, S. B. Cronin, and T. Koga, Low Dimensional Thermoelectric Materials, *Physics of the Solid State* **41**(5), 755 – 758 (1999).

9. F. G. Bass, A. A. Bilgakov, and A. P. Tetervov, *High-Frequency Properties of Superlattice Semiconductors* (Moscow: Nauka, 1989), 288p.
10. W. L. Liu, T. Borca-Tasciuk, J. L. Liu, K. Taka, K. L. Wang, M. S. Dresselhau, and G. Chen, In-Plane Thermoelectric Properties of Si/Ge Superlattice, *Proc. of 20th International Conference on Thermoelectrics* (2001). – P. 340 – 343.
11. R. Venkatasubramanian, E. Siivola, and T. S. Colpiits, In-Plane Thermoelectric Properties of Freestanding *Si/Ge* Superlattice Structures, *Proc. of 17th International Conference on Thermoelectrics* (1998). – P.191 – 197.
12. A. Lambrecht, H. Beyer, J. Nurnus, C. Künzel, and H. Böttner, High Figure of Merit *ZT* in *PbTe* and Bi_2Te_3 Based Superlattice Structures by Thermal Conductivity Reduction, *Proc. of 20th International Conference on Thermoelectrics* (2001). – P.335 – 339.
13. B. Yang, J. Liu, K. Wang, and G. Chen, Characterization of Cross-Plane Thermoelectric Properties of *Si/Ge* Superlattices, *Proc. of 20th International Conference on Thermoelectrics* (2001), 344 – 347.
14. Y. Zhang, D. Vashaee, R. Singh, and A. Shakouri, Influence of Doping Concentration and Ambient Temperature on Cross-Plane Seebeck Coefficient of *InGaAs*/*InAlAs* Superlattices, *Mat. Res. Soc. Symp. Proc.* **793**, 59 – 65 (2004).
15. J. C. Caylor, K. Coolney, J. Stuart, S. Nangoy, T. Colpiits, and R. Venkatasubramanian, Developing *PbTe*-Based Superlattice Structures with Enhanced Thermoelectric Performance, *2005 International Conference on Thermoelectrics*, P. 489 – 491.
16. R. F. Fivaz, Theory of Layered Structures, *J. Phys. Chem. Solids* **26**(5), 839 – 845 (1967).
17. N. F. Hinsche, I. Mertig, and P. Zahn, Lorentz function of Bi_2Te_3/Sb_2Te_3 Superlattices, *J. Electron. Mat.* **42**(7), 1406 – 1410 (2013).
18. B. M. Goltsman, V. A. Kudinov, and I. A. Smirnov, *Semiconductor Thermoelectric Materials Based on* Bi_2Te_3 (Moscow: Nauka, 1972), 320 p.
19. L. D. Ivanova, Yu. V. Granatkina, A. Dauscher, B. Lenoir, and H. Sherrer, Influence of the Purity and Perfection of Czochralski-Grown Single Crystals of Bismuth and Antimony Chalcogenides Solid Solution on Their Thermoelectric Properties, *Proc. of 5th European Workshop on Thermoelectrics, Pardubice, Czech Republic,* 1999, P. 175 – 178.
20. P. V. Gorskyi, (New York: *Layered Structure Effects as Realization of Anisotropy in Magnetic, Galvanomagnetic and Thermoelectric Phenomena* Nova Publishers, 2014), 366 p.
21. P. V. Gorskyi, Diagnostics of Functional Materials with Closed Fermi Surfaces Described by the Fivaz Model and Some Aspects of Their Use, *Dopovidi NAN Ukrainy* 12, 77 – 85 (2014).
22. P. V. Gorskyi, Electric Conductivity of Functional, Including Thermoelectric, Materials Described by the Fivaz Model, in Quasi-Classical Range of Magnetic Fields, *J. Thermoelectricity* **3**, 5 – 14 (2014).
23. P. V. Gorskyi, Are Layered Structure Effects Manifested with Close Fermi Surfaces? *Ukrainian J. Physics* **55**(12), 1297 – 1305 (2010).
24. P. V. Gorskyi, Power Factor of Layered Thermoelectric Material with Closed Fermi Surface in a Quantizing Magnetic Field, *Ukrainian J. Physics* **58**(4),1297 – 1305 (2013).
25. P. V. Gorskyi, Diagnostics of Functional Materials Described by Fivaz Model by the Dependence of Power Factor on Quantizing Magnetic Field. – *Collected Papers Based on Proc. of XX International Remote Scientific and Practical Conference "Scientific Discussion. Problems of Mathematics, Physics, Chemistry, Biology", №8(19), Moscow-2014* (Moscow: Nauka, Interperiodica), P.55 – 60.
26. P. V. Gorskyi, *Gigantic Negative Magnetoresistance of Nanoheterostructures, Described by Fivaz Model.* – arXiv:1503.06823v1 – 10 Mar 2015. – P. 1 – 3.

Submitted 10.07.2015.

D.M. Freik, B.S. Dzundza, O.B. Kostyuk, V.I. Makovishin

Vasyl Stefanyk Precarpathian National University,
57, Shevchenko St., Ivano-Frankivsk, 76018, Ukraine.

THERMOELECTRIC PROPERTIES OF THIN FILMS BASED ON STIBIUM-DOPED TIN TELLURIDE

The thermoelectric properties of thin films based on stibium-doped tin telluride with stibium content 2 at. % produced in open vacuum at different deposition temperatures on fresh chips (0001) of mica are investigated. It is established that samples of thickness close to 1.5 μm have maximum thermoelectric power 25 μW/K2cm, which is much better as compared to that of pure tin telluride.

Key words: thin films, tin telluride, doping, thermoelectric properties.

Introduction

Tin telluride is widely used in semiconductor technology. Moreover, it is also a promising thermoelectric material for medium-temperature range (500 – 750) [1 – 4]. Preparation of thin-film material largely expands the scope of application. Due to introduction of doping impurities the thermoelectric properties of material can be modified over wide range.

This paper is concerned with the thickness dependences of thermoelectric parameters of films based on stibium-doped tin telluride vapor-phase deposited on mica substrates.

Experimental procedure

Films to be investigated were prepared by vapor deposition of synthesized material *SnTe* in vacuum on the substrates of fresh chips (0001) of muscovite mica and glass ceramics. The evaporator temperature was $Te = 600\ ^{o}C$, and substrate temperature varied in the range of $Ts = 150 – 300\ °C$. The thickness of films was assigned by deposition time within (45 – 240) s and measured with the aid of a micro interferometer MII-4.

The electric parameters of films were measured in the air at room temperatures in constant magnetic fields on the developed automated plant that provides for measuring the electric parameters, as well as recording and primary processing of data with the possibility of constructing the plots of temporal and temperature dependences. The measured sample had four Hall and two current contacts. As the ohmic contacts, silver films were used. Current through the samples was ≈ 1 mA. A magnetic field was directed perpendicular to the surface of films at the induction of 1.5 T.

The results of investigations and the dependences of the electric conductivity σ and the Hall concentration of charge carriers n_h and the Seebeck coefficient S on the surface temperature and thickness are represented in Figs. 1 – 3.

Investigation results and their analysis

As can be seen from Fig. 1, the deposition temperature has a considerable impact on the thermoelectric parameters of material under study. The electric conductivity and the Hall concentration of charge carriers increase with a rise in deposition temperature, and the thermoelectric

power has a clear peak at deposition temperature 200 °C. With a rise in *Ts*, mobility grows up to temperatures 200 °C, and with a further increase in temperature, it is somewhat reduced. This is due to structural perfection of condensate. With a rise in deposition temperature, due to improved self-organization, material structure is better ordered, which reduces the impact of grain-boundary scattering mechanism. With a further increase in substrate temperature, the processes of condensate re-evaporation are considerably accelerated and thermoelectric parameters of material are somewhat degraded.

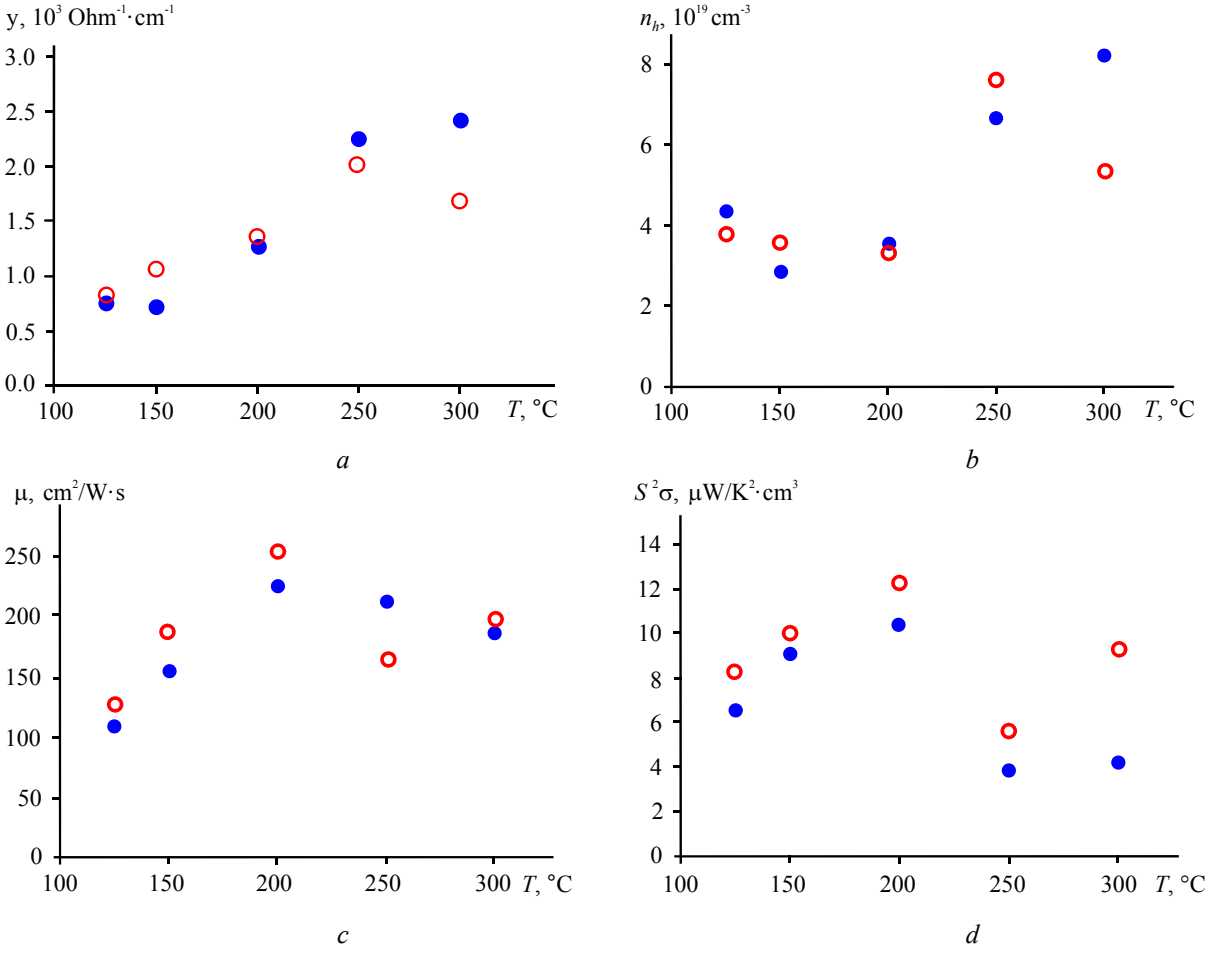

Fig. 1. Dependences of the electric conductivity σ (a), the Hall concentration n_h (b), charge carrier mobility μ (c) and the thermoelectric power $S^2\sigma$ (d) on the deposition temperature of films produced on fresh mica chips. Derivation time, s: ● – 120, ○ – 240.

With regard to a clear peak of thermoelectric power, subsequent studies versus condensate thickness were performed for samples produced at *Ts* = 200 °C.

The electric conductivity of films and the Hall concentration of charge carriers drastically increase in the area of low thicknesses. This is due to the acceptor action of oxygen. On the contrary, the Seebeck coefficient is reduced in the area of low film thicknesses. Therefore, for the thermoelectric power ($S^2\sigma$) a clear peak is observed in the area of thicknesses 1.5 μm (Fig. 3).

To determine the surface effect, the thickness dependences of thermoelectric parameters for films produced on different substrates were investigated (Fig. 2). Parameters of near-surface layers were estimated by means of Petritz's model. A thin film in this model is composed of two layers: near-surface (I) (surface charge region) of thickness d_s, with current carrier concentration n_s, and their mobility μ_s, and bulk (II), which is characterized by similar values d_b, n_b, μ_b, connected in parallel. The

thickness of the film is $d = d_s + d_b$.

In this case according to [5]:

$$\gamma = \frac{\gamma_s d_s + \gamma_b d_b}{d}; \tag{1}$$

$$R = \frac{R_s \gamma_s^2 d_s + R_b \gamma_b^2 d_b}{\left(\gamma_s d_s + \gamma_b d_b\right)^2} d; \tag{2}$$

$$S = \frac{\gamma_s d_s S_s + \gamma_b d_b S_b}{\gamma_s d_s + \gamma_b d_b}. \tag{3}$$

On condition of known experimental values of σ, R, μ and the bulk σ_b, R_b, μ_b and d, from these relationships one can approximately determine parameters of near-surface layers σ_s, R_s, μ_s respectively, the values of which are listed in the table. It is seen (Fig. 2 – solid lines) that calculated curves describe adequately the experimental results with the defined values of near-surface electric parameters d_s, σ_s, R_s, n_s, μ_s (Table 1).

Table 1

Parameter values of near-surface layer (*s*) and bulk (*b*) of *SnTe*: *Sb* films calculated according to a two-layer Petritz's model

	Parameters
d_s, μm	0.13
σ_s, $Ohm^{-1}cm^{-1}$	3100
σ_b, $Ohm^{-1}cm^{-1}$	300
R_s, cm^3C^{-1}	0.013
R_b, cm^3C^{-1}	0.15
n_s, cm^{-3}	$4.81\ 10^{20}$
n_b, cm^{-3}	$4.17\ 10^{19}$
μ_s, $cm^2V^{-1}s^{-1}$	40.3
μ_b, $cm^2V^{-1}s^{-1}$	45
S_s, μV/K	80
S_b, μV/K	150

Conspicuous are considerable values of near-surface electric conductivity and the Hall concentration of carriers, the Seebeck coefficient $S_s \approx 80$ μV/K (Table 1), which creates prospects for using *SnTe*:*Sb* as *p*-type legs in thin-film thermoelements.

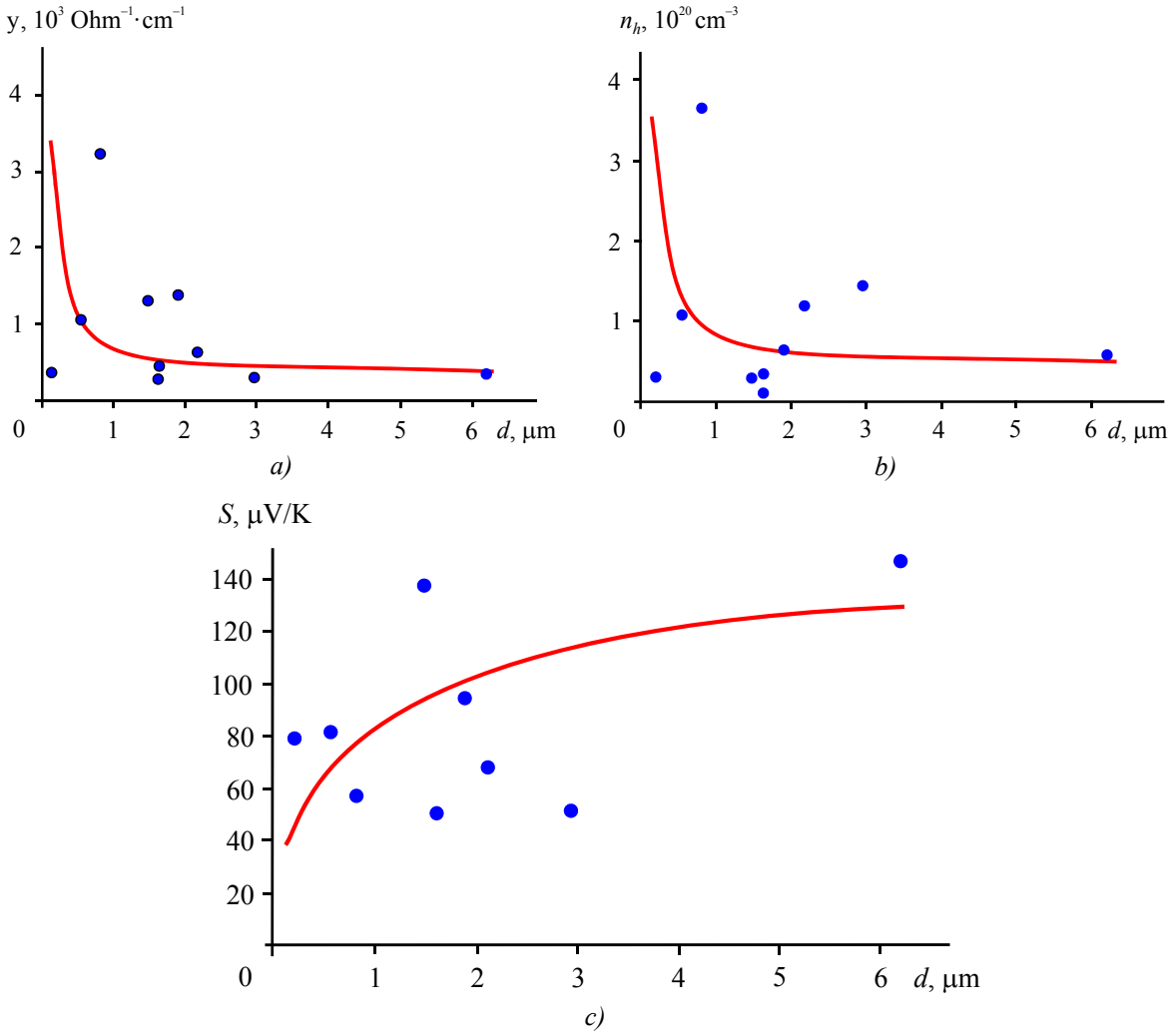

Fig. 2. Dependences of the electric conductivity σ (a), the Hall concentration n_h (b) and the Seebeck coefficient S (c) on the thickness d of SnTe:Sb films on mica substrates. Dots are for experiment, solid line – calculation according to Petritz's model.

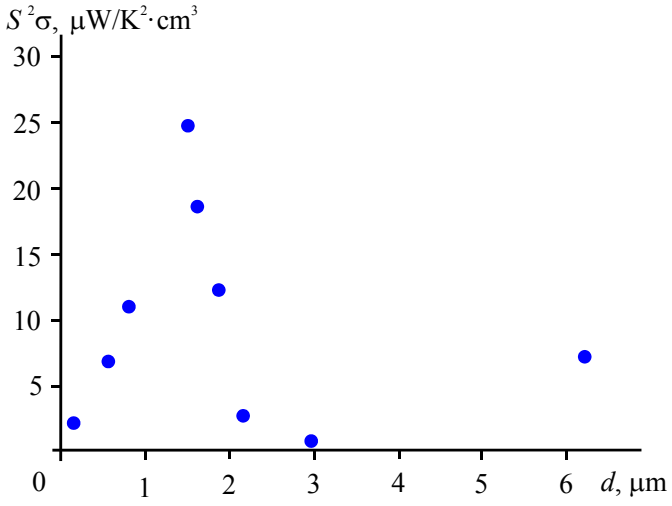

Fig. 3. Dependence of the thermoelectric power $S^2\sigma$ on the thickness d of SnTe:Sb films on mica substrates.

Conclusions

1. The thermoelectric properties of *Sb* doped tin telluride thin films produced by vapor-phase methods on mica substrates are studied. It is established that samples of thickness close to 1.5 μm have maximum thermoelectric power 25 $\mu W/K^2 cm$, which is much better as compared to that of pure tin telluride.

2. The thermoelectric parameters of near-surface layers are determined. It is shown that *p*-type *SnTe* films have improved thermoelectric parameters as compared to the bulk samples.

The work was performed in the framework of integrated science project of the Ministry of Education and Science of Ukraine (state registration number 0115U002303).

References

1. V. M. Shperun, D. M. Freik, and R. I. Zapukhlyak, *Thermoelectricity of Lead Telluride and its Analogs* (Ivano-Frankivsk: Plai, 2000), 250 p.
2. E. P. Sabo, Technology of Chalcogenide Thermoelements. Physical Fundamentals. Structure and Properties of Materials, *J.Thermoelectricity* 1, 61 (2002).
3. D. M. Freik, I. V. Horichok, N. I. Dykun, and Yu. V. Lysyuk, Influence of Manufacturing Technique on the Thermoelectric Properties of Nonstoichiometric and Doped Lead Telluride and Solid Solutions on its Basis, *J.Thermoelectricity* 2, 43 (2001).
4. D. M. Freik, M. A. Haluschak, and L. I. Mezhylovska, *Physics and Technology of Thin Films* (Lviv:Vyscha Shkola, 1988), 182 p.
5. R. L. Petritz, Theory of an Experiment for Measuring the Mobility and Density of Carriers in the Space-Charge Region of a Semiconductor Surface, *Phys. Rev*. 110, 1254 (1958).

Submitted 03.07.2015.

V.Ya. Mykhailovsky, M.V. Maksimuk

V. Ya. Mykhailovsky

Institute of Thermoelectricity
of the NAS and MES of Ukraine,
1, Nauky Str., Chernivtsi, 58029, Ukraine

M. V. Maksimuk

AUTOMOBILE OPERATING CONDITIONS AT LOW TEMPERATURES. THE NECESSITY OF APPLYING HEATERS AND THE RATIONALITY OF USING THERMAL GENERATORS FOR THEIR WORK

The main reasons for a complicated startup of transport means at low ambient temperatures are analyzed. The benefits and drawbacks of using start heating for a better startup of automobile engine are determined. The operating principle and structural features of starting pre-heaters are described. The rationality of using thermoelectric generators for the operation of such equipment is substantiated.

Key words: engine, start heating, compartment heater, thermoelectric generator.

Introduction

To date, startup of internal combustion engine at low ambient temperatures remains a relevant problem for any and every kind of transport means [1 – 6]. It is primarily due to a negative effect of low temperatures on the service life of internal combustion engines. Quick heating of "cold" engine creates temperature stresses leading together with mechanical loads to quick parts wear and their lifetime reduction [1, 3, 4]. Another negative factor of cold start is large fuel consumption due to its condensation and reduced volatility [2]. That is why prior to startup the engine must be warmed up [5, 6]. At the present time there are a lot of various methods for easy startup of engines in cold weather. In general, they are classified as group and individual [7].

Group methods realize start heating of engine by heat carriers heated from the external energy sources (electric grids, boiler facilities, and portable gas generators): water steam, hot air, infra-red rays, etc.

Individual heating methods include standard (required by design of engines) and supplementary heating means (liquid and air heaters, electric torch air heaters, and heating plugs mounted directly on the engines). The benefit of individual heating methods is their independence, i.e. they do not depend in their operation on the presence of external energy source.

Autonomous start heating of cooling liquid is one of the most widespread and efficient individual methods of engine warm-up at low temperatures. Such heaters are fit for practically all types of internal combustion engines, so they are used in cars and trucks, as well as in buses, planes, yachts and boats [8, 9].

However, despite powerful capabilities, starting pre-heaters have not found wide use yet. It is primarily due to their high cost. However, it is not the only constraining factor: according to statistics, even in economically developed Nordic countries the autonomous starting pre-heaters are installed only in one automobile of a thousand [10].

Therefore, the purpose of this paper is analysis of the benefits and drawbacks of start heating of automobile engines at low temperatures and expansion of the opportunities of practical use of starting pre-heaters with the aid of thermoelectric power converters.

Drawbacks of "cold" engine start

The main reasons complicating startup of internal combustion engine at low temperatures include [11 – 13]:

1. Resistance increase with crankshaft rotation due to increased viscosity of engine oil. Many years of experience in transport means operation show that at temperature –18°C the resistance to crankshaft rotary moment increases by a factor of 2 – 2.5.

2. Starter power decrease with reduction of dry starting current and accumulator capacity. For a completely charged accumulator battery of capacity 50 – 60 A·h, dry starting current is within 300 – 500 A. If starter current at temperature 25°C can reach 400 A at voltage 9 V, then at temperature – 30°C it will decrease to 200 A. And with each new starting attempt, its value will decrease. Though manufacturing techniques of accumulator batteries improve every day, they do not affect the degree of starter current reduction at low temperatures.

3. Fuel condensation and its volatility decrease. The quality of air-fuel mixture depends on fuel volatility. For instance, petrol fuel volatility occurs mainly in the range from 35°C to 200°C. In so doing, "light" fractions are volatilized which are most critical in the period of cold engine start. However, according to standards, the content of such fractions in petrol fuel is restricted, since their large amount in the hot engine will cause formation in fuel system of vapour locks that result in the internal combustion engine wobble. In this connection, "winter" petrol that has volatility almost three times higher compared to "summer" petrol is provided, which should assure a reliable engine startup at – 15…– 20°C. However, the use of "winter" petrol already at temperature +5°C leads to formation of vapour locks. With "summer" petrol sort engine startup is complicated at – 5°C, and at – 20°C it becomes impossible.

Effect of said factors at low temperatures is manifested simultaneously and leads to reduction of engine service life and increase of fuel consumption at its startup [13]. Preliminary investigations show that with each "cold" start of internal combustion engine (at temperature lower than + 5°C), the loss in its service life is nearly 400 – 600 km. Taking into account that over the year there are 100 – 120 days with the temperature lower than 0°C, the loss in engine service life will be ~80000 km [11].

4. Increase in the norm of toxic substances emission with exhaust gases. According to medical men, high emission of toxic substances into environment with the exhaust gases of automobiles leads to propagation of various allergic and asthmatic diseases and, as a consequence, to reduction in life expectancy at least by 4 – 5 years.

It has been established that the emission of toxic substances in the cars during first kilometers after "cold" engine start is 70 – 80% of total amount of automobile emission during this period. It is due to low efficiency of catalyst work under conditions of low temperatures. Depending on the ambient temperature, the automobile must drive several kilometers prior to the catalyst will be heated and start cleaning efficiently the exhaust gases.

Investigations of Norwegian Automobile Federation have shown that the emission at one "cold" engine start is 100 – 300 g. If throughout the year 500 such starts are made (on the average 2 times a day), the annual average emission of one automobile with account of start emission is 69 kg. In so

doing, the total amount of yearly emissions of all automobiles, for instance, for a city with population ~1 million inhabitants, will be 20000 tons.

Operating principle and structural features of starting pre-heaters

At the present time, autonomous starting pre-heaters for preliminary warm-up of engines of transport means at low temperatures are commercially produced by a number of foreign companies: Eberspacher, Webasto, Truma (Germany), Ateso (Czech Republic), Mikuni (Japan), Tepolostar (Russia) [14 – 17]. Staring pre-heaters are mainly classified:

- by the type of fuel as diesel, petrol and gas. Separation of heaters according to the type of fuel and the necessity of creation of corresponding structures is due to the fact that the heaters are mounted on a car with diesel, petrol and liquefied gas-operated engines. From the standpoint of ease of use, the fuel that the engine is operated by is advisable for the heaters;

- by the type of heat carrier heating as liquid and air.

Fig. 1 shows a schematic and appearance of a liquid starting pre-heater Hydronic (Eberspacher) of thermal power 4 kW.

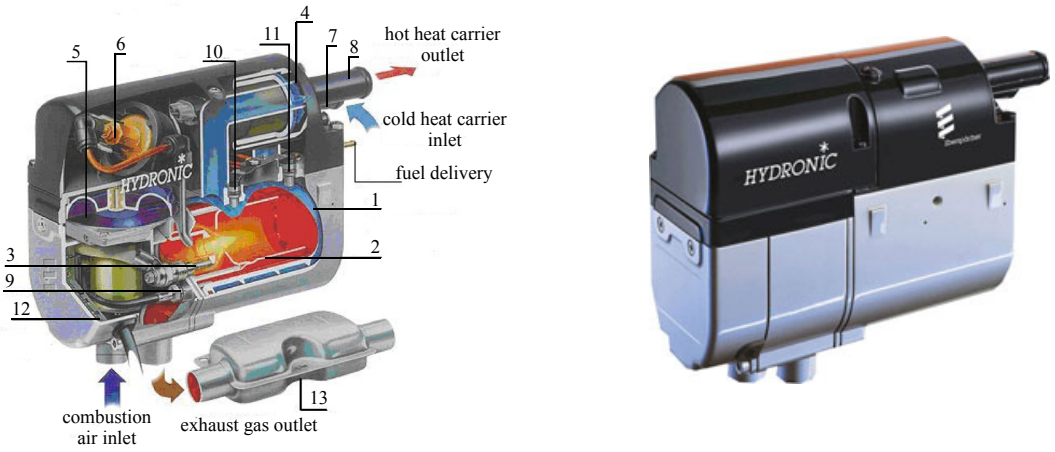

a) *b)*

Fig. 1. Schematic (a) and appearance (b) of a liquid starting pre-heater Hydronic:
1 – heat exchanger; 2 – combustion chamber; 3 –igniter;
4 – liquid circulation pump, 5 – fan; 6 – fuel pump;
7, 8 – inlet and discharge branch pipes; 9 – flame sensor; 10 – temperature sensor;
11 – overheat sensor; 12 – electronic unit; 13 – silencer [15].

A starting pre-heater combines in one housing heat exchanger 1, combustion chamber 2 with igniter 3, liquid circulation pump 4, fan 5 and pump 6 for air and fuel delivery to combustion chamber. The operating principle lies in heating of cooling liquid (heat carrier) of automobile engine. For this purpose, the heater through branch pipes 7 and 8 is connected to engine cooling system loop, which in turn is connected to automobile heating radiators. Liquid circulation in cooling system and heating radiators is done by a liquid pump. Fuel to the heater comes directly from the automobile tank or is taken from a separate special container. The presence of flame in combustion chamber is controlled by sensor 9. Sensors 10 and 11 are used to control heat carrier temperature. The diagnostic system in electronic unit 12 controls the work of the heater and disconnects it in case of emergency. The device is started manually or by means of a timer programmable for a specific time from a remote control desk. To provide for a noise-free work, the heater is additionally equipped with silencer 13.

Thus, liquid starting pre-heaters provide for not only engine warm-up at low temperatures, but also heating of cabins, passenger compartments and transport means. Moreover, this type of heaters can be also used in summer for blowing of passenger compartments when air-conditioner is inoperative.

In some cases the use of liquid starting pre-heaters is impossible (automobiles with air-cooled engine) or unreasonable – for instance, for heating of passenger compartments of buses, sailboat cabins, cabins of trucks during stops, and auto campings. For such cases autonomous air heaters of passenger compartments have been created (Fig. 2).

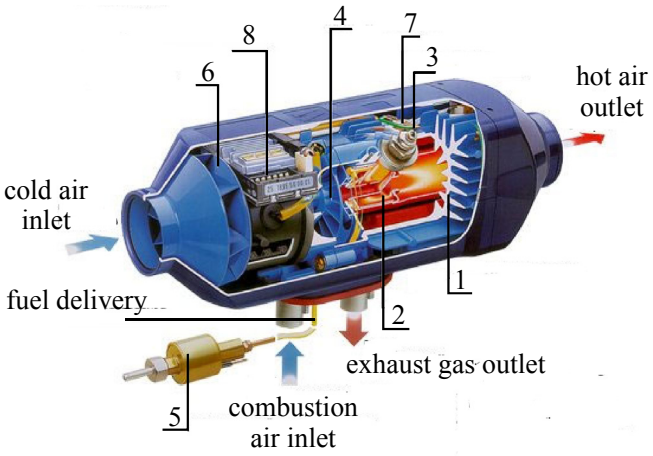

a)

b)

Fig 2. Schematic (a) and appearance (b) of autonomous air heater of passenger compartment Airtronic (Eberspacher) of thermal power 4 kW:
1 – heat exchanger; 2 – combustion chamber; 3 – igniter;
4 –fan for air supply to combustion chamber; 5 – metering fuel pump;
6 – cold air supply fan; 7 – overheat sensor; 8 – electronic unit [15].

Just as for liquid heaters, the basic structural elements of autonomous heaters are heat exchanger 1 and combustion chamber 2. Air blown by fan 4 is mixed with the fuel delivered to combustion chamber by metering pump 5. Firing of fuel-air mixture is done by ceramic igniter 3. Air flow created by means of another fan 6, passes through the external finned part of heat exchanger to be heated by thermal energy from combustion of diesel or petrol fuel. Following

this, the hot air is fed to passenger compartment or cabin. Located on heat exchanger housing is overheat indicator 7, and air temperature sensor (not shown in Fig. 2), necessary for control of thermal condition, is arranged in cold air flow directly in front of the heat exchanger. Control unit 8 maintains given air temperature in passenger compartment, changing the number of fan rotations and consumption of fuel coming to combustion chamber. The exhaust system provides for a discharge of combustion products beyond the cabin of passenger compartment.

Moreover, this type of heaters can be also used in summer for blowing of passenger compartments when air-conditioner is inoperative.

An alternative to autonomous air heaters of buses, microbuses, off-roaders, jeeps and special machines are non-autonomous air heaters (Fig. 3). Such devices are composed of a radiator heated by engine heat carrier and a fan delivering heat from the heated radiator to space. On delivery of heat carrier to radiator, the heater through deflectors or air ducts blows hot air to passenger compartment. Pumping of heat carrier is done by a standard automobile pump, so the heater works only when the engine is in operation.

Fig. 3. Nonautonomous air heater Xerox-4000 (Eberspacher):
1 – heat exchanger; 2 – inlet and discharge branch pipes; 3 – fan [15].

The unique feature of these devices lies in the fact that they are used in transport means with large internal volumes as supplementary heaters for standard heating system.

Benefits of engine start heating

From technical standpoint, engine start heating at low ambient temperatures as compared to "cold" start provides for the following [11, 18]:

- engine startup at 1 – 2 attempts due to reduced time of starter rotation by a factor of 2 – 3;
- reduction of engine oil viscosity and increase of its pumping rate;
- increase of crankshaft speed;
- reduction of fuel consumption by 0.1 – 0.5l per one start. Preliminary studies that were conducted in the Technological Institute of Oslo (Norway) show that with the use of start heating fuel consumption at startup is reduced by 15 – 30% for petrol engines and 8 – 12% for diesel engines. In so doing, already after passing the distance of 3 – 4 km the engine is warmed-up completely, and fuel consumption practically does not depend on the fact whether or not start heating took place. Thus, the most evident fuel saving at engine warm-up occurs in the process of startup itself and with the first 2 – 3 km of running. This allows saving 90 – 150 liters of fuel during one winter season;

reduction of engine service life loss. Fig. 4 shows the results of study on automobile engine oil after 30 starts at ambient temperature – 20°C with and without start heating. As is seen from the presented data, the content of metals in the oil of automobile for which start heating was used is more than 3 times less than for automobile with no start heating. It is due to the fact that at low temperatures the rate of oil flow is reduced, and it cannot efficiently oil the surfaces of parts, which results in their quick wear due to friction and engine service life reduction in general. Engine start heating allows increasing the operational period of internal combustion engine and essentially saves its service life. For instance, under conditions of middle climate zone and the North where the temperature does not raise above +5 °C within six months, with a daily use of start heating the saving of engine service life is 50-60 thousand km;

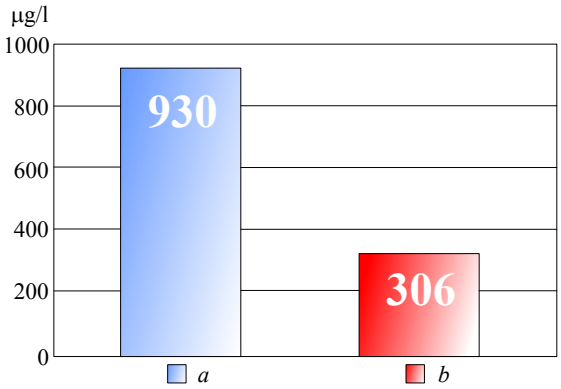

Fig. 4 – Metal amount, µg in 1 l of car engine oil: a) without start heating; b) with start heating.

– reduction of toxic substances emission to environment with the exhaust gases. Figs. 5, 6 show the results of recent research on the determination of toxic emissions with exhaust gases for automobile with a preheated and cold engine.

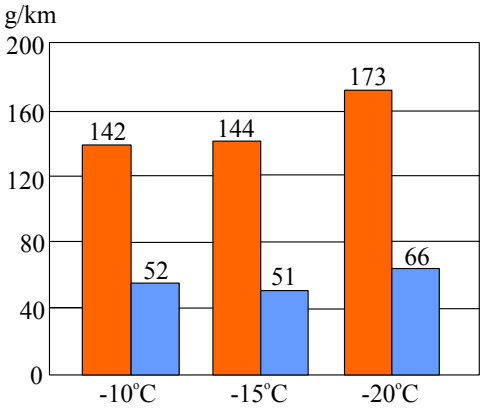

Fig. 5. Carbon monoxide level in automobile exhaust with a cold and preheated engine.

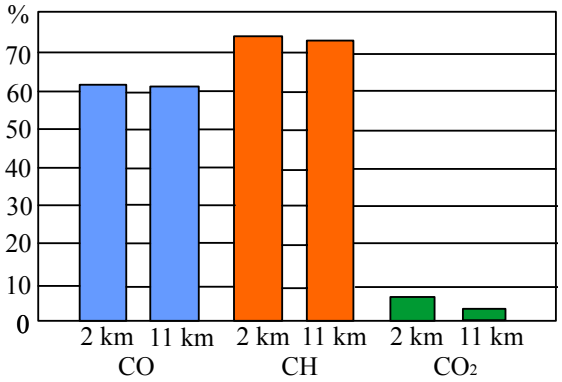

Fig. 6. Relative reduction of emission in automobile exhaust with a preheated engine.

From the analysis of presented data it follows that depending on the number of cold starts during the year engine preheating allows reducing toxic emissions of automobile during the first kilometers of running by 60-80%. Moreover, at the startup of preheated engine the content of toxic gases in the exhaust is reduced by a factor of ~ 5, which in turn allows reducing the early amount of

emissions from one automobile by 80%. Given below are the values of reduction of yearly emissions with the use of start heating of automobile engine, on condition of its yearly mileage 10000 km (Table 1).

Table 1

Reduction of yearly automobile emission with the use of start heating

Emission level	Without start heating	With start heating
Carbon monoxide (*CO*), kg	63	12.6
Hydrocarbons (*CH*) + nitrogen oxides (NO_x), kg	6	1.25
Total emission, kg	69	13.8

It is noteworthy that today the norms of toxic emissions with exhaust gases are regulated by international standards EURO-4 – for cars and EURO-5 – for trucks. Apart from the total norm of emissions for heated engine, these standards partially specify the amount of emissions under start-up conditions.

Another benefit of engine start heating lies in higher safety of travel. Psychologists emphasize essential effect of cold on humans. The actions of chilled person are delayed and retarded, his attention is diminished. These factors account for accident statistics according to which 15 % of all traffic collisions occur within the first 15 minutes of travel. Under comfortable conditions provided by start heating of engine and passenger compartment, such negative factors are completely excluded.

Use of thermoelectric generators for engine start heating

Despite several positive features, automobile heaters, as mentioned above, do not find mass application, in particular, in cars and microbuses.

This is mainly due to the need for electric energy for power supply to components of starting pre-heaters, namely fuel pump, fan for air supply to combustion chamber, circulation pump for pumping of liquid heat carrier.

Preliminary studies have shown that in operation of liquid heater of thermal power 4 kW and electric power requirement 37 – 40 W, making 60 W together with a standard fan of automobile heating system, a battery of capacity 60 A·h during 4.5 h loses 50% of capacity. One should also take into account the fact that under reduced temperatures the capacity of automobile battery loses is further reduced by another 15 – 20% [19]. So, liquid starting pre-heaters are recommended to be used not more than for 40 min in automobiles with the engine up to 3 liters, and not more than for 1 h in other automobiles, which can be insufficient for warm-up of internal combustion engine to operating temperature [20]. In so doing, the work of standard automobile heating system should be adjusted so that the electric current of fan motor does not exceed 2.5 A.

Practice shows that by strong frosts (– 10…– 30 °C) the problem of passenger compartment warm-up becomes irrelevant. The problem of automobile operation in principle is much more acute. Under such conditions, essential rise in the temperature of passenger compartment by means of start heating is practically impossible. Though air heaters allow passenger compartment to be warmed before everything else, to warm up the engine, battery capacity is not sufficient. To prevent from a "deep" battery discharge, by strong frosts it is recommended not only to disconnect the function of compartment heating, but also to refuse from the use of additional equipment installed in the car (audio- and video complexes, GPS-navigators, warning systems). Drivers who throughout the day use

a car for less than 30 min (home-office-home), and in so doing a heater operates for 20 – 30 min prior to each engine startup, will not avoid weekly battery charging.

It is noteworthy that none of known models of starting pre-heaters solve the problem of battery discharge. The most widespread ways of cold engine heating without the use of battery energy is electric heating and heating by means of thermal accumulators. However, in this case a driver is permanently tied to external energy source.

Said problem can be solved with the aid of a thermoelectric generator operated from heater and providing for autonomous power supply to its components [22]. A schematic of thermoelectric automobile heater is given in Fig. 7.

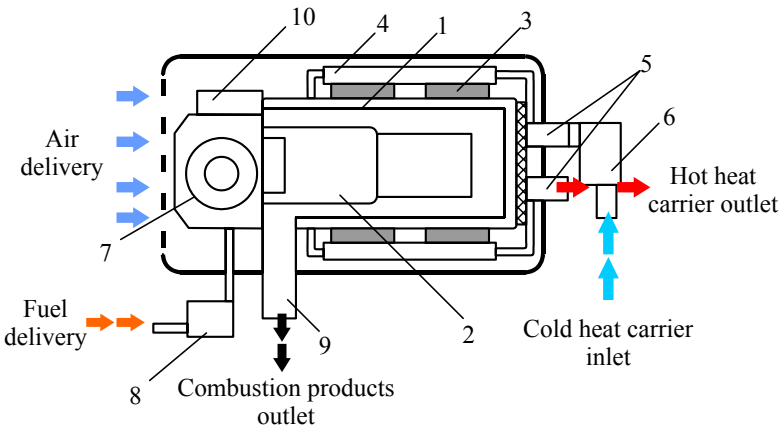

Fig. 7. Schematic of thermoelectric automobile starting pre-heater:
1 – hot heat sink; 2 – heat source; 3 – thermoelectric modules; 4 – liquid cold heat exchangers;
5 –inlet and outlet connecting branches; 6 –liquid circulation pump; 7 – fan; 8 –fuel pump;
9 –exhaust pipe; 10 –electronic unit.

Structurally, such thermoelectric heater is composed of hot heat sink 1 which accommodates heat source 2 inside. On the external surface of the heat sink there are thermoelectric modules 3, the heat from which is rejected by liquid heat exchangers 4. Liquid heat exchangers are combined into one hydraulic loop which is connected to engine cooling system by connecting branches 5. Circulation of liquid heat carrier in heater-engine loop is done by pump 6. Moreover, the heater must comprise fan 7 and fuel pump 8 – for air and fuel delivery to combustion chamber. Combustion products are rejected to environment by exhaust pipe 9. The heater start and control is done by electronic unit 10.

The heater will work as follows. Thermal energy obtained due to fuel combustion heats the hot heat exchanger, passes through thermoelectric converter and is rejected by liquid heat carrier circulating in the heat exchanger of the heater and engine cooling system. Due to the difference in temperatures between the hot and cold sides, thermal converter generates an electric current. Thermal energy rejected by heat carrier from thermal converter is used for engine warm-up and heating of automobile passenger compartment.

Apart from preliminary engine warm-up and heating of compartments, vehicle cabins at reduced ambient temperatures, the thermoelectric heater will provide for electric energy supply to:

- inherent components: fuel and circulation pumps, fan, electronic unit;
- battery during engine warm-up;
- standard fan of automobile heating system;
- automobile warning systems;
- automobile audio and video equipment.

Besides, thermoelectric starting pre-heaters can find wide practical application in ambulances to maintain stable temperature conditions in passenger compartment and power supply to medical devices (cardiographs, defibrillators, etc.) and in transport means of military purpose – for additional power supply to communication systems during engine warm-up.

Thus, owing to the fact that the thermoelectric heater will not depend in its operation on the availability of battery or other external source of electric energy, this opens up vast prospects for such devices in various scopes of activity.

Conclusions

1. It is shown that the drawbacks of transport means startup under low ambient temperatures include reduction of engine service life and overconsumption of fuel during first kilometers of running.

2. It is determined that the use of start heating allows increasing engine life by 50 – 60 thousand km per year and reducing emissions of toxic substances by a factor of 5, saving 90 – 150 l of fuel during one winter season. Moreover, comfortable conditions provided by start heating of engine and automobile compartment exclude completely the possibility of accidents caused by the effect of cold on the driver.

3. It is shown that the main drawback of starting pre-heaters is a need for electric energy for power supply to components (fuel and circulation pumps, fan, and electronic control unit), leading to battery discharge. It creates essential difficulties during engine startup.

4. The possibility of creation and the expedience of using thermoelectric generator to solve the problem of automobile battery discharge during the operation of starting pre-heaters are substantiated. With the aid of thermoelectricity the process of start heating becomes completely autonomous, without the use of battery electric energy. Moreover, excess energy of thermal generator can be used for battery charging and power supply to other automobile equipment. This opens up new vistas for thermoelectric starting pre-heaters in various scopes of activity.

References

1. O. V. Antoshkiv, Means for Easy Engine Start During Winter Operation and Evaluation of the Possibility of Their Use for Peugeut J9 Karsan Automobiles, *Herald of State University "Lvivska Politekhnika"* 396, 3 – 7 (2000).
2. S. O. Yakushenko, A. M. Budyatskyi, and R. R. Kuzmyak, Effect of Fuel Temperature on Technical and Economic Performance of Engine, *Innovatsiini Tekhnologii v Osviti, Nautsi ta Vyrobnytstvi* **5**(10), 56 – 62 (2014).
3. A. I. Ponomarev, V. N. Sidorov, and S. B. Vanyushin, Analysis of the Main Properties of Liquid Starting Pre-Heaters, *Proc. of Regional Scientific and Technical Conference "Science-Intensive Technologies in Instrument and Machine Building and Development of Innovation Activity in Higher Educational Institution",* Vol. **2**, 2015, p.2 – 7.
4. L. M. Matyukhin, *Heating Devices of Automobiles: Teaching Guide (*Moscow: MADI, 2009), p. 89.
5. V. L. Derkach, Analysis of Using Start Heating for Automobile Transport, *Interuniversity Collected Papers "Naukovi Notatky*" **43**, 75 – 78 (2013).
6. A. V. Gnatov, Starting Pre-Heater for Petrol Engine, Application Peculiarities*, Herald of Scientific Technical University "Kharkiv Polytechnic Institute"* **8**(1117), 58 – 63 (2015).
7. http://stroy-technics.ru/article/klassifikatsiya-sredstv-i-sposobov-bezgarazhnogo-khraneniya-avtomobilei

8. http://avtoexperts.ru/article/predpuskovoi-podogrevatel/
9. http://oooksis.ru/Podogrevobzor.htm
10. http://5koleso.ru/articles/Tehnika/Predpuskovie_podogrevateli_dvigatelya
11. V. S. Naiman, *All about Starting Pre-Heaters* (Moscow: ACT, 2007), p. 213.
12. http://auto.potrebitel.ru/data/11/14/p55podogr.shtml
13. O. P. Sitovsky, Study of Automobile Fuel Economy with Cold Engine Start and its Warm-Up during Automobile Motion, *Interuniversity Collected Papers "Naukovi Notatky*" **35**, 166 – 170 (2011).
14. http://www.webasto.com/ua/
15. http://www.eberspaecher.ua
16. http://www.mikuni.co.jp/e/
17. http://www.trumatic.ru
18. http://www.lpg.ru/auto/heating/
19. Yu. I. Bubnov, S. B. Orlov, *Hermetically Sealed Chemical Sources of Current: Cells and Storages, Testing and Operation Equipment, Reference Book* (Saint-Petersburg, KHIMIZDAT, 2005).
20. http://autosiga.ru/gidronik/175-akkumulyator-sovmestnaya-rabota-akkumulyatora-i-predpuskovogo-podogrevatelya
21. *Patent UA № 72304*, InCl: F01N 5/00; H01L35/00. Automobile Heater with Thermoelectric Power Source /L. I. Anatychuk, V. Ya. Mykhailovsky. Publ.10.08.2012, Bul. № 15, Application u2012 02055 of 23.02.2012.
22. *Patent UA for Invention № 102303*, InCl F01N 5/00 H01L 35/00. Thermoelectric Power Source for Automobile / L. I. Anatychuk, V. Ya. Mykhailovsky. Publ. 25.06.2013, Bul. № 12, Application u2011 13957 of 28.11.2011.

Submitted 17.07.2015.

L. I. Anatychuk[1,2], N. V. Pasechnikova[3], O. S. Zadorozhnyi[3], R. R. Kobylianskyi[1,2], M. V. Havrylyuk[1], R. E. Nazaretyan[3], V. V. Mirnenko[3]

[1]Institute of Thermoelectricity of the NAS and MES of Ukraine,
1 Nauky str., Chernivtsi, 58029, Ukraine;
[2]Yu. Fedkovych Chernivtsi National University,
2, Kotsyubinsky str., Chernivtsi, 58012, Ukraine;
[3]State Institution "The Filatov Institute of Eye Diseases and Tissue Therapy
of the National Academy of Medical Sciences of Ukraine",
49/51, Frantsuskiy Boulevard, Odessa, 65061, Ukraine.

THERMOELECTRIC DEVICE FOR MEASUREMENT OF INTRAOCULAR TEMPERATURE

This paper presents the results of development and experimental research on a multi-channel thermoelectric device intended for measurement of intraocular temperature. The operating principle, design and technical characteristics of such device, as well as its advantages over known world analogs are given. The method for the intraocular introduction of thermoelectric measuring probes and the method for measurement of intraocular temperature have been developed in an in vivo experiment. With the aid of the elaborated device the regularities of temperature distribution in different sections of the rabbit eye have been determined in an in vivo experiment.

Key words: thermoelectric device, measuring probe, intraocular temperature, rabbit eye.

Introduction

It is known that physicochemical processes in a sound eye, as well as hemo- and hydrodynamic parameters of the eye are in direct relationship to temperature of intraocular media [1 – 3]. However, the issue of temperature distribution in different sections of the human and animal eye remains to be studied.

There are contact and noncontact methods of measuring eye temperature. Noncontact measurement methods (for instance, infrared thermography) allow recording only the temperature of the outer surface of the eye, the temperature of intraocular media remaining unknown [4]. A number of devices and measuring probes have been developed in the world for recording the temperature of biological tissues and liquids. Some of them have been employed for contact measurement of intraocular temperature [5 – 7]. However, the existing devices and measurement methods have considerable disadvantages. First, the use of measuring probes of high thermal conductivity materials results in appreciable temperature measurement errors. Second, proposed methods of surgical approach produce a considerable impact on the intraocular temperature recorded [8].

Therefore, *the purpose of the paper* is to develop a thermoelectric device for contact measurement of intraocular temperature and to determine in experiment the regularities of temperature distribution in different parts of the rabbit eye.

Thermoelectric temperature measuring device

Thermoelectric device for measurement of intraocular temperature has been developed at the Institute of Thermoelectricity of the NAS and MES of Ukraine in the framework of cooperation agreement with the Filatov Institute of Eye Diseases and Tissue Therapy of the NAMS of Ukraine [9].

The device is intended for measurement of the temperature of biological object tissues and investigation of the dynamic thermal processes occurring in the organs of biological objects.

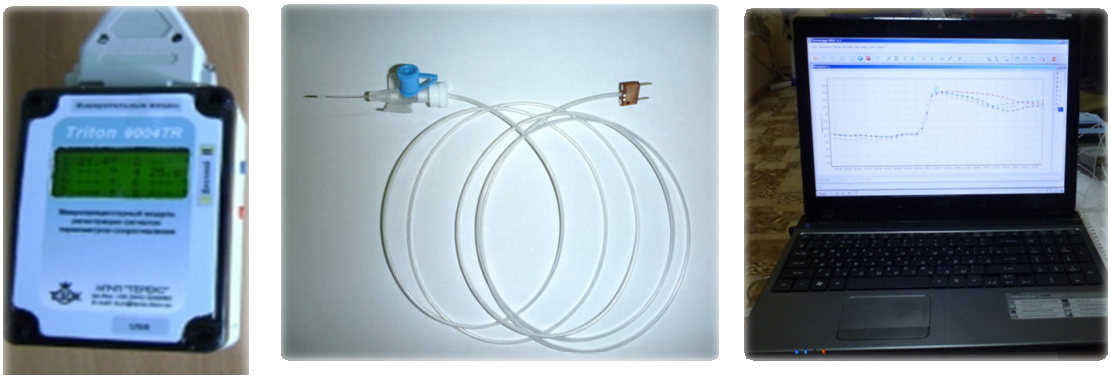

Fig. 1. Outside view of thermoelectric device for measurement of intraocular temperature.

Table 1

Specificationsof thermoelectric device
for measurement of intraocular temperature

№	Technical characteristics	Value
1.	Temperature measurement range	(-10° ÷ +120) °C
2.	Temperature measurement accuracy	± 0.05°C
3.	Number of temperature measurement channels	4
4.	Temperature recording period	from 4 s to 2 h
5.	Dimensions of temperature measuring microprobes	22 G and 24 G
6.	Temperature measurement in real-time mode	+
7.	Time of continuous operation of device from fully charged batteries	100 h
8.	Device power supply: Li-Ion battery 950 mA/h mains adapter AC220V/DC12V, 1A	 + +
9.	Charging of batteries from USB interface	+
10.	Type of interface for data exchange with PC	USB
11.	Geometric dimensions of microprocessor temperature recording module	(125 × 90 × 60) mm
12.	Geometric dimensions of docking device	(70 × 55 × 25) mm
13.	Device weight	0.5 kg

The device consists of a microprocessor temperature recording module, thermocouple measuring microprobes, a docking device, as well as a computer with software for visualization and recording of temperature in real-time mode. By means of USB-cable the results of temperature measurement can be passed to a personal computer. The outside view of the thermoelectric device is given in Fig. 1.

Microprobe temperature sensors are based on *L*-type thermocouples (chromel-copel) [10, 11]. The sensor probe is arranged in a case of standard cannula made of polytetrafluoroethylene. Thermocouple junction is welded to heat concentrator of medical stainless steel and fixed at the end of cannula needle. Thermocouple leads pass from cannula to a cable 1.5 m long and end in a plug. The

cable and cannula joint is sealed with a medical silicon sealant which is chemically neutral and permits thermal or chemical sterilization of device (as a standard medical instrument).

With the aid of a plug through the docking device the microprobe is connected to a microprocessor temperature recording module. The docking module has 4 sockets to which up to 4 microprobes can be connected simultaneously. The docking device of temperature recording module is connected by means of DB-37f connector. Sockets in the docking device are mounted on a copper heat concentrator which also accommodates a precision temperature sensor (platinum resistance thermometer). It is used to measure the temperature of "cold" thermocouple ends – the reference temperature. A diagram of microprobes connection to microprocessor temperature measuring device is shown in Fig. 2.

The plugs of the microprobes and the sockets of the docking device have polarity marks. To reduce the level of crosstalk, the unused inputs of the meter are shorted with pegs – individual plugs with shorted pins.

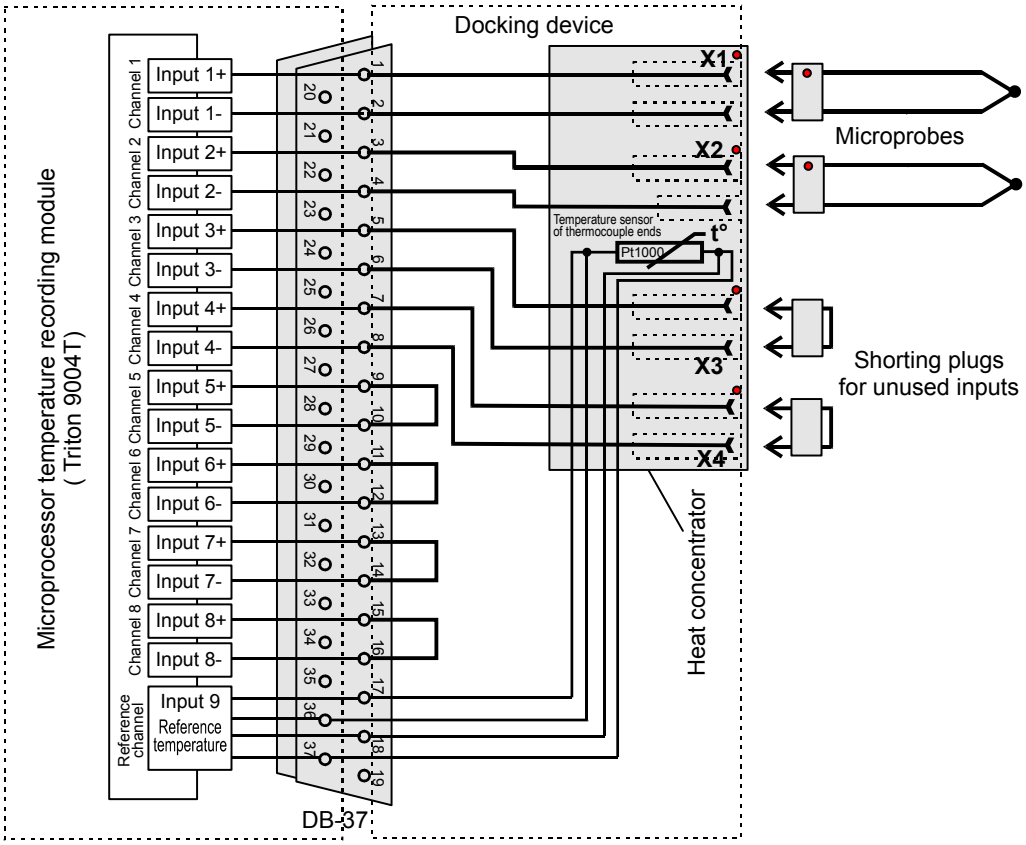

Fig. 2. Diagram of microprobes connection to thermoelectric temperature measurement device.

Microprocessor temperature recording module is based on Triton-9004T device that has an 8-channel 24-digit analog-to-digital converter (ADC). This temperature meter employs the first 4 channels, and the rest of the channels are shorted. If necessary, they can be "unshorted" and used for further measurement with another 4 channels. Maximum input voltage of measuring channel is ± 1.17 V. Temperature recording module is powered from a storage battery, and can also operate on mains adapter or powered from USB-cable with a joint work with computer. This adaptor is used for charging of storage battery. Device battery is also recharged from personal computer.

The specific feature of microprocessor temperature recording module is a possibility to set individually the sensitivity for each channel depending on thermocouple type. The device can measure temperature with the assigned time interval in the range from 4 s to 2 hours. The measured results are recorded in a non-volatile memory. The device memory capacity is 50 thousand cells. Programming of channels of microprocessor recording module and information readout is done by means of a personal computer through USB-cable.

Experiment description

The thermoelectric device for measurement of intraocular temperature was tested in the Filatov Institute of Eye Diseases and Tissue Therapy of the NAMS of Ukraine. Its operating characteristics (temperature recording speed, measured temperature range, measurement error) were studied in an *ex vivo* experiment on 10 isolated pig eyes (Figs. 3). The optimal properties of thermoelectric measuring probes were tried out (Fig. 4), namely material, diameter, length, method of insertion, fixation and temperature recording. To simulate natural thermal effect of choroid, the experiment was carried out under bath water temperature 39 °C.

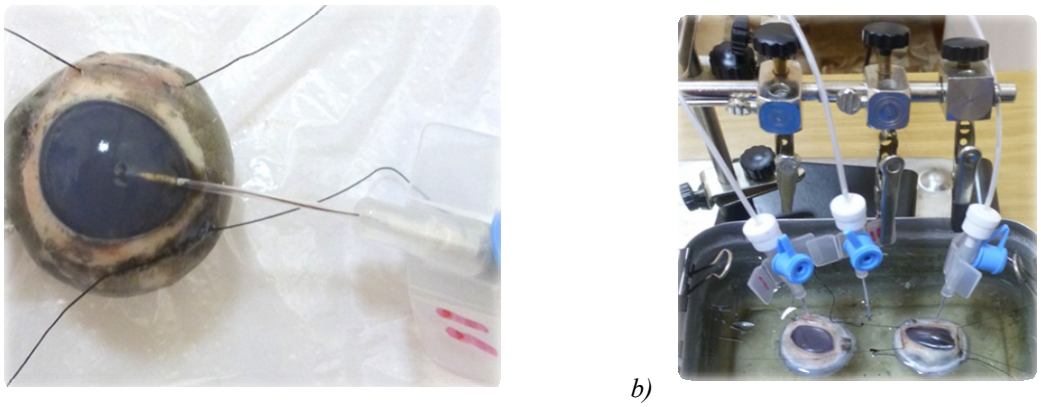

a) *b)*

Fig.3 a, b. An ex vivo experiment on the isolated pig eyes.

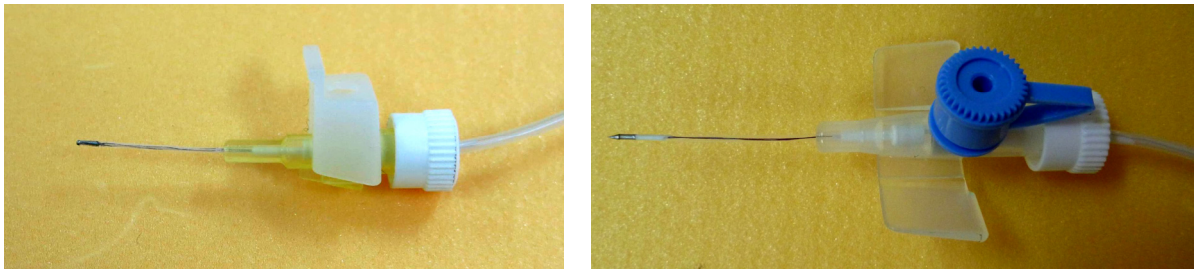

a) *b)*

Fig.4. Thermoelectric measuring probes for contact measurement of eye temperature:
a) gauge 24G (outer diameter of measuring probe needle 0.7 mm, length 19 mm);
b) gauge 22G (outer diameter of measuring probe needle 0.8 mm, length 25 mm).

In an *in vivo* experiment, on 11 chinchilla rabbits (22 eyes) (age 1 year, weight 3.5 - 4 kg) prior to the anesthetic management of the rabbit the outer surface temperature of cornea and conjunctiva was measured (Fig. 5). Cornea temperature was measured by direct contact of probe tip to central part of the outer surface of cornea up to recording of constant temperature data. After that the temperature was recorded with the measuring probe placed into lower conjunctival fornix, and then into upper conjunctival fornix. After the anesthetic management of the rabbit the temperature was measured

again on the outer surface of cornea and in conjunctival fornices, and then, on formation of surgical approach, the temperature was measured in the ocular anterior chamber, in the anterior, medial and posterior sections of vitreous humor, in retina/choroid, in subtenon space. The measuring probe was introduced into the anterior chamber through tunnel paracentesis 0.7 mm. The probe was introduced into vitreous humor through sclerotomy of diameter 0.6 mm in the projection of flat part of ciliary body 2 – 3 mm away from limbus. The probe was introduced into subtenon space through conjunctival incision in the upper internal quadrant. Moreover, measurements were made of the rabbit rectal temperature, the temperature and relative air humidity in the room.

a) *b)* *c)*

Fig.5 a,b,c. An in vivo experiment on chinchilla rabbits.

The work with experimental animals was performed in conformity with the "European Convention for the Protection of Verterbrate Animals" used for research and other scientific purposes (Strasbourg, 1986) and the Law of Ukraine "On Protection of Cruelty to Animals" (2006).

Results of experimental research

In an *ex vivo* experiment it was established that the elaborated device permits temperature measurement in real-time mode (with data display as graphic images) in the range from -10°C to +120°C simultaneously by 4 thermal probes with measurement error up to ± 0.05°C. In so doing, the difference in readings of 4 thermal probes was not more than 0.04°C.

During the first stage, in an *ex vivo* experiment, on the isolated pig eye the method of measuring temperature in the ocular anterior chamber, in the anterior, media and posterior sections of the vitreous humor, retina/choroid, as well as the on the outer surface of cornea by proposed device was adapted for application *in vivo*. The method of intraocular introduction of thermal probes (into anterior chamber, into vitreous humor) on the isolated eye was developed. Then, using the elaborated device, at constant water bath temperature on the average 39 ± 0.5°C and ambient temperature 23.5 ± 0.6°C, the temperature was measured in the sections of the eye. Maximum intraocular temperature was recorded in the posterior section of vitreous humor at contact with retina and made 38.5 ± 0.8°C. With the probe displacement from the posterior to medial section of vitreous humor the temperature was reduced to 38 ± 0.6°C, and with the probe displacement to anterior section of vitreous humor – to 37 ± 0.7°C. The temperature in the anterior chamber proved to be lower that that of the vitreous humor and made 35 ± 0.8°C, which is due to the contact of cornea to the environment, whereas water bath simulates the role of retina, forming and maintaining the constancy of intraocular temperature. Thus, in an *ex vivo* experiment the hypothetic temperature distribution in different sections of the eye was demonstrated.

During the next stage, in an *in vivo* experiment, the method of application of the elaborated device was worked out for measuring temperature of the outer surface of cornea and conjunctiva, in the ocular anterior chamber, in the anterior, medial and posterior sections of the vitreous humor, retina/choroid, as well as in the subtenon space of the rabbit eye. The research was performed at an average ambient temperature 23.8 ± 0.6°C, an average relative air humidity 80.7 ± 1.6 %, and an average rectal temperature of the rabbit 38.73 ± 0.94°C. The temperature of different sections of the eye recorded in the experiment is represented in Table 2.

Table 2

Temperature distribution in different sections of the rabbit eye

Eyball and ocular adnexa section	Average value of *t* *, °C ± SD
lower conjunctival fornix	37.65 ± 0.70
upper conjunctival fornix	36.82 ± 0.66
outer surface of cornea	34.41 ± 0.80
ocular anterior chamber	35.97 ± 0.73
anterior section of vitreous humor	36.96 ± 0.77
medial section of vitreous humor	37.40 ± 0.87
posterior section of vitreous humor	37.50 ± 0.88
retina/choroid	37.64 ± 0.87
subtenon space	37.78 ± 0.77

* *t* – temperature data obtained after the anesthetic management of the rabbit.

So, the *in vivo* experiment has confirmed the existence of temperature gradient between different sections of the eye. Thus, temperature gradient between the outer surface of cornea and ocular anterior chamber has made 1.56°C, between the outer surface of cornea and retina – 3.23°C, between the outer surface of cornea and subtenon space – 3.37°C (Fig. 6).

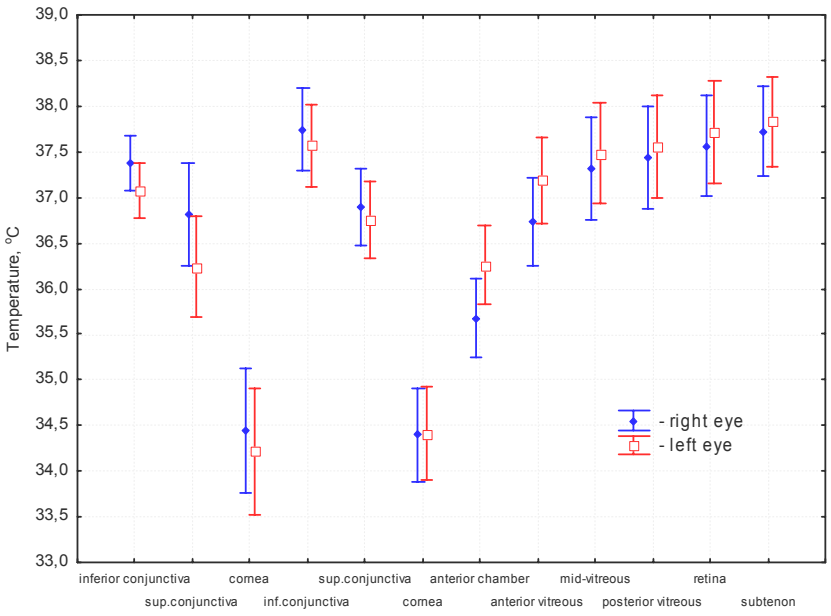

Fig. 6. Temperature in different sections of the rabbit eye.

When analyzing the obtained results it was marked that no essential differences in the temperature of the right and left eyes of experimental animals were revealed. These observations refer both to the outer sections of the rabbit eye where measurements were performed (lower conjunctival fornix, upper conjunctival fornix, outer surface of cornea), and the inner sections of the rabbit eye (anterior chamber, different sections of vitreous humor, retina/choroid, subtenon space). Hence, it can be stated that the temperature in all the sections of the right and left eye of the same experimental animal does not differ essentially. Moreover, these results confirm the reproducibility of temperature measurements performed by the elaborated thermoelectric device.

Further analysis of the obtained results revealed high correlation between the temperature of conjunctival fornices and intraocular temperature in vitreous humor, retina and subtenon space. Thus, high correlation was revealed between the temperature of lower conjunctival fornix and retina temperature ($r = 0.857$, $p = 0.000$), as well as the temperature in subtenon space ($r = 0.86$, $p = 0.000$). Presumably this observation can be explained by the well-defined vascularity of conjunctiva and superficial arrangement of vessels in it. Also, high correlation was revealed between the temperature in the anterior section of vitreous humor and the temperature of retina ($r = 0.92$, $p = 0.000$), as well as between the temperature in the anterior section of vitreous humor and in the subtenon space ($r = 0.88$, $p = 0.000$).

At the same time, it was mentioned that the temperature of the outer surface of cornea less correlates with the intraocular temperatures recorded in the anterior chamber, vitreous humor, retina and subtenon space. Thus, low correlation was observed between the temperature of cornea and that of retina ($r = -0.13$, $p = 0.57$). The obtained results are obviously attributable to the nonvascular structure of eye cornea and a direct contact between the outer surface of cornea and the environment. It is known that the temperature of the outer surface of cornea is very variable and strongly dependent on the ambient temperature, air motion velocity and air humidity.

Based on the obtained experimental results a schematic distribution of temperature in the rabbit eye was constructed (Figs. 7 – 8).

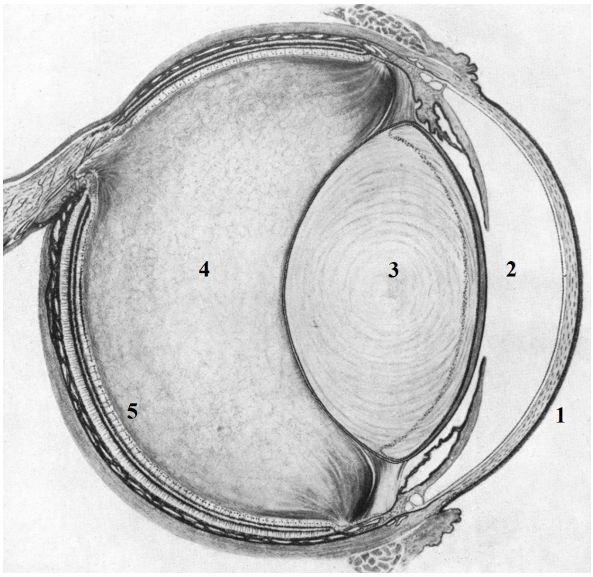

Fig. 7. Schematic of the rabbit eye:
1 – cornea, 2 – anterior chamber, 3 – lens,
4 – vitreous humor, 5 – retina.

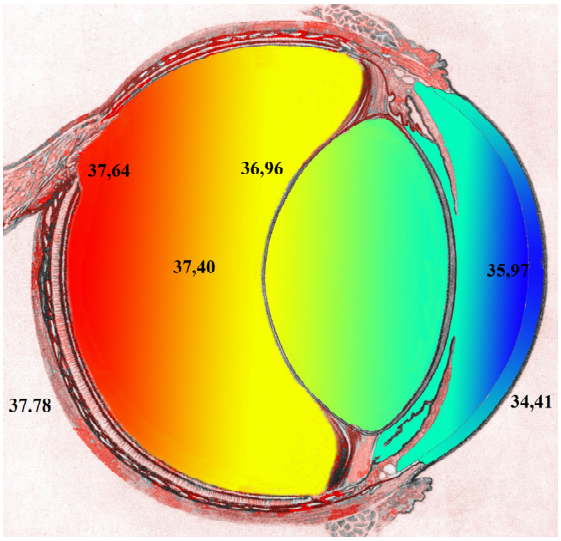

Fig. 8. Schematic of temperature distribution in the rabbit eye.

Discussion

In 1962 B. Schwartz and M. R. Feller published a paper dedicated to measurement of temperature in different eye sections of white New Zealand rabbits. For measuring the intraocular temperatures the authors employed a device based on a thermistor and several modifications of measuring probes. As a probe for recording the intraocular temperatures, a metal needle of length 7.62 cm and diameter 0.7 mm was used. Measurement in different eye sections was performed by gradual introduction of the probe through cornea, lens, vitreous humor and retina into the eye socket. The ambient temperature varied from 22 to 24°C, the relative air humidity was 33 – 53%. After the anesthetic management of seven experimental animals the average rectal temperature was 39.13°C. The work resulted in the following average figures: the temperature of the outer surface of cornea – 32.30 ± 0.49°C, lower conjunctival sac – 38.74 ± 0.54°C, anterior chamber – 32.98 ± 0.74°C, lens – 35.42 ± 1.0°C, medial section of vitreous humor – 36.56 ± 0.9°C, retina/choroid – 37.03 ± 0.86°C, socket – 37.68 ± 0.71°C [7].

In 1983 D. R. May with coauthors determined the effect of perfusion of anterior chamber with irrigating solutions of different temperature on temperature variations in the eye sections of Dutch rabbits. In this work they employed a thermocouple-based thermometer which is a metal probe with a blunt tip of diameter 0.64 mm and length 2.5 cm. Thermometer measurement error was ± 1°C. Air temperature was 25 °C. After the anesthetic management of experimental animals the average rectal temperature was 39.4°C. The authors represented the following average initial temperatures in the eye sections: anterior chamber – 32.5°C, anterior section of vitreous humor – 35.0°C, medial section of vitreous humor – 35.5°C, posterior section of vitreous humor – 36.6°C, retina – 36.8°C [5].

It should be noted that in these works use was made of high thermal conductivity metal probes. Moreover, in the work by D. R. May with co-authors, prior to temperature measurement, for irrigation/aspiration processes of the anterior chamber two punctures of the cornea were made with metal needles of diameter 0.7 and 0.8 mm, and then one of the punctures was widened with metal scissors up to 3 mm. From the experimental data (in vitro) and theoretical studies performed by I. Fatt

and J. F. Forester in 1972 it is known that the temperatures of eye tissues recorded by metal probes can prove to be several degrees lower than the temperatures recorded by low thermal conductivity probes [8].

In our work, the temperature recorded in the ocular anterior chamber was 35.97°C and proved to be higher as compared to the data published before (32.5°C in the work by D. R. May and 33°C in the work by B. Schwartz) by about 3 – 3.5°C. Essential differences in temperatures recorded in ocular anterior chamber apparently are related to a small volume of humidity in the rabbit's ocular anterior chamber which is as low as 0.25-0.3 ml, as well as to a direct contact of the cornea to the environment. Therefore, introduction into anterior chamber of metal instrument at formation of surgical approach and metal measuring probe results in essential heat loss and recording of lower temperatures. In our work, measuring probe was made of low thermal conductivity polytetafluoroethylene, and a minimum surgical approach which is only necessary for the introduction of thermal probe was formed, which resulted in heat loss reduction at the moment of temperature measurement and recording of higher figures.

Heat loss is less appreciable when measuring temperature in vitreous humor, since its volume for the rabbit is 1 – 1.5 ml and there is no direct contact of vitreous humor to the environment. The temperature in the medial section of vitreous humor in our study was 37.4°C and was less different from the data reported by the above authors (35.5 and 36.56°C).

Therefore, the recorded intraocular temperatures are largely affected by the scope of surgical intervention at formation of access to different eye sections and by the application of surgical instruments made of high thermal conductivity materials. Moreover, considerable effect on the recorded data is produced by the material of probe for measurement of intraocular temperatures.

Conclusions

1. For the first time, a multi-channel thermoelectric device with computer software has been developed for recording and visualization of intraocular temperature, allowing high-precision measurements in real-time mode (in the temperature range of -10°C ÷ +120°C with measurement error ± 0.05°C).
2. For the first time, a thermoelectric measuring probe based on L-type thermocouples has been developed and manufactured in a case of standard cannula made of low thermal conductivity polytetrafluoroethylene, which allowed increasing the accuracy of measuring intraocular temperature through reduction of heat loss through the probe.
3. A method has been developed for measuring temperature of the outer surface of cornea and conjunctiva, in the anterior chamber, in the anterior, medial and posterior sections of vitreous humor, retina/choroid, in the subtenon space of the rabbit eye in an *in vivo* experiment.
4. Using the elaborated thermoelectric device, in an *in vivo* experiment the regularities of temperature distribution in different sections of the rabbit eye have been determined (lower conjunctival fornix – 37.65°C; upper conjunctival fornix – 36.82°C; cornea surface – 34.41°C; ocular anterior chamber – 35.97°C; anterior section of vitreous humor – 36.96°C; medial section of vitreous humor – 37.40°C; posterior section of vitreous humor – 37.50°C; retina/choroid – 37.64°C; subtenon space – 37.78°C at the ambient temperature 23.8°C). In an *in vivo* experiment high correlation has been revealed between the temperature of lower conjunctival fornix and retina temperature, as well as the temperature in the subtenon space of the rabbit eye.

References

1. B. Becker, Hypothermia and Aqueous Humor Dynamics of the Rabbit Eye, *Trans. Am. Ophthalmol. Soc.* **58**, 337 – 363 (1960).

2. V. I. Lazarenko, G.F.Chanchikov, I.M.Kornilovskii, and V.G.Gaidabura, Effect of Moderate Local Hypothermia on Hemo- and Hydrodynamic Indices of Sound Eyes, *Ophthalmological Journal* **6**, 419 – 422 (1976).
3. V. I. Lazarenko, S.V.Petrova, I.M.Kornilovskii, and V.G.Gaidabura, Effect of Local Hypothermia on Carbohydrate Metabolism of Sound Eye in Experiment, *Ophthalmological Journal* 3, 227 – 230 (1977).
4. C. Purslow, J. Wolffsohn, Ocular Surface Temperature: a Review, *Eye and Contact Lens* **31**, 117 – 123 (2005).
5. D. R. May, R. J. Freedland, Ocular Hypothermia: Anterior Chamber Perfusion, *British Journal of Ophthalmology* **67**, 808 – 813 (1983).
6. J. M. Katsimpris, T. Xirou, K. Paraskevopoulos, I. K. Petropoulos, and E. Feretis, Effect of Local Hypothermia on the Anterior Chamber and Vitreous Cavity Temperature: in vivo Study in Rabbits, *Klin. Monbl. Augenheilkd*. **220**(3), 148 – 151 (2003).
7. B. Schwartz, M. R. Feller, Temperature Gradients in the Rabbit Eye, *Investigative Ophthalmology* **1**(4), 513 – 521 (1962).
8. I. Fatt, J. F. Forester, Errors in Eye Tissue Temperature Measurements when Using a Metallic Probe, *Exp. Eye Res*. **14**, 270 – 276 (1972).
9. L. I. Anatychuk, N. V. Pasechnikova, O. S. Zadorozhnyi, R. R. Kobylyanskii, N. V. Havrylyuk, R. E. Nazaretyan, and V. V. Mirnenko, Use of Thermoelectric Device for Studying Temperature Distribution in Different Parts of the Rabbit Eye, *Proceedings of research and practical conference with international engagement "The Filatov Readings 2015" dedicated to 140 anniversary of V.P.Filatov (May 21 – 22, 2015) (Odessa, Ukraine, 2015), p.188.*
10. L. I. Anatychuk, *Thermoelements and Thermoelectric Devices. Reference Book* (Kyiv:Naukova Dumka, 1979), 768 p.
11. L. I. Anatychuk, *Thermoelectricity. Thermoelectric Power Converters. Vol.II* (Kyiv, Chernivtsi: Institute of Thermoelectricity, 2003), 376 p.

Submitted 05.07.2015.

S. O. Filin, B. Jasinska

S. O. Filin

West Pomeranian University of Technology,
Aleja Piastów 17, Szczecin, 70310, Poland

B. Jasinska

ECONOMICAL TRANSPORT THERMOELECTRIC REFRIGERATORS WITH TWO-LEVEL TEMPERATURE CONTROL: THE EXPERIENCE OF CREATION AND TEST RESULTS

The article describes the experience of creating Transport Thermoelectric Refrigerators (TTER) on the basis of household cabinets of thermoelectric refrigerators by Ravanson Company with a useful volume of 48 liters. Also the results of comparative tests of the basic model and the two new TTER samples with different types of thermoelectric modules are presented. Using two-level temperature control has significantly improved the energy performance of refrigerators, which enables their long-term operation with the power supply from the vehicle's battery without the risk of rapid discharge.

Key words: thermoelectric refrigerator, temperature control, electrical power, energy saving.

Introduction

The main and global objective of technical progress in the early XXI century, beyond question, is energy efficiency increase. The reduction of energy consumption of thermoelectric refrigerators is not only in this tideway, but also is prerequisite for competitive ability of thermoelectric products in the world market, primarily with respect to compressor analogs.

At Department of Air Conditioning and Refrigerated Transport of West Pomeranian University of Technology in Szczecin, investigations of mostly experimental nature have been pursued for more than 15 years with the aim of improving the energy parameters of various-purpose thermoelectric refrigerators. The above improvement is a consequence of selected approach to design of stationary thermoelectric coolers and displays, namely optimization of refrigeration unit design and its power supply circuit, combined with a respective method of temperature control in the refrigerator chamber. New samples of refrigerators offer not only lower power requirement, but also reduced daily energy consumption due to maximum increase of operation time in energy-saving mode. The results of these efforts are regularly published in the "Journal of Thermoelectricity". Several monographs in Polish and Russian have appeared. Within recent two years, investigations have been pursued with a view to apply the above approach to transport refrigerators powered from direct current mains 12 V. Preliminary results of these works were reported to XV International Forum on Thermoelectricity [1]. The work phase represented in this paper was performed in the framework of a project of "Inkubator innowacyjnosci" program, which is supported by Ministry of Science and Higher Education of Poland and aimed at promoting new technologies [2].

Purpose, objects and methods of investigation

The purpose of the project was to create and test new designs of low-cost transport

thermoelectric refrigerators (hereinafter – TTER) powered from direct current mains 12 V or from a battery using the principle of two-level temperature control. This idea has been earlier tested on stationary thermoelectric refrigerators and displays with chamber volume from 40 to 100 liters and power supply from alternating current mains 230 V. Transport refrigerators of such volume find application on yachts, in railway cars, tourist buses, mobile homes and truck trailers, auto shops, mobile coffee houses and in summer cottages. In the absence of external electrical grid or diesel-generator, continuous operation of refrigerator from a battery can result in its discharging. Therefore, a reduction of TTER power requirement at least by several watts is of principal significance.

Since the above TTER are only custom-built, and the budget of and terms of the project were very limited, it was decided to take as the basic model a retail household thermoelectric refrigerator Ravanson LK-48 with chamber volume 48 liters. Its technical specifications are represented in Table 1. Four refrigerators were purchased, of which two were intended for comparative tests and the other two – for adaptation to transport version. When creating two samples of new products, from the basic model only thermally insulated cabinets were used where new units were placed according to principal diagrams described in [1]. The models of new refrigerators with abbreviation ChTT-48 were different only in the type of thermoelectric modules used: MT2-2.5-127 (ChTT-48-1) and MT2-2.0-127 (ChTT-48-2). The general view of the refrigerators is represented in Fig. 1.

Table 1

Technical specifications of thermoelectric refrigerator Ravanson LK-48
(according to manufacturing data)

Parameters	Measuring unit	Value
1. Temperature range in the chamber	ºC	5…12
2. Total chamber volume	dm^3	48
3. Supply voltage	V	~230
4. Current frequency	Hz	50
5. Overall dimensions (width, depth, height)	mm	480 × 460 × 840
6. Power consumption (at t_{amb} = 32ºC)	W	70
7. Weight	kg	11.6
8. Daily energy consumption	kW h/24h	0.8*

* – manufacturer does not indicate the conditions when this parameter was measured.

Fig. 1. Refrigerators ChTT-48 in the process of laboratory test.

The research program provides for comparative testing of new samples and basic model, as well as individual testing of new samples at different ambient temperatures and thermostat settings. Apart from he tests performed in department laboratory, part of them were performed in COCH certified Refrigeration Centre in Krakow, in particular, tests at ambient temperature t_{amb} = 32ºC and tests with a loaded chamber. The main measured values were the energy and dynamic characteristics, such as: chamber temperature, power requirement, daily energy consumption, time and conditions of transition into energy-saving mode.

A correct comparison of parameters of refrigerators with different supply voltage, kind of current and different temperature control principle was assured by the following techniques:

- according to the results of preliminary tests, the electrical efficiency of power supply LK-48 and its dependence on temperature and voltage on the module was determined, which made it possible to a sufficient degree of precision to recalculate the refrigerator power requirement from ~230V supply mains to = 12 V;

- with regard to the differences in temperatures in the chamber of compared models, use was made of practically approved parameter of specific power consumption, proposed in [3].

An experimental bench described in [1] was modernized, in particular, supplemented with a battery of HZY-EV12-100 type and electronic meters of direct current power consumption FRER C15UCL with the division value 1 Wh. The meter C15UCL (Fig. 2) also makes possible recording of current strength, power consumption actual values and a number of other parameters, computer data recording. Using of this rather rare and precise instrument makes it possible to detect even a small difference in the energy consumption of objects with power requirement 10...20 W without the need for performing many days, and even many weeks of testing.

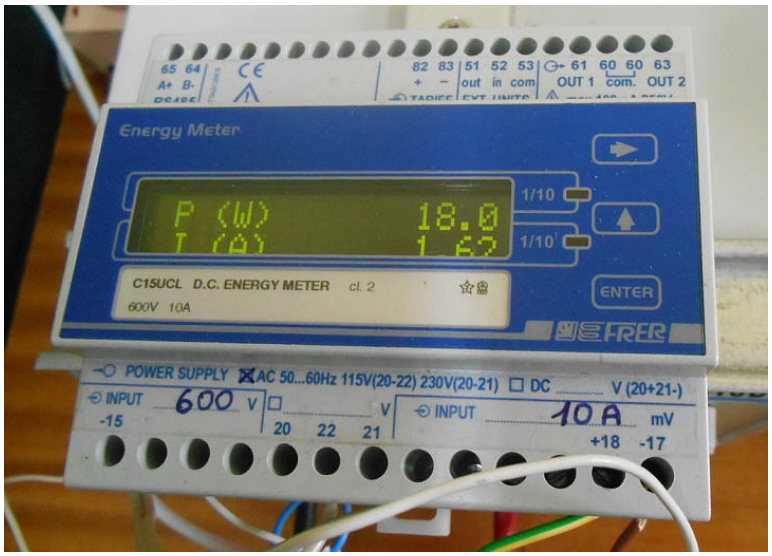

Fig. 2. Direct current energy parameters meter FRER C15UCL.

Results of testing refrigerator LK-48

Analysis of design and operating principle of refrigerator LK-48 was performed by "reverse engineering" method. Restoration of refrigerator electric circuit diagram according to its wiring diagram has shown that the refrigerator employs not a manometric, but electronic temperature controller wherein temperatures sensor (thermal resistor) is switched into a bridge leg. Temperature controller is the inseparable part of supply circuit with a high-frequency voltage converter, pulse-width modulation and feedback. In other words, proportional temperature control was used as the most

efficient method known [1]. Though, in principle, one can also use proportional regulation at refrigerator supply from direct current mains, nevertheless technical decisions used in LK-48 do not provide this opportunity.

When testing LK-48, measurements were performed of the electrical parameters both in alternating current and direct current circuits (in thermoelectric module circuit), as well as of energy parameters. Tables 2 and 3 represent extracts from testing protocols of this refrigerator at the ambient temperature 23ºC for two thermostat settings "4" (middle) and "1" (min)[1]. Parameters at the moment beginning transition to energy-saving mode are shown against the grey background.

Table 2

Results of testing thermoelectric refrigerator Ravanson LK-48
with empty chamber at ambient temperature 23ºC and thermostat setting "4"

Time		Alternating current	Direct current			Temperatures	
absolute [h:min]	relative [min]	Power requirement *P*, [~W]	*V*, [V]	*A*, [A]	*P*, [=W]	Average in chamber, [ºC]	of hot heat sink, [ºC]
11:50	0	75.9	12.0	5.,20	62.4 (65.4)	21.5	21.5
12:05	15	64.4	12.0	4.38	52.6	16.1	40.0
12:20	30	64.3	12.0	4.37	52.4	12.8	39.8
13:20	90	64.1	12.0	4.37	52.4	7.0	38.8
13:37	107	64.0	12.0	4.37	52.4	6.5	38.7
13:40	110	63.9	11.9	4.36	51.9 (54.9)	6.4	38.7
13:55	125	61.6	11.6	4.27	49.5	6.0	38.6
14:10	140	56.8	10.9	4.10	44.8	5.7	37.8
15:03	193	51.7	10.4	3.89	40.4	5.7	36.8
16:00	250	51.7	10.5	3.89	40.8	5.7	37.0
16:05	255	51.8	10.5	3.90	40.9 (43.4)	5.7	37.1

Table 3

Results of testing thermoelectric refrigerator Ravanson LK-48
with empty chamber at ambient temperature 23ºC and thermostat setting "1"

Time		Alternating current	Direct current			Temperature	
absolute [h:min]	Relative [min]	Power consumption *P*, [~W]	*V*, [V]	*A*, [A]	*P*, [=W]	Average in chamber, [ºC]	Hot heat sink, [ºC]
14:05	0	78.9	12.0	5;12	61.4 (64.4)	22.0	23.2
14:20	15	63.9	12.0	4.36	52.3	16.3	40.4
14:35	30	63.6	12.0	4.35	52.2	12.8	40.2
14:45	40	63.6	12.0	4.35	52.2	11.1	39.5
14:49	44	62.8	11.9	4.33	51.5 (54.5)	10.7	39.5
15:00	55	48.7	10.1	3.76	38.0	9.5	37.0
15:20	75	28.8	7.5	2.75	20.6	9.1	33,6
15:40	95	23.5	6.6	2.40	15.8	9.3	32.4
16:18	133	25.4	6.9	2.53	17.4 (19.1)	9.5	33.0

[1] Setting scale of refrigerator thermostats, irrespective of their operating principle, is from "1", which corresponds to maximum, i.e. higher temperature in the chamber, to "7", which, in turn, corresponds to minimum temperature. Accordingly, setting "4" is middle. It is generally recommended by the manufacturer of refrigerators for everyday use.

At the ambient temperature of 23ºC and thermostat setting "4", a transition to energy-saving operation mode starts in 110 minutes after switching (Table 1), when the temperature in the chamber falls to 6.4ºC and lasts nearly 1.5 hours. The transition lies in a smooth reduction of module supply voltage with the respective reduction of current and power consumption. During this time the temperature in the chamber falls to 5.7ºC and is stabilized at this level, and the power consumed from the rid is reduced from 63.9 to 51.8 W. With regard to energy consumption of the fans (the values in brackets in *P* [=W]) column, and taking into account that their supply voltage is synchronized with modules supply voltage, a reduction of power consumption in direct current circuit 12 V is, respectively, from 54.9 to 43.4 W.

At the same ambient temperature and thermostat setting "1", a transition to energy-saving operating mode starts 44 minutes after switching, when the temperature in the chamber falls to 10.7ºC, and lasts nearly an hour. During this time the temperature in the chamber is reduced to 9.3..9.5ºC and is stabilized at this level, whereas power consumption from the grid is reduced from 62.8 to 25.4 W. Accordingly, reduction of power consumption in direct current circuit is from 12 V is from 54.5 to 19.1 W.

At thermostat setting "4", transition to energy-saving mode is observed at ambient temperature not above 24ºC, and at thermostat setting "1" – not above 28ºC. In so doing, the refrigerator energy consumption should be determined in conformity with standard EN ISO 8561:1995 + A1:1997 at ambient temperature 25ºC and mean thermostat setting, i.e. in position '"4". It means that under these conditions refrigerator LK-48 does not pass into energy-saving mode. The tests have shown that its power requirement (on conversion to direct current) is in this case 53.16 W, and daily energy consumption, accordingly, made 1.276 kWh. The value 0.8 kWh indicated by the manufacturer in passport specifications of the refrigerator refers to setting "1". We have more than once mentioned in our previous publications that concealment of conditions of determination of such important parameter as daily energy consumption can disorient the buyer concerning its economical operation.

Some results of comparative tests and their analysis

Apart from structural differences, the basic difference of a new transport refrigerator ChTT-48 from known analogs with temperature controller is that its energy consumption and temperature in the chamber in energy-saving mode depend only on ambient temperature and do not depend on thermostat setting. Thermostat setting has impact only on the refrigerator's dynamic characteristics. The time from switching to transition to energy-saving mode can vary from 15 minutes at setting "1", i.e. for maximum temperature in the chamber, to 1...2 hours at settings "4"– "7". Time of temperature stabilization in the chamber on switching to energy-saving mode, on the contrary, will be less at thermostat setting for lower temperatures. On the whole, a new refrigerator has much better dynamic characteristics than the counterpart LK-48, especially with regard to the fact that transition to energy-saving mode and back occurs immediately. This peculiarity also has a positive effect on the daily energy consumption.

In the process of testing, the modules ChTT-48 were powered from a direct current source D3010 which provides for two operating modes: voltage stabilization and current regulation (restriction). On switching of refrigerator ChTT-48-1, power source for 15...30 seconds worked in current restriction mode, following which it automatically passed to 12.0 V voltage stabilization mode. When testing the model ChTT-48-2, the source remained in current restriction mode up to transition to energy-saving mode, and supply voltage in operating mode was 10.5... 10.6 V.

Table 4

Some results of comparative test of refrigerators LK-48 and ChTT-48
with empty chamber at ambient temperature 23ºC and thermostat setting "4"

Parameters	LK-48	ChTT-48-1	ChTT-48-2
Maximal created temperature difference, K	17.8	19.8	22.0
Temperature difference created in energy-saving mode, K		14.5	14.9
- setting "4"	17.3		
- setting "1"	13.9		
Power requirement, W			
- in working mode	64.1 (53.16*)	61.0	50.0 (73.0**)
- in energy-saving mode		16.0	19.0
setting "4"	52.1 (41.0*)		
setting "1"	25.4 (19.1*)		
Parameter of specific power requirement P_{spec} for energy-saving mode, W/dm^{3}K			
- setting "4"		0.023	0.0266
- setting "1"	0.063 (0.049*)		
	0.038 (0.029*)		

* – on conversion to power supply from direct current circuit 12 V.

** – for battery power supply.

As is seen from Table 4, new refrigerator models, especially ChTT-48-1, which employs lower-power modules, outperforms in the energy parameters the counterpart, even with a conventional conversion of its characteristics to power supply from direct current circuit. In this model, a parameter of power requirement 16 W is achieved, which is more than 3 W less than the respective parameter LK-48 in the most economy mode of its operation. In practice, besides energy saving it may mean increased rime of refrigerator operation from the battery without recharging from several hours to several days as a function of operating conditions.

It is true that foe the improvement of energy figures one had to "pay" with a slight (2 K on the average) average temperature increase in the chamber in energy-saving mode, but, on the other hand, new models offer a higher refrigerating capacity and larger maximum temperature difference created in operating mode.

Conclusion

The paper presents certain most important results. The tests of refrigerators are underway. On their completion and processing of the results, full data will be published. However, even at this stage one can assert that the adopted technical decisions gave the expected results. The major of them is confirmation of feasibility and efficiency of a two-level temperature control in TTER by switching cooling unit feed from a parallel to series circuit and back.

Apart from improving the energy parameters, the operating temperature range of thermoelectric refrigerators has been expanded by about 2 – 3ºC, making possible a transition to

energy-saving operation mode. This data needs verification and refinement, which is to be done in the nearest future.

Patent applications have been filed to the Polish and European patent agencies for technical decisions used in TTER [4, 5].

Fig. 3. Presentation of ChTT-48 refrigerator at EuroGastro Exhibition 2015 in Warsaw.

One of the models ChTT-48 in March 2015 was exhibited at EuroGastro exhibition in Warsaw (Fig. 3) where it aroused great interest of potentail end buyers.

References

1. S. Filin, B. Jasińska, Experimental Investigations of Two-Level Temperature Controllers for Transport Thermoelectric Refrigerators, *J.Thermoelectricity* **5**, 43 – 53 (2013).
2. Raport na Temat Transportowej Chłodziarki Termoelektrycznej. Inwestycje w Innowacje. 2014, www.inwestycjewinnowacje.pl.
3. S. O. Filin, A. Owsicki, and B. Zakrzewski, *Experimental Investigation of Stationary Thermoelectric Refrigerators* (Odessa, Astroprint, 2011).
4. S. Filin, B. Jasińska, B. Zakrzewski, M. Chmielowski, Sposób Redukcji Zużycia Energii przez Chłodziarkę Termoelektryczną i Chłodziarka Termoelektryczna. *Zgłoszenie patentowe nr P.408768 z dnia 07.07.2014.*
5. S. Filin, B. Jasińska, B. Zakrzewski, and M. Chmielowski, The Method of Reducing an Energy Consumption of Thermoelectric Refrigerator and Thermoelectric Refrigerator. *European patent. Application number EP14461596.0, 12 December 2014*.

Submitted 15.06.2015.

T. A. Ismailov, Z. A. Khulamagomedova

T. A. Ismailov

State Budgetary Educational Institution of Higher Professional Education "Dagestan State Technical University", 70, Imam Shamil avenue, Makhachkala, 367015, Russia

Z. A. Khulamagomedova

NEONATAL INTENSIVE CARE COMPLEX BASED ON THERMOELECTRIC POWER CONVERTERS

This paper is concerned with a calculation of temperature mode of thermoelectric neonatal complex. The fundamental design ratios based on differential equations describing convective heat exchange in the system are given. The results of a numerical experiment in the form of temperature variation at different complex points and with time as a function of cooling capacity and heat productivity of thermopiles are presented.

Key words: thermoelectric complex, neonatology, thermopile, thermal conductivity, heat exchange.

Introduction

For treatment of premature newborns of great significance are optimal temperature conditions, since a baby with a low birth weight has an ill-defined subcutaneous tissue with respect to large skin area and minimal energy reserves. This factor is primary not only for survival, but also for further adequate development of newborns with pathology.

Maintenance of optimal temperature ambient conditions during the first days of baby's life is one of the primary factors not only for survival, but also for further adequate development of newborns with pathology, owing to which the immature baby's organism can resist the aggressive effect of other environmental factors. Such a newborn has a limited potential of thermoregulation. This is due to a relatively larger surface of skin cover as compared to body mass, which results in considerable loss of heat by a premature newborn. Insufficient development of a subcutaneous layer, combined with a marked vascular bed, contributes to intense heat exchange. Such children are easily cooled, and excessive external heating quickly leads to overheating, which creates difficulties for medical staff in nursing process.

For the efficient restoration of vital functions of newborns, special neonatal resuscitation complexes are used nowadays, providing for the opportunity of accurate maintenance and control of microclimate, namely temperature, humidity, pressure, etc. [1].

For the initial control of ambient air temperature in the incubator depending on the body weight and age, it is necessary to meet the accepted medical requirements given in Table 1 [2].

Among the developers and producers of such complexes one can single out companies DRAEGERMEDICAL (Germany), TAXAT (Belarus), AIR-SHIELDS (USA), FANFM (Brazil), Axion-Holding (Russia), Closed JSC SPE Medintekh-M (Russia), et al. [3, 4, 5]. In Russia, investigations in this field are pursued in D. O. Ott Research Institute of Obstetrics and Gynecology (Saint-Petersburg), Ivanovo Research Institute of Maternity and Childhood, Research Institute of

Pediatrics and Human Reproduction (Irkutsk), I. M. Sechenov Moscow Medical Academy, Moscow Regional Research Institute of Obstetrics and Gynecology, et al. The main emphasis in the development and research in this field is made on the use as thermoregulation systems of units based on vapor compression, absorption, air and liquid methods. The use of thermoelectric power converters as a means of microclimate control in resuscitation chamber is impractical because of low reliability characteristics of low-current thermopiles. However, if the above disadvantage is removed, the use of thermoelectric power converters for temperature control inside a resuscitation incubator will be efficient in view of their absolute ecological safety, ease of transition from cooling to heating mode, and vice versa, fire safety, noise-free operation, and long service life.

Table 1

Age and body weight	**Temperature**	**Age and body weight**	**Temperature**
C – 6 *hours*		24 – 36 *hours*	
less than 1200 g	34.0 – 35.4	less than 1200 g	34.0 – 35.0
1200 – 1500 g	33.9 – 34.4	1200-1500 g	33.1 – 34.2
1501 – 2500 g	32.8 – 33.8	1501-2500 g	31.6 – 33.6
2500 (36 weeks)	32.0-33.8	2500 (36 weeks)	30.7 – 30.5
6 – 12 *hours*		36 – 48 *hours*	
less than 1200 g	34.0 – 35.4	less than 1200 g	34.0 – 35.0
1200 – 1500 g	33.5 – 34.4	1200 – 1500 g	33.0 – 34.1
1501 – 2500 g	32.2 – 33.8	1501 – 2500 g	31.4 – 33.5
2500 (36 weeks)	31.4 – 33.8	2500 (36 weeks)	30.5 – 33.3
12 – 24 *hours*		48 – 72 *hours*	
less than 1200 g	34.0 – 35.4	less than 1200 g	34.0 – 35.0
1200 – 1500 g	33.3 – 34.2	1200 – 1500 g	33.0 – 34.0
1501 – 2500 g	31.8 – 33.8	1501 – 2500 g	31.2 – 33.4
2500 (< 36 weeks)	31.0 – 33.7	2500 (36 weeks)	30.1 – 33.2

The purpose of this work is design study of neonatal resuscitation system based on thermopiles characterized by rather high supply currents [6].

Description of system design

The system design is shown in Fig. 1, and its external view – in Fig. 2.

Neonatal intensive care complex comprises a mobile table 1 with incubator 2 with double walls, upper flap lid 3 and lateral sliding lid 4. On the bottom of the incubator 2 there is a gel mattress for preventing pressure sores 5 of high thermal conductivity materials whose cells 6 are filled with gel 7 with high thermal conductivity coefficient. Each of the cells 6 of the gel mattress 5 is in thermal contact with the hot junctions 8 of thermopile 9, whose second junctions 10 are connected with a single air heat exchanger 11. The thermopile is divided into sections that can be connected in series according to signals from temperature sensors located at different points of the mattress. Inside the incubator there is a head hypothermic device 12 shaped as a cylinder glass 13 with a spherical inner cavity 14 and gel layer 15, which is in contact with the hot junctions 16 of thermoelectric module 17, the second junctions of which are in contact with liquid heat exchanger 18. Thermoregulation of a newborn body is done by means of temperature sensors 19 connected to control unit 20 and located on the surface of mattress 5 and in gel layer 15 of head hypothermic device 12.

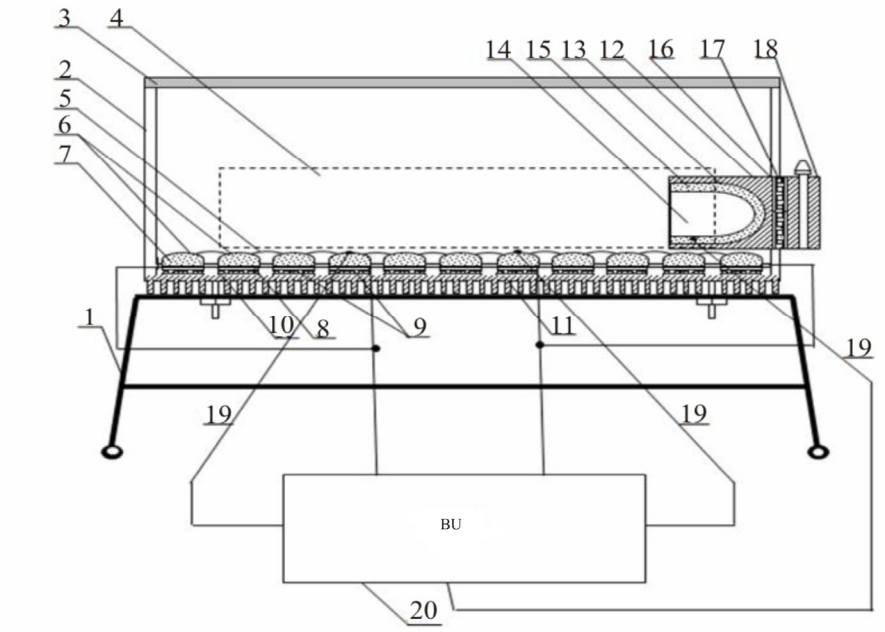

Fig. 1. Structural schematic of a system for the intensive therapy of newborns.

The operating principle of proposed device is as follows. A newborn patient is placed in the incubator 2, and his head in case of need is placed into a spherical inner cavity 14 of head hypothermic device 12. Special sensors are mounted for temperature control of newborn body, following which power supply to thermopile 9 and thermoelectric module 17 is switched.

Fig. 2. External view of neonatal intensive care complex.

Depending on the selected method, the necessary level of thermal effect is set on control unit 20. A change in supply current of thermopile 9 and thermoelectric module 17, as well as a series connection of sections of thermopile 9 will allow a smooth temperature control of a gel mattress for preventing pressure sores 5, and supply current reversal will permit to pass from cooling to heating mode. Simultaneously, heat pickup is done from the second junctions of thermopile 9 and thermoelectric module 7 by means of heat exchangers 11 and 18.

Simulation results

A generalized thermal scheme of neonatal complex comprises a chamber filled with air and a special bed for the newborn. A thermopile with cooling capacity q_{TEB} is brought into a good thermal contact with the lateral surface. Heat pickup from the hot thermopile junctions can be done by means of fan-blown air heat exchangers, as well as by means of liquid cooling. The lower surface of the neonatal resuscitation complex chamber exchanges heat with the environment with heat exchange coefficient α_{amb}.

Mathematical formulation of the problem of temperature field calculation for such system is given by [7]:

at $x, y, z \in D_1$

$$\rho_1 C_1 \frac{\partial T_1}{\partial t} = \lambda_1 \left(\frac{\partial^2 T_1}{\partial x^2} + \frac{\partial^2 T_2}{\partial y^2} + \frac{\partial^2 T_3}{\partial z^2} \right) + Q_{ext}, \tag{1}$$

at $x, y, z \in D_2$

$$\rho_2 C_2 \frac{\partial T_2}{\partial z} = \lambda_2 \left(\frac{\partial^2 T_2}{\partial x^2} + \frac{\partial^2 T_2}{\partial y^2} + \frac{\partial^2 T_3}{\partial z^2} \right),$$

at $x, y, z \in D_3$

$$C_3 \rho_3 \left(\frac{\partial T_3}{\partial t} + \omega_x \frac{\partial T_3}{\partial x} + \omega_y \frac{\partial T_3}{\partial y} + \omega_z \frac{\partial T_3}{\partial z} \right) = \lambda_3 \left(\frac{\partial^2 T_3}{\partial x^2} + \frac{\partial^2 T_3}{\partial y^2} + \frac{\partial^2 T_3}{\partial z^2} \right),$$

$$\frac{\partial \omega_x}{\partial x} + \frac{\partial \omega_y}{\partial y} + \frac{\partial \omega_z}{\partial z} = 0,$$

$$\rho_3 \left(\frac{\partial}{\partial \tau} + \omega_x \frac{\partial}{\partial} + \omega_y \frac{\partial}{\partial} + \omega_z \frac{\partial}{\partial} \right) \omega_y =$$

$$= -\frac{\partial P}{\partial y} + \frac{\partial}{\partial x} \left[\mu_3 \left(\frac{\partial \omega_y}{x} + \frac{\partial \omega_x}{y} \right) \right] + 2 \frac{\partial}{\partial y} \left(\mu_3 \frac{\partial \omega_y}{\partial y} \right) + \frac{\partial}{\partial z} \left[\mu_3 \left(\frac{\partial \omega_y}{\partial z} + \frac{\partial \omega_z}{\partial y} \right) \right] - \frac{2}{3} \times$$

$$\times \frac{\partial}{\partial y (\mu_3 div \varpi)} - g_y \times \rho_3$$

$$\rho_3 \left(\frac{\partial}{\partial \tau} + \omega_x \frac{\partial}{\partial} + \omega_y \frac{\partial}{\partial} + \omega_z \frac{\partial}{\partial} \right) \omega_y =$$

$$= -\frac{\partial P}{\partial z} + \frac{\partial}{\partial x} \left[\mu_3 \left(\frac{\partial \omega_z}{\partial x} + \frac{\partial \omega_x}{\partial z} \right) \right] + \frac{\partial}{\partial y} \left[\mu_3 \left(\frac{\partial \omega_z}{\partial y} + \frac{\partial \omega_y}{\partial z} \right) \right] + 2 \frac{\partial}{\partial_z} \left(\mu_3 \frac{\partial \omega_z}{\partial z} \right) - \frac{2}{3} \times$$

$$\times \frac{\partial}{\partial y (\mu_3 div \varpi)} - g_y \times \rho_3$$

$$\rho_3 \left(\frac{\partial}{\partial t} + \omega_x \frac{\partial}{\partial x} + \omega_y \frac{\partial}{\partial y} + \omega_z \frac{\partial}{\partial z} \right) \omega_z =$$

$$= -\frac{\partial P}{\partial z} + \frac{\partial}{\partial x} \left[\mu_3 \left(\frac{\partial \omega_z}{\partial x} + \frac{\partial \omega_x}{\partial z} \right) \right] + \frac{\partial}{\partial y} \left[\mu_3 \left(\frac{\partial \omega_z}{\partial y} + \frac{\partial \omega_y}{\partial z} \right) \right] + 2 \frac{\partial}{\partial_z} \left(\mu_3 \frac{\partial \omega_z}{\partial z} \right) - \frac{2}{3} \times$$

$$\times \frac{\partial}{\partial z} (\mu_3 div \varpi) + g_z \times \rho_3$$

$$\beta = -\frac{1}{\rho_3} \frac{\partial \rho_3}{\partial \rho T_3},$$

where T is temperature; indexes 1, 2, 3 correspond to newborn, bed and air medium in the volume of neonatal complex; ρ_1, ρ_2, ρ_3 is the density of D_1, D_2 , D_3 domains; C_1, C_2, C_3 is the heat capacity of D_1, D_2, D_3 domains; λ_1, λ_2, λ_3 is the thermal conductivity of D_1, D_2, D_3 domains; t is time, Q_{ext} is specific amount of heat released by a newborn per unit time; ω_x, ω_y, ω_z are components of air motion velocity vector; P is air pressure; μ_3 is air dynamic viscosity; g_x, g_y, g_z are components of free fall acceleration vector; β is air thermal expansion coefficient.

The single-valuedness conditions are as follows.

The initial conditions:

$$T_{2,3}(x,\ y,\ z,\ t) = T_{amb},\ T_1(x,\ y,\ z,\ t) = 309.6 \text{ K at } t = 0, \tag{2}$$

$$\omega_x = 0;\ \omega_y = 0;\ \omega_z = 0 \text{ at } t = 0, \quad P = 100 \text{ kPa at } t = 0;$$

The boundary conditions:

$$\lambda_3 \frac{\partial T_3}{\partial n} = q_{TEB} \quad \text{for } S_{3\text{-}0},\ \lambda_2 \frac{\partial T_2}{\partial n} = q_{OP} \quad \text{for } S''_{3\text{-}0},$$

$$\lambda_2 \frac{\partial T_2}{\partial n} = \alpha_{amb} T_{amb} - T_2 \quad \text{for } S_{2\text{-}0},\ \lambda_2 \frac{\partial T_2}{\partial n} = \lambda_x \frac{\partial T_1}{\partial n} \quad \text{for } S_{2\text{-}1},$$

$$\omega_x = \omega_y = \omega_z = 0 \quad \text{for } S_{3\text{-}0} \text{ in the general case,}$$

$$\omega_x = \omega_y = \omega_z = 0 \quad \text{for } S'_{3\text{-}0},\ S''_{3\text{-}0},\ S_{3\text{-}1},\ S_{3\text{-}2},\ S_{2\text{-}1},\ S_{2\text{-}0},$$

where $S_{3\text{-}0}$ is D_3 domain-environment contact area along the lateral surface; $S_{3\text{-}2}$ is D_3 domain-D_2 domain contact area; $S_{3\text{-}1}$ is D_3 domain-D_1 domain contact area; $S_{2\text{-}0}$ is D_2 domain-environment contact area; $S_{2\text{-}1}$ is D_2 domain-D_1 domain contact area; $S'_{3\text{-}0}$ is D_3 domain-environment contact area along the upper surface; $S''_{3\text{-}0}$ is D_3 domain-environment contact area along the lower surface; α_{amb} is coefficient of heat exchange with the environment; $\alpha_к$ coefficient of heat exchange with the chamber air; T_{amb} is ambient temperature.

Solution of this set of differential equations (1) with single-valuedness conditions (2) will make it possible to determine temperature variation at each point of the system at any time instant, as well as to follow its variation depending on cooling capacity and heat productivity values of thermopile and ambient conditions. Calculation of the above problem was done by finite-element numerical method offering high efficiency and accuracy in the calculation of heat exchange in the inhomogeneous systems of complicated configuration.

The results are represented in Figs. 3 – 5 as the plots of temperature variation at different system points as well as with time at different values of thermopile cooling capacity and thermal conductivity.

According to the plots, the temperature in the volume of neonatal resuscitation complex strongly depends on the refrigerating capacity of thermopile. According to estimated data, at q_{TEB} = 700 W/m^2 the minimum value of temperature near the wall is 293 K, and in the centre – 309 K. With increase of q_{TEB} to 800 and 900 W/m^2, the respective temperature values are reduced to 290 K and 308 K and 289 K and 307 K. Thus, adjusting the refrigerating capacity of thermopile, one can control baby temperature. In case of newborn hyperthermia, the thermopile power should be increased, and at hypothermia it should be reduced, thus creating optimal conditions for developmental care.

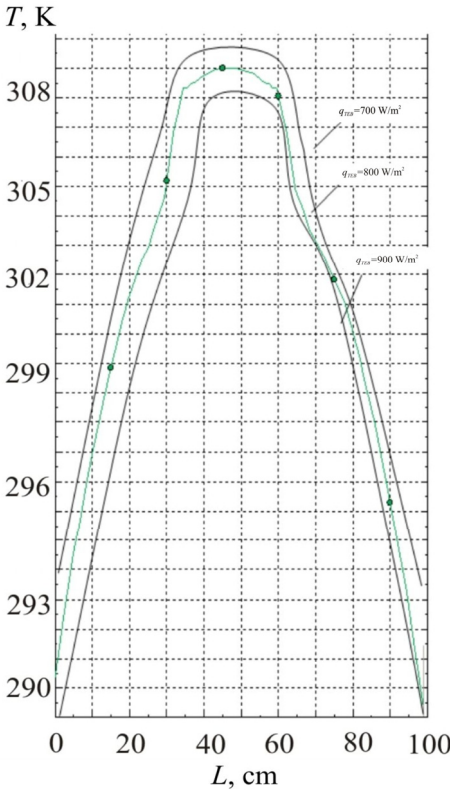

Fig. 3. Temperature distribution along central axial line in cross direction at different q_{TEB}.

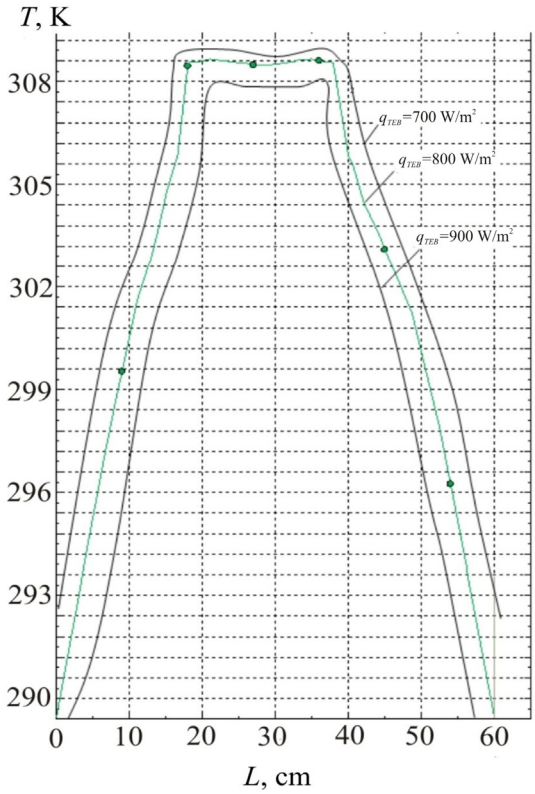

Fig. 4. Temperature distribution along central axial line in longitudinal direction at different q_{TEB}.

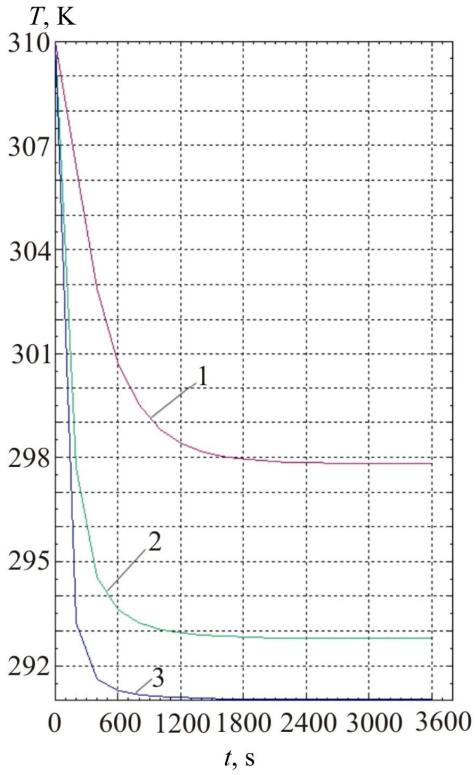

Fig. 5. Temperature variation of different parts of neonatal resuscitation complex with time.

To estimate time dependence of temperature at different points of chamber volume, the plots of temperature variation with time of different parts of neonatal resuscitation complex have been

obtained. Fig. 3 shows temperature variation with time in the centre of the chamber (plot 1), at the distance of 30 cm from the centre of the chamber (plot 2) and from the lateral surface (plot 3). According to calculated data, time of reaching the steady state is about 35 min. This value is quite acceptable, since accelerated time of reaching the operating mode can cause newborn heatstroke.

Conclusions

1. A neonatal resuscitation complex based on high-current thermopiles has been developed, which allows improvement of its power and reliability characteristics.
2. A model of the complex has been created which includes a set of equations describing convective heat exchange in its chamber with regard to using of thermopiles as the source of heat (cold).
3. Based on the elaborated model, dependences of temperature variation at different complex points and with time for different cooling capacity and heat productivity values of thermopile have been obtained which show utilization efficiency of the latter.

References

1. N.N. Volodin, D.N. Degtyarev, Development Care of Newborns with Extremely Low Body Weight, *Voprosy Ginekologii, Akusherstva i Perinatologii* **2**(2), 64 – 69 (2003).
2. N.P. Shabalov, *Neonatology*. Tutorial, 2 vol. (Moscow: MEDpress – Inform, 2009).
3. http://www.draeger.com
4. http://www.axion-med.ru
5. http://medconcept.kz
6. *Patent 2494715 RF*: InCl A61G 10/02, A61G 11/00, Resuscitation System for Newborns / T.A.Ismailov, M.A.Khazamova, O.V.Yevdulov, Z.A.Kamilova; applicant and patent holder Federal State Budgetary Educational Institution of Higher Professional Education “Dagestan State Technical University”, №2012102167/14; filed 23.01.2012; publ. 10.10.2013, Bul. № 28.
7. *Theory of Heat and Mass Transfer*, Ed.by A.I. Leontyev (Moscow: Bauman MSTU, 1997).
8. D.Shi, *Numerical Methods in Heat Exchange Problems* (Moscow: Mir, 1988).

Submitted 16.06.2015.

L. I. Anatychuk[1,2], R. R. Kobylianskyi[1,2], O. I. Denisensko[3], T. Ya. Kadenyuk[1]

[1]Institute of Thermoelectricity of the NAS and MES of Ukraine,
1, Nauky Str., Chernivtsi, 58000, Ukraine;
[2]Yu. Fedkovych Chernivtsi National University,
2, Kotsyubinsky str., Chernivtsi, 58012, Ukraine;
[3]Higher state educational institution of Ukraine "Bukovinian State Medical University",
2, Theatre Sq., Chernivtsi, 58002, Ukraine.

ON THE USE OF THERMOELECTRIC COOLING IN DERMATOLOGY AND COSMETOLOGY

A review of current status of thermoelectricity application in dermatology and cosmetology is given. The paper presents currently used thermoelectric devices for treatment of skin diseases, their classification and a brief description of technical specifications.
It has been established that thermoelectric devices for treatment of skin diseases offer a number of advantages over medical equipment based on liquid nitrogen, namely: temperature control of work instrument, high temperature accuracy, self-containment, compactness, reliability, simplicity and safety of application.The priority lines of using thermoelectric devices in dermatology and cosmetology have been determined.
Key words: thermoelectric cooling, dermatology, cosmetology.

Introduction

General characterization of the problem. Thermoelectric cooling is widely used in many fields of science and technology, in particular, medicine [1 – 3]. It is commonly known in medical practice that thermal effect is an important factor of treatment of many human health problems, including skin diseases.

The scientific line and methods related to effect on the organism of extremely low temperatures is called cryotherapy. Cryotherapy methods are conventionally divided into cryodestruction and cryomassage. During cryodestruction, specialists remove warts, including pointed condylomas, as well as molluscum contagiosum, benign skin neoplasms (keratomas, papyllomas, etc), various scars, restricted hyperkeratoses, etc. At the same time, cryomassage is widely used for treatment of acne vulgaris, acne rosacea, allopeacia, lochen rubber planus, patchy neurodermatitis and other dermatoses. In cosmetology, low temperatures are used for cryorejuvenation, whereby skin elasticity is enhanced, cellulite signs disappear or are reduced, and all skin aging processes on human face and body are decelerated [4 – 8].

However, devices used for this purpose in medical practice in the majority of cases are cumbersome, without proper opportunities of temperature control and thermal modes simulation. In order to achieve low temperatures, in national dermatology and cosmetology use is preferably made of liquid nitrogen, which is quickly evaporated and requires special storage, which restricts considerably the possibilities of its use in medical and cosmetology institutions. That is why the use of thermal effect of low temperatures on patient organism is involved today with certain difficulties and disadvantages, which motivates the *relevance* of development of novel, more state-of-the-art and controlled equipment for cryotherapy realization in medical practice. This, in turn, creates certain difficulties with the use of temperature effect on human body.

The relevance of the work lies in creation of new up-to-date thermoelectric medical equipment and its proof of concept study for the purpose of development of practical recommendations and treatment of skin diseases.

All known thermoelectric devices for treatment of skin diseases by the temperature effect can be divided into the following groups [9]:

- Thermoelectric devices using strong cooling (-60 ÷ -25)°C for freezing out (cryodestruction) of skin defects, treatment of skin neoplasms and carrying out surgical interventions;
- Thermoelectric devices using moderate cooling (for performance of cryomassage) or heating (-25 ÷ +60)°C, for treatment of skin diseases by contrast temperature effect.

Therefore, the purpose of this work is to analyze current status of thermoelectric cooling application in dermatology and cosmetology, as well to develop recommendations as to the use of thermoelectric device ALTEC-7010 for treatment of skin diseases in medical practice.

Thermoelectric devices for dermatology

An example of modern developments in the field of medical equipment that are based on thermoelectric modules is Kryotur 600 (Fig. 1, *a*). The device is intended for local cryotherapy, in particular, for arrest of bleeding, pain control, prevention of inflammation, avoidance of edemas, and is used in case of dislocations, strains, shocks, damages of muscles or joints, preoperative preparation of patients. The temperature of device working applicator is set with a step of 1°C to -10°C and maintained at given level during the therapeutic procedure. The applicator temperature is controlled by means of temperature sensor and displayed on computer screen. Apart from the applicator, a changeable applicator-cuff can be connected to the device for moderate cooling to +12°C, as well as a changeable applicator with a head that can be cooled to -35°C for dermatocosmetology [10].

a) *b)* *c)* *d)* *e)* *f)*

Fig. 1. a) Kryotur 600 (Germany) [10]; b) Kholod-01 (Russia) [11]; c) Cryos Card (Italy) [12]; d) Ar Tek Spot (USA) [13]; e) Ar Tek Air (USA) [14]; f) Cryocell (Korea) [15].

Apparatus for local contrast cooling of surface layers of biological tissue Kholod-01 (Fig. 1, *b*) is used to achieve therapeutic effect and cryomassage performance [11]. Structurally, the apparatus is composed of thermoelectric therapeutic device and power supply unit. Maximum cooling temperature is -12ºC.

One of modern devices for cryotherapy is a compact medical apparatus Cryos Card (Fig. 1, *c*), intended for cryotherapy, thermotherapy, treatment of inflammatory processes, pain control, posttraumatic rehabilitation, treatment of rheumatic diseases, psoriasis, etc. Analgetic end-point is achieved due to temperature effect on sensitive nerve fibers. The apparatus is equipped with a cryoradiator and thermal cone for cryotherapy, with possible control of temperature range from -10°C to +50°C [12].

Cryomassage device ArTek Spot (Fig. 1, *d*) is intended for local cooling of damaged human body area and is used in various medical institutions and beauty salons for pain syndrome control at depilation and removal of tattoos, reduction of edemas, sores and thermal traumas. The device is composed of cooling and control unit, as well as of several work of various shape intended for therapeutic procedures on the face, back, hands and legs. Precise temperature control of work instruments eliminates the risk of freeze burn and damage of biological tissues. The operating temperature range of device is 0 ÷ +40 ºC [13].

Cryotherapy device ArTek Air (Fig. 1, *e*) is intended for cooling of human skin surface. It is used for cryomassage, pain control, reduction of edemas and temporary pain relief at injections. The device operating principle is based on air flux cooling by means of thermoelectric Peltier modules. Later on, using air cooled to the required temperature, therapeutic procedures on patient skin are performed. The device is composed of cooling thermoelectric unit and operating probe for delivery of "cold" or "hot" air [14].

Cryocell device (Fig. 1, *f*) is intended for cryomassage and treatment of human skin diseases by means of cryoelectrophoresis method. Such device makes it possible to perform cryotherapy, "hot" therapy, ionophoresis, electric therapy, as well as combined thermal effect on patient skin. The device is used for pain attenuation at traumas [15].

Table 1 lists examples of patented developments of thermoelectric devices for dermatology (Figs. 2 – 13) [16 – 27].

Thermoelectric devices for cosmetology

Modern apparatus Cryolift 3 (Fig. 14, *a*) is used in many beauty salons for cryotherapy and luminotherapy. For pain abatement when performing cosmetic procedures, use is made of local cooling of patient skin by means of work applicator with an embedded thermoelectric cooler. Apparatus Cryolift 3 provides for two modes of light effect: pulsed and continuous. Pulsed mode assures more effective stimulation of collagen synthesis due to deep penetration to biological tissues and influence on intracellular organs. Luminotherapy is successfully used in anti-cellulite programs, for correction of age skin changes, for treatment of inflammatory processes (erythema, edema, etc.), in a complex treatment of alopecia, in the prophylaxis of hypertrophic scars and post-inflamatory hyperpigmenttaion, to accelerate their healing. Combination in one procedure of luminotherapy and cryotherapy creates a synergetic "anti-age" effect (biorevitalization and skin amelioration) [28].

Table 1

Patented developments of thermoelectric devices for dermatology

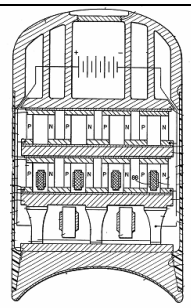 *Fig. 2. Instrument for therapeutic hypothermia (US 4483341A) [16].*	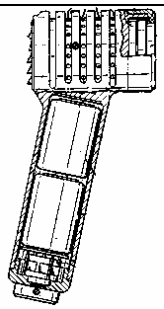 *Fig. 3. Device for heating and cooling of skin (US 5097828, US5209227) [17].*	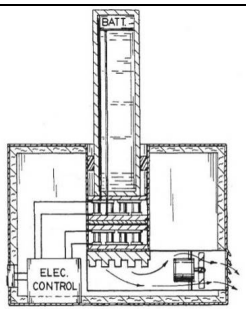 *Fig. 4. Support for precooling of probe (US 5277030) [18].*
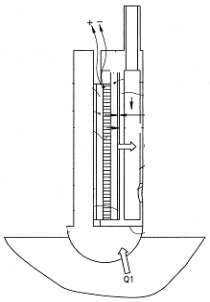 *Fig. 5.Cryocatheter (WO 2013164820A1) [19].*	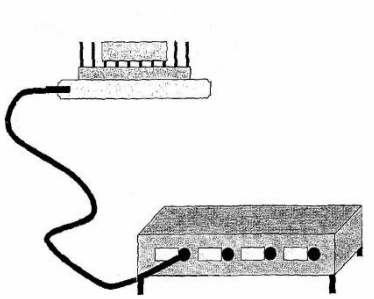 *Fig. 6. Device for thermal exposure of skin (DE 10147563) [20].*	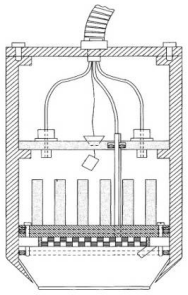 *Fig. 7.Cryoprobe (US 6017337) [21].*
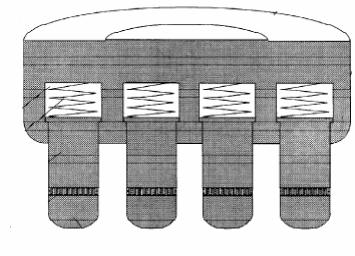 *Fig. 8. Thermoelectric device for treatment of head skin diseases (RF 2341737) [22].*	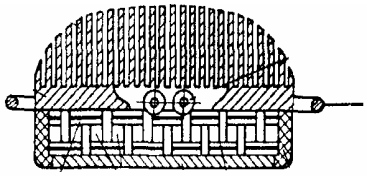 *Fig. 9. Microcooler for treatment of skin diseases [23].*	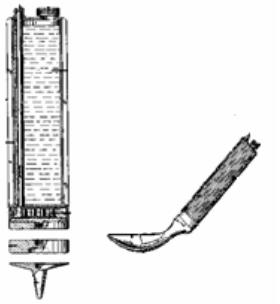 *Fig.10. Thermoelectric medical device – cold lancet (US3133539) [24].*
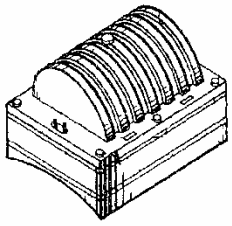 *Fig. 11. Hypothermal device (US 3327713) [25].*	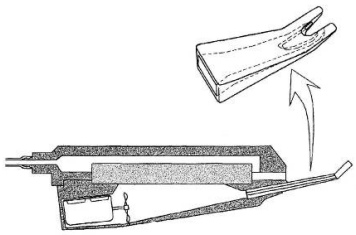 *Fig.12. .Device for treatment of skin diseases and surgical operations (US 7037326)) [26].*	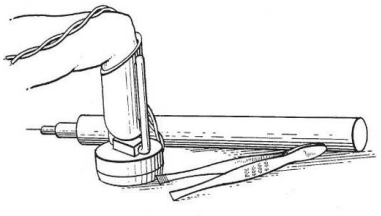 *Fig. 13. Cooling probe for skin (US 4614191) [27].*

Fig.14.: a) Cryolift 3 (Italy) [28]; b) FormaxPlus (Israel) [29]; c) Broad Band Light (BBL)(USA) [30]; d) HS 810 diode laser (China) [31]; e) SkinPulse 500 (Germany) [32]; f) ProShockIce (China) [33].

Device FormaxPlus (Fig. 14, *b*) is used for depilation, reduction of wrinkles and scars after acneiform rash, reduction of vessels and pigment spots on patient skin. With a contact cooling the device allows maintenance of constant epidermis temperature, close to +5 °C, due to thermoelectric cooling. Cooling temperature is shown on device display and kept constant during long-term procedures. This unique method guarantees maximum safety, cooling control, patient comfort and eliminates the need for anesthesia [29].

BroadBand Light (BBL) (Fig. 14, *c*) is a system of high-intensity broadband light radiation for depilation, vessel pathology, benign pigment formations, photorejuvenation, treatment of acne, etc. The device employs integrated thermoelectric system for monitoring of cooling temperature of work instruments which provides for precise temperature control from 0 °C to 30 °C to an accuracy of 1 °C. Large radiation range allows a wide spectrum of procedures without additional heads. Adapters of various sizes assure flexible adaptation even to skin areas difficult of approach [30].

HS 810 diode laser (Fig. 14, *d)* is used for laser epilation and rejuvenation of patient skin. To achieve prompt effect, HS 810 diode laser makes 10 laser flashes per second, making the epilation procedure less sensitive and painless. The apparatus utilizes thermoelectric cooling of a system with water reservoirs, as well as work instrument tip to the temperature of 0÷5 °C. Continuous operating mode of the apparatus is 24 hours [31].

Compact apparatus SkinPulse 500 (Fig. 14, *e*) is a desktop device intended for epilation by means of light pulses technology. It is helpful for treatment of skin vessel injuries, acme, pigmentation, and erythema. Contact cooling of local area of patient skin is done by means of thermoelectric modules and varies in the temperature range of -4°C ÷ +10°C [32].

ProShockIce (Fig. 14, *f*) is a device reducing local depot fact and cellulite signs using Ice-shock-lipolysis technology. It is a novel method which consists in the reduction of subcutaneous fat and fibrous cellulite in the areas where only liposuction has been used so far. For the first time this technology employs a combination of two methods: cryolipolysis and shock wave effect of acoustic

waves. During local freezing of problematic area by means of special cooling head with imbedded thermopile, hardening and destruction of subcutaneous fat tissue takes place [33].

Table 2 lists examples of patented developments of thermoelectric devices for cosmetology (Fig. 15 – 23) [34 – 42].

Table 2

Patented developments of thermoelectric devices for cosmetology

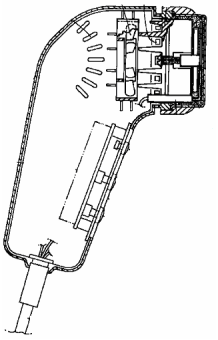 *Fig. 15. Cooling device (JP 2000037412A) [34].*	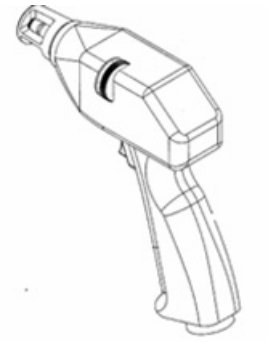 *Fig. 16. Skin care device (KR 20100060222(A) [35].*	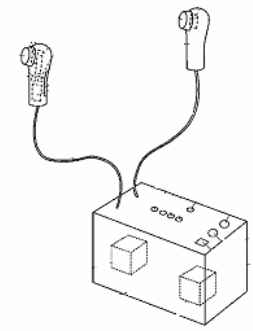 *Fig. 17. Device for cooling local areas of face skin (JP 2012152307(A)) [36].*
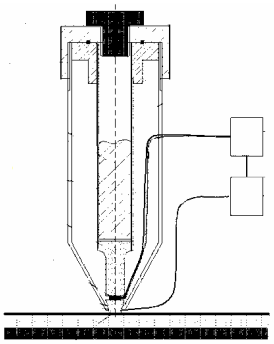 *Fig. 18.Cryotherapy apparatus (JP 2006130055(A)) [37].*	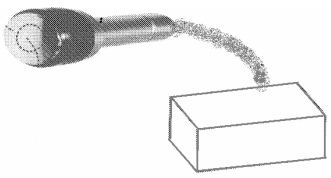 *Fig. 19. Skin care apparatus (KR 20130043299(A)) [38].*	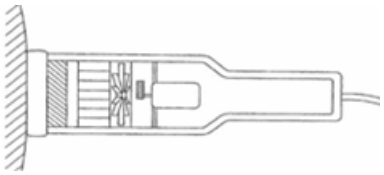 *Fig. 20. Device for face massage (KR 20010077967(A)) [39].*
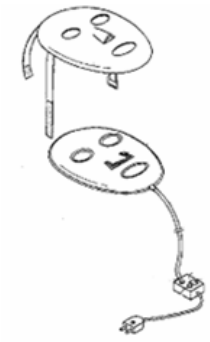 *Fig. 21. Cosmetic mask (CN 1640370(A)) [40].*	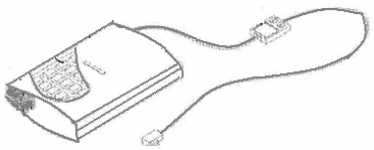 *Fig. 22. Cooling belt (KR 20120090862(A)) [41].*	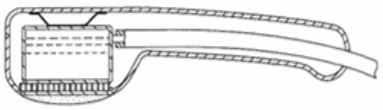 *Fig. 23. Device for cold and hot soaking therapy (US 6311497) [42].*

Thus, from the foregoing review of the literature it follows that today there are numerous developments of thermoelectric medical devices for dermatology and cosmetology. However, information is still lacking on the methods of using such devices and the expected treatment result. In particular, it is important to study the curative effect of moderate skin cooling. For this purpose, the work employs a device "ALTEC-7010" developed at the Institute of Thermoelectricity of the NAS and MES of Ukraine for treatment of skin diseases in the operating temperature range (–35 ÷ +5) °C [43].

Thermoelectric device for treatment of skin diseases "ALTEC-7010"

Device "ALTEC-7010" developed at the Institute of Thermoelectricity [43] is intended for cryomassage the mechanism of which lies in a stimulated effect on the microcirculation flow and skin nerve terminals, which ameliorates metabolic and reparation processes and accelerates the regression of inflammatory processes with chronic dermatoses. Owing to positive effect on the skin, cryomassage method is used in complex treatment of such skin diseases as patchy allopecia, acne rosacea and acne vulgaris, Vidal's disease, skin itch, chronic eczema, lichen planus, flat warts, granulema annulare, etc. The general view of device is shown in Fig. 24.

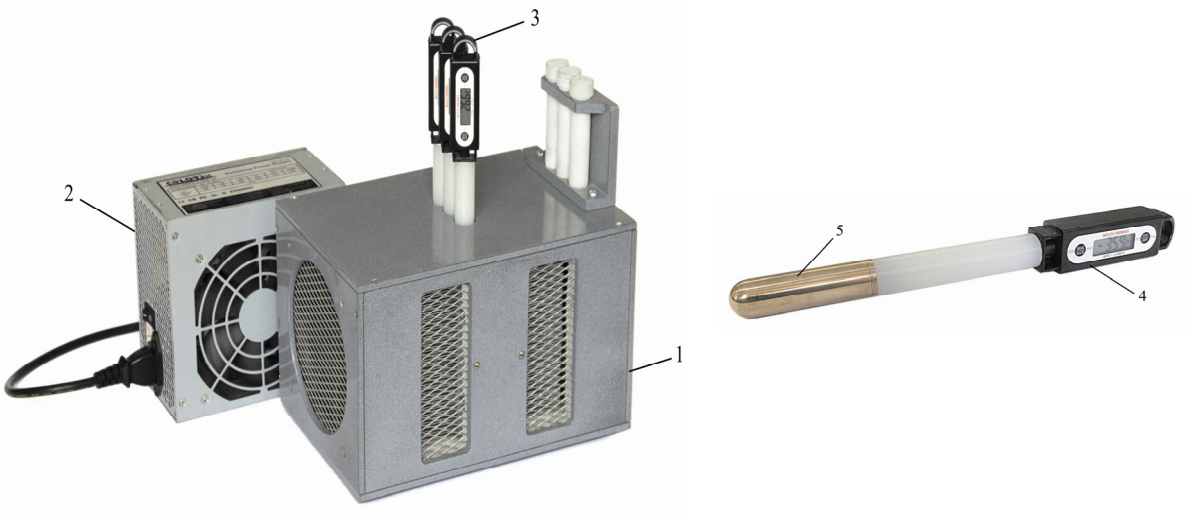

Fig.24. External view of thermoelectric device for treatment of skin diseases [43]:
1 – thermoelectric cooling unit, 2 –power supply unit,
3 – kit of work instruments, 4 – embedded electronic thermometer,
5 – cylinder container filled with a liquid with high heat capacity.

The device is composed of three main functional units: cooling unit 1, power supply unit 2 and a kit of work instruments 3 (Fig. 24). In turn, cooling unit has a case, cooling chamber for work instruments, two-stage thermoelectric modules "Altec–11" and air heat exchangers with the fans for cooling the hot sides of thermoelectric modules. Device work instruments comprise embedded electronic thermometers 4 with autonomous power supply sources and cylinder empty heads 5 with a liquid with high heat capacity.

The operating principle of "Atec-7010" device lies in cooling work instruments by means of thermoelectric Peltier modules. Cooled work instrument is used to produce a thermal effect on the respective areas of human skin.the advantages of this device include: the availability of electronic thermometers of work instruments for controlled thermal effect on the respective skin area, absence of work instruments connection to cooling unit and small dimensions of work instruments. Technical specifications of this device are given in Table 3.

Table 3

Technical specifications of device for treatment of skin diseases"ALTEC-7010"

№	Device technical characteristics	Parameter values
1.	Device operating temperature range	(–35 ÷ +5) °C
2.	Time to achieve temperature mode by device	10 min.
3.	Temperature measurement accuracy	±1 ºC
4.	AC current supply voltage of device	(220 ± 10) V
5.	Device power requirement	250 W
6.	Thermoelectric cooler dimensions	(240 × 160 × 15) mm
7.	Work instrument dimensions	(18.5 × 23 × 215) mm
8.	Work instrument weight	0.08 kg
9.	Device weight	6.5 kg
10.	Device continuous work duration	8 h.

From the known counterparts the most similar in technical characteristics is thermoelectric device for treatment of skin diseases [44] which is composed of supply unit, cooling unit and a kit of work instruments with replaceable tips of different shape. Cooling of work instruments takes place in cooling unit based on thermoelectric Peltier modules, the heat from the hot junctions of thermoelectric modules is rejected by cooling liquid flowing through liquid heat exchangers. The unique feature of this device is that the work instruments are galvanically isolated from the supply and cooling units. The device offers the opportunity to maintain the temperature of work instruments in the range of -50 ÷ 0 °C. However, the main disadvantages of this device is connection to central water supply, restricting its application potential, and the absence of temperature control of the surface of work instruments during therapeutic procedures.

The proposed device "Altec-7010" is different in that the heat from the hot sides of thermoelectric modules is rejected to environment by means of air heat exchangers, and each work instrument has an electronic thermometer with a digital display for temperature control of work instrument tip. This device allows therapeutic procedures under unstationary treatment conditions with a possibility of simultaneous visual control of work instruments temperature.

Results of clinical use of thermoelectric device for treatment of skin diseases "ALTEC-7010"

Inspected were 24 patients (among them 19 women and 5 men) of the age from 19 to 69 years who suffered from chronic skin diseases (acne rosacea, acne vulgaris, patchy allopecia, psoriasis and lichen amyloidosis), the complex therapy of which employed cryomassage method with the use of thermoelectric device "Altec-7010". Clinical investigations were performed at Department of Dermatovenerology of Bukovonian State Medical University. Examples of device clinical application are given below.

Acne rosacea. Acne rosacea were diagnosed in 9 persons. Acne rosacea is chronic dermatosis with a poly-factor etiopathogenesis resulted from the effect of external factors (alimentary, meteo- and professional factors, activity of Demodex mites) against the background of hormone, immune, metabolic, microcirculation disorders, etc. Dermatosis is localized on face skin, shown as erythema, surface vasodilatation (telangiectasia), small indurated nodes (papules), pustules. According to known

classification, 5 patients had erythematic-papular-pustular form of rosacea, 4 persons – erythematic-papular form of dermatosis. All the patients were prescribed standard dermatosis therapy which included methods of systemic and external (topical) actions, as well as cryomassage method with the use of thermoelectric device "Altec-7010" – immediately for patients with the erythematic-papular form of dermatosis, and for patients with erythematic-papular-pustular form only after the regression of pustules (on the 6 – 7 day after the initiation of treatment).

Cryomassage sessions were prescribed for 30 – 40 seconds 2 – 3 times on each area (with total exposure 10 min) daily for 5 days and every second day during the next 10 – 12 days (altogether 10 – 11 procedures per course). The dynamics of rash elements regression with patients suffering from acne rosacea as a result of employment in complex therapy of cryomassage sessions with the use of thermoelectric device "Altec-7010" (in scores according to known classification of V.P. Adaskevich, 2004 [45]) is represented in Fig. 25 and in the pictures in Fig. 26.

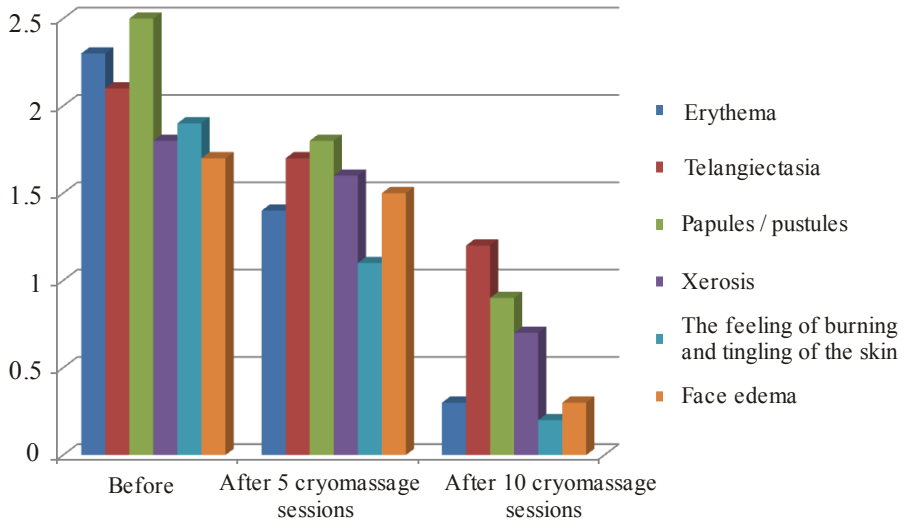

Fig. 25. Dynamics of rash elements regression with patients suffering from acne rosacea due to cryomassage with the use of thermoelectric device "Altec-7010" (in scores according to V.P.Adaskevich's classification, 2004 [45]).

a) *b*)

Fig. 26. Patient K., 69 year. Diagnosis: Acne rosacea, erythematic-papular form, prior to (a) and after (b) the course of treatment (disappearance of greater part of telangiectasias, size reduction of popular rash elements).

Acne vulgaris. Acne vulgaris were diagnosed in 11 patients. Acne vulgaris is a polyetiologic chronic skin disease caused by a number of microorganisms (Propionibacterium acnes, Staphylococcus epidermidis and other cocci), developed against the background of neuroendocrinal, immune, metabolic disorders, microcirculation disorders, etc. Dermatosis is localized on the skin of face, shoulders and body, is manifested as comedones, popular acne, pustular acne, nodes (indurative, acne conglobata). According to severity, there can be light, mean and severe forms of acne [46]. Among the investigated patients, acne vulgaris of mean severity were diagnosed in 7 persons, severe form was diagnosed in 3 persons and light form – in 1 person. All the patients were prescribed standard dermatosis therapy which included methods of systemic and external (topical) actions, as well as cryomassage method with the use of thermoelectric device "Altec-7010" (Fig. 27).

Fig.27. Patient N., 19 years. Diagnosis: Acne vulgaris, mean severity.

Patients suffering from acne vulgaris were prescribed cryomassage sessions for 30 – 40 sec 3 – 4 times on each area (with total exposure time 10 min) daily for 5 – 8 days and every second day 10-12 days (total course – 11 – 14 procedures). According to the dynamics of rash elements regression on completion of treatment course, a light degree of acne vulgaris was diagnosed in 4 patients, mean degree – in 6 patients and severe form – in 1 patient (Fig. 28).

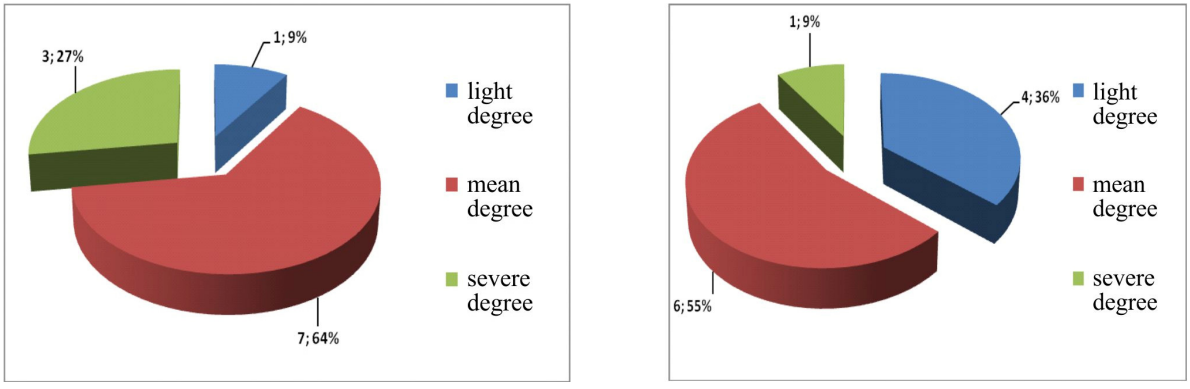

Fig.28. Distribution of patinets suffering from acne prior to and after treatment according to dermatosis severety.

Patchy allopecia (circumscribed) was diagnosed in 2 patients. Dermatosis has a multi-factor pathogenesis and is created, as a rule, against the background of combined co-morbidity of inner organs, chronic sites of focal infection, etc. Treatment of this disease provides for complex

observation of patient and correction of diagnosed co-morbid pathology. Cryomassage has long since been an important component of this dermatosis treatment.

Patients suffering from patchy alopecia were prescribe cryomassage sessions for 40 – 50 seconds in 2 – 3 steps for 5 min daily (total course – 15 – 20 procedures). In a month, on completion of treatment, a refresher course of treatment by the same scheme was prescribed. The results of patient treatment after 5 months are represented in Fig. 29.

a) *b*)

Fig. 29. Patient M., 39 years. Diagnosis: Patchy alopecia of hair area (prior to (a) and after (b) 5 months of treatment).

Psoriasis is a common chronic skin disease characterized by benign hyperprolification of surface skin layers with formation of inflammatory plaques and massive lamellar exfoliation of their surface. There are progressive, stationary and regression stages in the course of this disease. Complex therapy of such patients widely employs phototherapy which has a cytostatic effect, namely it suppresses a hypernormal division of cells. Physiotherapy methods are recommended to be used during stationary dermatosis stage and regression stage. Information on using cryotherapy methods in the available home literature was not found. We used this method for patient with the diagnosis: common psoriasis, exudative form, regression stage. The dermatosis of this patient had a lengthy torpedo course that did not respond easily to standard treatment methods. After 3 weeks of standard therapy, moderately infiltrated plaques remained on the skin of lower limbs, for which cryomassage sessions were prescribed with the use of thermoelectric device "Altec-7010" (Fig. 30).

Patients suffering from psoriasis were prescribed cryomassage sessions for 30 – 40 sec in 2 – 3 steps for 5 min daily (total course – 10 procedures, following which the process on the skin was gradually solved, and only signs of secondary hyperemia remained.

Lichen amyloidosis is a rare skin disease occurring as a consequence of metabolic, neuroendocrinal and microcirculation disorders with formation mostly on the legs skin of small semiround nodes accompanied by intensive itch.

Patient C., 29 years was the case with a diagnosis: lichen amyloidosis of legs. In parallel with standard therapy, the patient was subject to a course of cryomassage with the use of thermoelectric device "Altec-7010" for 30 – 40 sec in 3 – 4 steps for 8 min daily (total course – 10 procedures), following which the status of skin was considerably ameliorated, the itch practically ceased, and papules on the skin became flat (Fig. 31).

a) *b)*

Fig. 30. Patient T., 53 years. Diagnosis: Common psoriasis, exudative form (a), regression stage (b).

a) *b)*

Fig.31. Patient C., 29 years.
Diagnosis: lichen amyloidosis of legs (prior to(a) and after(b) treatment course).

On completion of treatment course, the patient was recommended to repeat the therapy course in 3 – 4 weeks with the use of regression cryomassage by thermoelectric device "Altec-7010".

Conclusions

1. Analysis of current status of using thermoelectric devices for treatment of various skin diseases in dermatology and cosmetology has been made. The priority lines of using such devices have been determined and their technical specifications have been given.

2. It has been established that thermoelectric devices can be used in dermatology and cosmetology with curative purpose, in particular, for treatment of chronic dermatoses (acne rosacea, acne vulgaris, residual symptoms of psoriasis, patchy alopecia and other skin diseases). This is because thermoelectric devices are convenient in application, do not require additional maintenance on operation, and easily realize temperature control of work instruments.

3. It has been established that thermoelectric device for treatment of skin diseases "Altec-7010", providing for cooling of work instruments to -35 °C, makes it possible to perform cryomassage in a complex therapy of chronic skin diseases, nevertheless, its design should be improved for the purpose of expanding its operating temperature range and treatment efficiency.

References

1. L.I.Anatychuk, *Thermoelements and Thermoelectric Devices: Reference Book* (Kyiv:Naukova Dumka, 1979), 768 p.
2. L.I.Anatychuk, *Thermoelectricity,Vol.2, Thermoelectric Power Converters* (Kyiv, Chernivtsi: Institute of Thermoelectricity, 2003), 376 p.
3. E.A.Kolenko, *Thermoelectric Cooling Devices* (Leningrad: Nauka, 1967), 283p.
4. V.K.Albrova, Treatment of warts, freckles and keloid scars with liquid nitrogen, *In: Aesthetic medicine Problems* (Moscow: Medicine, 1968), 19 – 25.
5. B.A.Zadorozhnyi, *Cryotherapy in Dermatology (Practitioner's Library)* (Kyiv:Zdorov'ya, 1985), 72 p.
6. M.A.Rozentul, *Guidebook on Cosmetics* (Moscow: Medicine, 1964), 337 p.
7. V.I.Grischenko, B.P.Sandomirskiy, and Yu.Yu.Kolontai, *Practical Cryomedicine* (Kyiv:Zdorovye, 1987), 248p.
8. A.L.Mashkilleison, *Treatment of Skin Diseases* (Moscow: Kron-Press, 2000), 250 p..
9. V.S.Zemskov, L.I.Gasanov, *Low Temperatures in Medicine* (Kyiv:Naukova Dumka, 1988), 278 p.
10. http://www.gymna.ru/shop/krioterapiya/kriotur-600-kryotur-600/
11. http://www.elamed.com/catalog/catalog/kriooborudovanie/apparat-dlya-lokalnoy-gipotermii-kholod-01
12. http://osd.prom.ua/p3913869-krioterapiya-cryos-card.html
13. http://www.thermotekusa.com/md_artekspot.php
14. http://www.thermotekusa.com/md_artekair.php
15. http://www.ec21.com/offer_detail/Sell_Medical_Device_Business_Unit--19708108.html
16. *Patent US 4483341(A).* Therapeutic Hypothermia Instrument / Witteles Eleonora. – 1984.
17. *Patent US 5097828*. Thermoelectric Therapy Device/ Richard Deutsch. – 1992.
18. *Patent US 5277030*. Preconditioning Stand for Cooling Probe/ William R. Miller. – 1994.
19. *Patent WO 2013164820(A1).* Cryocatheter with Coolant Fluid Cooled Thermoelectric Module / Berger Avi, Hazan Avri. – 2013.
20. *Patent DE 10147563.* Die folgenden Angaben sind den vom Anmelder eingereichten Unterlagen entnommen/ Maurer, Marcus. – 2003.
21. *Patent US 6017337*. Cryoprobe Based on a PeltiIer Module/ Luc Pira. – 2000.
22. *Patent RF 2341737*. Thermoelectric Device for Treatment of Head Skin Diseases / T.A.Ismailov, G.I.Aminov, O.V.Popova, M.A.Khazamova, 2008.
23. E.A.Kolenko, A.A.Isaakyan, and A.G.Scherbina, Thermoelectric Device for Temperature Skin Excitations, *J.of Physiology* 65(11), 1959.
24. *Patent US 3133539*. Thermoelectric Medical Instrument/ Eidus William. – 1964.

25. *Patent US 3327713*. Portable Thermoelectric Hypothermia Device / Eidus William. – 1967.
26. *Patent US 7037326*. Skin Gooling Device using Thermoelectric Element/ Hee-Young Lee. – 2006.
27. *Patent US 4614191*. Skin-Cooling Probe/ Robert F. Perler. – 1986.
28. http://www.mciti.ru/main.php?k=8
29. http://volkovabeauty.ru/nashe-oborudovanie/sharplight
30. http://sciton.com.ua/products/sciton-joule/bbl
31. http://www.apolo-laser.com/products_detail/&productId=30.html
32. http://perukar.sells.com.ua/kompaktnyij-skinpulse-500-tsena-10-880-evro/p1857
33. http://t-clinic.ru/cryolipolys
34. *Patent JP 2000037412A*. Skin Beatifying Implement / Miyabayashi Kiyomi. – 2000.
35. *Patent KR 20100060222(A)*. Device for Skin Beauty and Medical Treatment / Gim Yang Soo. - 2010.
36. *Patent JP 2012152307(A)*. Beauty Appliance / Hitachi Maxell. – 2012.
37. *Patent JP 2006130055(A)*. Cryotherapy Apparatus by Peltier Module / Element and Temperature Control Method for Cryotherapy by Peltier Module / Element / Maruyama Shigenao, Yamaya Tomoyuki, Alba Setsuya. – 2006.
38. *Patent KR 20130043299(A)*. Medical Skin Beauty Care Apparatus for Heating and Stimulating Skin using Thermoelectric Module and Ultra-Sonic Vibrator / Kim Ki Tae. – 2013.
39. *Patent KR 20010077967(A)*. Facial Treatment Implement / Shimizu Hirohisa. – 2001.
40. *Patent CN 1640370(A)*. Beauty Cover / Myong – Ha Kim. – 2005.
41. *Patent KR 20120090862(A)*. An Apparatus for Hot and Cold Therapy which Utilizes Thermoelectric Module / Kang Sung Mo. – 2012.
42. *Patent US 6311497*. Device for Cold and Warm Formentations/ Young-Chun Chung. – 2001
43. L.I.Anatychuk, R.R.Kobylyanskyi, and Yu.M.Mochernyuk, Thermoelectric Device for Skin Treatment, *J.Thermoelectricity* **4**, 90 – 96 (2009).
44. *Patent UA 8462*. Skin Treatment Device / L.I.Anatychuk, LYa.Kushneryk, 2005.
45. V.P.Adaskevich, *Diagnostic Indexes in Dermatology* (Moscow: Med.Kniga, 2004), 164 p.
46. *Dermatology, Venerology*, Ed. by V.I.Stepanenko (Kyiv: KIM, 2012), 848 p.

Submitted 20.07.2015.

T. A. Ismailov, R. Sh. Kazumov, D. K. Ramazanova

Federal State Budgetary Educational Institution of Higher Professional Education
"Dagestan State Technical University", 70, Imam Shamil avenue,
Makhachkala, 367015, Russia

THERMOELECTRIC RECUPERATIVE-TYPE HEAT EXCHANGE APPARATUS WITH THERMAL BRIDGES

This paper dwells upon the design of a thermoelectric heat-exchange apparatus with thermal bridges. The results of its mathematical simulation and full-scale test of the prototype are presented. Calculated and experimental plots of temperature variation at different points of the apparatus are given. The results obtained allow for a conclusion on the efficient practical application of heat-exchange apparatus.

Key words: heat-exchange apparatus, thermopile, heat carrier, temperature field, mathematical model, prototype, experiment.

Introduction

At the present stage of science and technology development the problems of studying special facilities for provision of intensive heat transfer from the sources with high thermal loads, creation of basically new high-performance cooling and temperature stabilization systems meeting special requirements, design of heat exchangers with improved characteristics become increasingly vital and relevant [1]. This is due to world market saturation with novel technical facilities offering great functional opportunities and high-speed performance but characterized by increased thermal overloads and overheating problems, which has an adverse effect on their operating reliability.

One of promising lines when creating cooling and temperature stabilization systems is the use of semiconductor thermoelectric converters providing for construction of economical, small-size coolers and temperature stabilizers with broad functional capabilities of maintaining given thermal mode [2, 3]. The theory and possibilities of practical application of such devices are adequately described in the works by A. F. Ioffe, L. S. Stilbance, A. E. Kolenko, A. I. Burshtein, M. A. Kaganov, M. P. Privin, L. I. Anatychuk, A. L. Vainer, E. K. Iordanishvili, I. V. Zorin, et al. In these works, parameters of devices working in different modes are calculated, the energy efficiency of their application is determined. The main emphasis here is made on the investigation of thermophysical processes with constant temperature on the junctions of thermoelectric power converters.

However, there exist many application areas of thermoelectric devices with temperature variation of heat carriers along the thermopile surfaces absorbing and releasing heat. They include various types of heat exchangers: coolers and heaters of liquid flows, air coolers, air conditioners, etc., i.e. all devices where circulation of heat carriers occurs along thermopile junctions. Despite considerable progress in thermoelectric technology, papers on such devices are lacking, their theoretical foundations are not developed to the full extent, no efficient operating modes are indicated, no areas of reasonable application are determined, etc.

Not without interest is investigation of thermoelectric heat exchangers of special structure with improved energy characteristics, their optimization, determination of the basic parameters and rational

application areas. The above interest is due to insufficient research in this field, alongside with the urgent need for development of highly efficient heat exchangers with improved properties. Said factors determine the relevance of the present research.

The purpose of the paper is to study a thermoelectric recuperative-type heat exchange apparatus with thermal bridges with improved energy, weight-size and reliability parameters.

Mathematical model of heat exchange apparatus

Design circuit of the apparatus is given in Fig. 1. Here, in the elementary section dx of thermopile length, heat transfer is provided both through thermoelements and high thermally conductive thermal bridges with heat exchange intensity determined by the Biot numbers $Bi_{1,2}$ and $Bi'_{1,2}$ for thermopile and thermal bridge, respectively. The concept of filling factor ξ, is introduced which in this case is characterized by the ratio of thermopile area in the elementary section to the elementary section area. Then, in the elementary section of length dx the area of thermoelement junctions occupies the surface ξLdx, and the surface area of thermal bridge is $(1-\xi)\,L$dx, where L is thermopile width.

Coefficients of heat transfer, thermal conductivity and thickness, respectively, for thermopile and thermal bridge will be denoted through $\alpha_{1,2}$, $\alpha'_{1,2}$, $\lambda_{1,2}$, $\lambda'_{1,2}$, d, d'. Let us assume that the temperatures of cooled and heated heat carriers at thermopile inlet are related as $T_1 > T_2$. The rest of assumptions are generally accepted for straight-flow thermoelectric heat pumps: the flows are absolutely mixed in the direction perpendicular to motion direction; the properties of heat carriers and materials are temperature-independent; heat transfer through unaccounted structural members is absent.

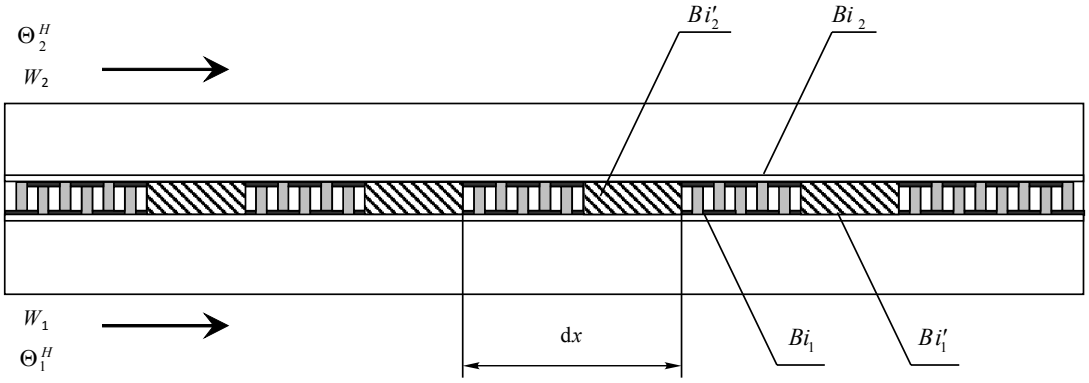

Fig. 1. Design circuit of thermoelectric heat exchange apparatus with thermal bridges.

Heat balance equations according to heat carrier flows for the above circuit under parallel flow conditions are given below:

$$W_1 \frac{dT_1}{dx} = \alpha_1 \xi L(T_{1TEB} - T_1) + \alpha_1^{'}(1-\xi)L(T_{1м} - T_1),$$

$$W_2 \frac{dT_2}{dx} = \alpha_2 \xi L(T_{2TEB} - T_2) + \alpha_2^{'}(1-\xi)L(T_{2м} - T_2),$$

where $T_{1TEB,\ 2\mathrm{TEB}}$ are temperatures of thermoelement junctions, $T_{1b,2b}$ are surface temperatures of thermal bridges, $T_{1,\,2}$ are temperatures of cooled and heated heat carriers.

Heat balance equations on the surfaces exposed to heat carrier flows for TE junctions are of the form:

$$\alpha_1(T_1 - T_{1TEB}) = \overline{e}jT_{1TEB} - \frac{1}{2}j^2\rho d - \frac{\lambda}{d}(T_{2TEB} - T_{1TEB}),$$

$$\alpha_2(T_{2TEB} - T_2) = \overline{e}jT_{2TEB} + \frac{1}{2}j^2\rho d - \frac{\lambda}{d}(T_{2TEB} - T_{1TEB}),$$

where $\bar{e}$ is the Seebeck coefficient, j is electric current density;
for thermal bridges:

$$\alpha'_1(T_1 - T_{1,м}) = K'(T_1 - T_2),$$

$$\alpha'_2(T_{2,м} - T_2) = K'(T_1 - T_2),$$

where $K' = \left(\frac{1}{\alpha'_1} + \frac{1}{\alpha'_2} + \frac{d'}{\lambda'}\right)^{-1}$ is coefficient of heat transfer through thermal bridge.

On excluding the surface temperatures $T_{1TEB,\ 2TEB}$ and $T_{1b,2b}$ and reducing the equation to dimensionless form, the expressions for temperature variation of heat carrier flows along the heat exchange surface of heat exchange apparatus take on the form:

$$\frac{d\Theta_1}{dx} = b\xi\left\{\left[m\beta\nu^2 - (1+\nu)\right]\Theta_1 + \Theta_2 + \frac{\nu^2}{2}\left[1 + (2-\nu)m\beta\right]\right\} + b'(1-\xi)(\Theta_2 - \Theta_1), \quad (1)$$

$$\frac{d\Theta_2}{dx} = \eta b\xi\left\{\left[\beta\nu^2 - (1-\nu)\right]\Theta_1 + \Theta_2 + \frac{\nu^2}{2}\left[1 + (2+\nu)\beta\right]\right\} + \eta b'(1-o)(\Theta_1 - \Theta_2), \quad (2)$$

where $b' = \frac{K'}{W_1}S; \quad \Theta_1 = \frac{\overline{e}^2}{\rho\lambda}T_1; \quad \Theta_2 = \frac{\overline{e}^2}{\rho\lambda}T_2; \quad \nu = \frac{\overline{e}d}{\lambda}j;$

$$b = \frac{K}{W_1}S;\ K = \left[\frac{1}{\alpha_1} + \frac{1}{\alpha_2} + \frac{d}{\lambda} + \nu\left(\frac{1}{\alpha_1} - \frac{1}{\alpha_2} - \frac{\nu\lambda}{\alpha_1\alpha_2 d}\right)\right]^{-1}.$$

The boundary conditions are written for the case of parallel flow as

$$\Theta_1\big|_{x=0} = \Theta_1^H; \Theta_2\big|_{x=0} = \Theta_2^H. \quad (3)$$

Solution of the resulting system of differential equations (1)-(2) with the boundary conditions (3) for parallel flow condition is written as follows:

$$\Theta_1 = C_1(\Psi_1 - b_2)\frac{e^{\Psi_1 X}}{b_1} + C_2(\Psi_2 - b_2) - -\frac{P_1}{\Psi_1 b_1}(\Psi_1 - b_2) - \frac{P_2}{\Psi_2 b_1}(\Psi_2 - b_2),$$

$$\Theta_2 = C_1 e^{\Psi_1 X} + C_2 e^{\Psi_2 X} - \frac{P_1}{\Psi_1 b_1} - \frac{P_2}{\Psi_2 b_1},$$

where $C_1 = \left[\Theta_1^H b_1 - (\Psi_1 - b_2)\Theta_2^H + (\Psi_2 - b_2)V - b_1\delta\right]/(\Psi_1 - \Psi_2),$

$$C_2 = \left[\Theta_1^H b_1 - (\Psi_1 - b_2)\Theta_2^H + (\Psi_1 - b_2)V - b_1\delta\right]/(\Psi_2 - \Psi_1),$$

$$P_1 = (a_3 b_1 - b_3\Psi_2 + b_3 b_2)/(\Psi_1 - \Psi_2),$$

$$P_2 = (a_3 b_1 - b_3\Psi_1 + b_3 b_2)/(\Psi_2 - \Psi_1),$$

$$\delta = \frac{P_1}{\Psi_1 b_1}(\Psi_1 - b_2) - \frac{P_2}{\Psi_2 b_1}(\Psi_2 - b_2),\ V = -\frac{P_1}{\Psi_1} - \frac{P_1}{\Psi_2},$$

$$\Psi_{1;2} = \frac{b_2 + a_1 \pm \sqrt{(b_2 - a_1)^2 + 4a_2 b_1}}{2},$$

$$a_1 = b\xi\left[\nu^2 m\beta - (1+\nu)\right] - b'(1-\xi),\ a_2 = b\xi + b'(1-\xi),$$

$$a_3 = b\xi\frac{\nu^2}{2}\left[1 + (2-\nu)m\beta\right],\ b_1 = \eta b\xi + \eta b'(1-\xi),$$

$$b_2 = \eta b\xi\left[\nu^2\beta - (1-\nu)\right] - b'\eta(1-\xi),\ b_3 = \eta b\xi\frac{\nu^2}{2}\left[1+(2+\nu)\beta\right].$$

In the case of counter flow, the sign of the left side of the second equation of the initial system for the description of temperature fields of heat carriers along the heat exchanger should be changed for the opposite. It is the same as if in all the expressions for determination of Θ_1 and Θ_2 in the case of parallel flow instead of b_1, b_2, b_3 it is necessary to take $-b_1$, $-b_2$, $-b_3$.

Moreover, constants C_1 and C_2 must be found from the boundary conditions:

$$\Theta_1\big|_{x=0} = \Theta_1^H, \Theta_2\big|_{x=1} = \Theta_2^H.$$

In conformity with the foregoing, for determination of C_1 and C_2 in the case of a counter flow the following relations are used:

$$\begin{cases} \Theta_1^H = C_1(\Psi_1 - b_2)\dfrac{1}{b_1} + C_2(\Psi_2 - b_2)\dfrac{1}{b_1} + \delta, \\ \Theta_2^H = C_1 e^{\Psi_1} + C_2 e^{\Psi_2} + V. \end{cases} \tag{12}$$

From the system we obtain:

$$C_1 = \frac{-b_1(\Theta_1^H - \delta)e^{\Psi_2} + (\Theta_2^H - V)(\Psi_2 - b_2)}{(\Psi_2 - b_2)e^{\Psi_2} - (\Psi_1 - b_2)e^{\Psi_2}}, \tag{13}$$

$$C_2 = \frac{-b_1(\Theta_1^H - \delta)e^{\Psi_1} + (V - \Theta_2^H)(\Psi_1 - b_2)}{(\Psi_2 - b_2)e^{\Psi_1} - (\Psi_1 - b_2)e^{\Psi_2}}. \tag{14}$$

In these expressions, one should also replace b_1, b_2, b_3 by $-b_1$, $-b_2$, $-b_3$. And heat carrier temperatures in this case are found by the same formulae as for parallel flow.

The distinctive feature of counter flow mode is that in this case the radical expression in Ψ_1 and Ψ_2 may prove to be a negative value, i.e.

$$(b_2 - a_1)^2 + 4a_2b_1 < 0.$$

If such is the case, then Ψ_1 and Ψ_2 can be represented in a complex form:

$$\Psi_1 = \phi + j\Psi,\ \ \Psi_2 = \phi - j\Psi,$$

where $$\phi = (b_2 + a_1)/2,\ \ \Psi = \sqrt{\left|(b_2 - a_1)^2 + 4a_2b_1\right|}.$$

In this case, changes in the temperatures Θ_1 and Θ_2 along the heat exchanger will have the nature of harmonic oscillations.

In the case when Ψ_1 and Ψ_2 are real in counter flow mode, full temperature variations in the flows of cooled and heated heat carriers when passing through heat exchanger are equal to:

$$\Delta\Theta_1 = \Theta_1\big|_{x=0} - \Theta_1\big|_{x=1} = \frac{C_1}{b_1}(\Psi_1 - b_2)\left(1 - e^{\Psi_1}\right) + \frac{C_2}{b_1}(\Psi_2 - b_2)\left(1 - e^{\Psi_2}\right),$$

$$\Delta\Theta_2 = \Theta_2\big|_{x=0} - \Theta_2\big|_{x=1} = C_1\left(1 - e^{\Psi_1}\right) + C_2\left(1 - e^{\Psi_2}\right).$$

The results of computational experiment are given in Figs. 2 – 4.

As it follows from Fig. 2 showing plots of temperature variation at heat exchanger outlet versus its length, for the best use of thermoelectric heat exchange apparatus one should proceed from the requirements to it. For instance, to obtain a deeper cooling with the same current value, it is necessary to use a longer thermopile and a lower filling factor. In so doing, saving of thermoelements as compared to the case when they cover the entire surface ($\xi = 1$) is tangible enough. The plot suggests that at $\xi = 1$ maximum thermopile length in heat exchange apparatus for the above conditions is 1.1 m,

and liquid is cooled from 318 K to 312 K. The surface area of thermopile in this case is $S_1 = L \cdot \xi = 1.1\ L$ m^2. When $\xi = 0.2$, the length of thermopile in the heat-exchange apparatus whereby maximum possible cooling of liquid is attained is 3.6 m. In this case heat carrier is cooled from 318 K to 308 K, with the surface area of thermoelement $S_2 = 0.38$ m^2.

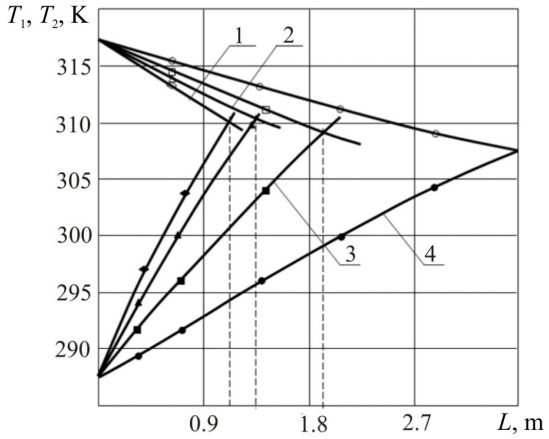

Fig. 2. Temperature variation of liquids at heat exchanger outlet versus length at different filling factors (1 – ξ = 1; 2 – ξ = 0,8; 3 – ξ = 0,5; 4 – ξ = 0,2; I = 10 A).

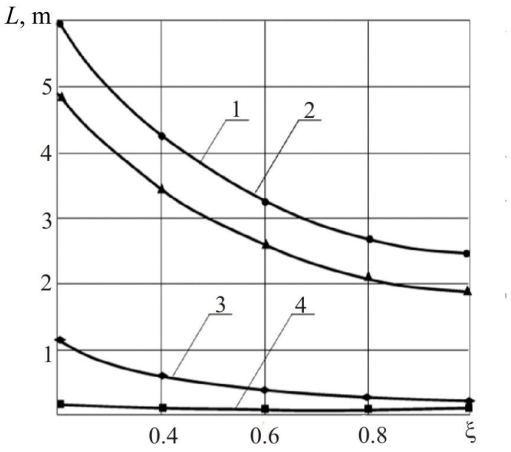

Fig. 3. Ultimate thermopile lengths in the intensification mode versus filling factor at different temperatures (1 – T^H = 327 K; 2 – T^H = 318K; 3 – T^H = 297 K; 4 – T^H = 293 K; T^H_2 = 287K; I = 5 A).

If we now compare these two cases, cooling of outlet liquid in the second case is deeper than in the first one. Moreover, surface area in the second case is smaller than the area in the first case, i.e. $S_2 < S_1$, which means saving of thermoelement material and consumable electric energy.

Fig. 3 represents the plots of change in ultimate thermopile lengths versus filling factor, i.e. the lengths whereby liquid temperatures at heat exchanger outlet are equal. As it follows from the represented data, the larger temperature difference of heat carriers at heat exchanger inlet, the larger thermopile length is necessary to hold the intensification mode. The plots are monotonously decreasing versus filling factor. The larger temperature difference of heat carriers at the inlet, the more drastically functions $L = L(\xi)$ decay at constant supply current $I = 5$ A.

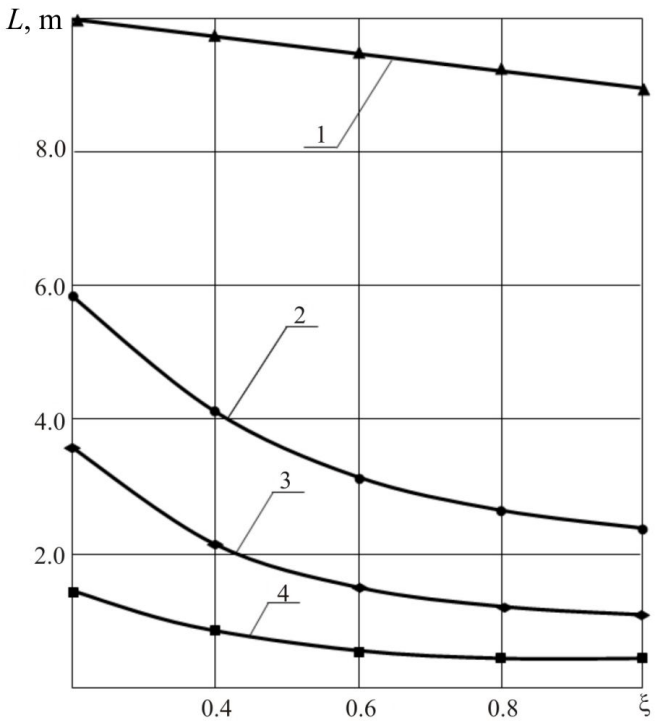

Fig. 4. Ultimate thermopile lengths in the intensification mode versus filling factor at different supply currents(1 – I = 1 A; 2 – I = 5 A; 3 – I = 10 A; 4 – I = 20 A; T^H_1 = 318 K; T^H_2 = 287 K).

Fig. 4 represents the plots of ultimate thermopile lengths in the intensification mode versus filling factor at various supply currents and constant temperature difference of heat carriers at heat exchanger inlet. Functions $L = L(\xi)$ are also monotonously decaying. In so doing, the larger supply current value, the smaller thermopile length is required to hold the intensification mode.

Analysis of calculation results shows that current value whereby the work of heat exchanger in the intensification mode is still possible essentially depends on temperature difference of heat carriers at heat exchanger inlet. The higher this difference, the larger is current magnitude in the intensification mode with otherwise equal parameters.

The results of calculation of coefficient of performance ε(ν), coefficient of conversion μ(ν) and heat carrier temperatures at heat exchanger outlet 1 m and 0.5 m, T_{1inl} = 45°C, T_{2inl} = 14°C are given, where T_{1inl}, T_{2inl} are inlet temperatures of cooled and heated heat carriers. According to these data, the larger filling factor, the smaller current variation area for the intensification mode. A deeper cooling can be achieved in the intensification mode with smaller currents, but with larger values of filling factor ξ. However, with lower ξ values such cooling may not be, since considerable current increase leads to further heating of cooled heat carrier. As regards heated heat carrier, with the same current value a more intensive heating occurs at low values of factor ξ. Comparison of coefficients of performance or conversion coefficients shows that under otherwise equal conditions these coefficients are higher in the lower length heat exchanger. If we consider one and the same heat exchanger with different ξ values, these coefficients are higher for lower ξ values.

The results of calculations of ε(ν), μ(ν) and heat carrier temperatures at heat exchanger outlet with thermopile length 0.24 m, T_{1inl} = 30°C, T_{2inl} = 21°C are given. In this case the ranges of current values whereby the intensification mode is observed for different filling factors are close to each other. These ranges decay more slowly than in the case of higher temperature difference of heat carriers at

heat exchanger inlet. And the difference in temperatures at heat exchanger outlet for ultimate current values in the intensification mode is not more than one degree.

Experimental investigations of heat exchange apparatus.

To perform full-scale investigations of heat exchange apparatus, a test bench was developed the basic diagram of which is shown in Fig. 5.

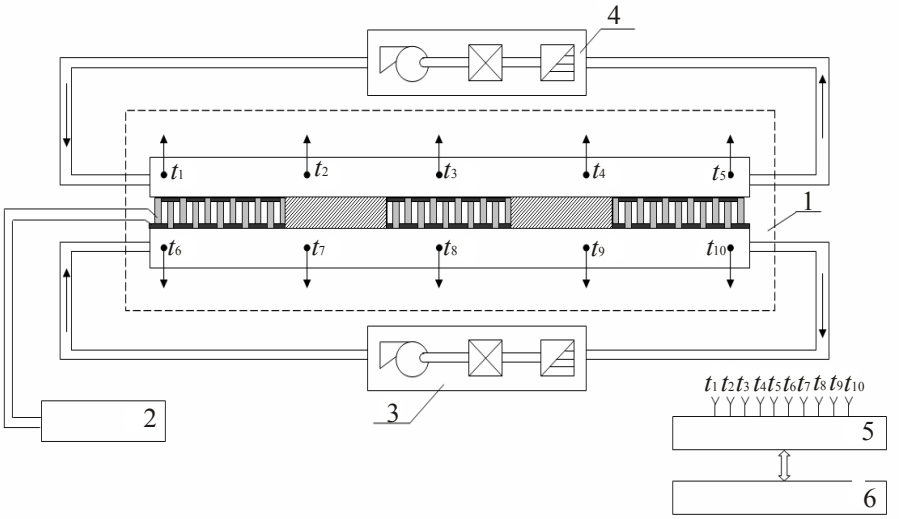

Fig. 5. Basic diagram of test bench.

Heat exchange apparatus 1 is connected to circulation loops of cold and heat carriers in which capacity water is used, as well as to adjustable direct current source 2. Ultra thermostats 3 and 4 maintain given temperatures of cold and heat carriers at heat exchange apparatus outlets to an accuracy of 0.1°C and provide for their circulation. Flow rates in the cold and heat carrier loops are adjusted by valves located on the respective ultra thermostats.

Recording of current temperature values is done by measuring system IRTM 2402/M3 5 which is connected to PC 6 and provides for possible connection of up to 24 temperature sensors.

The object for experimental studies was a thermoelectric heat exchange apparatus of flow-through type (Fig. 6), consisting of two steel pipes with internal diameter 7 mm and length 250 mm. The outer surface of the pipes was polished as a tetrahedron 20 × 20 mm. As thermopiles, unified thermoelectric modules (TEM) of BPTM and TEM types, developed in the laboratory of semiconductor thermoelectric instruments and devices of Dagestan State Technical University, were used.

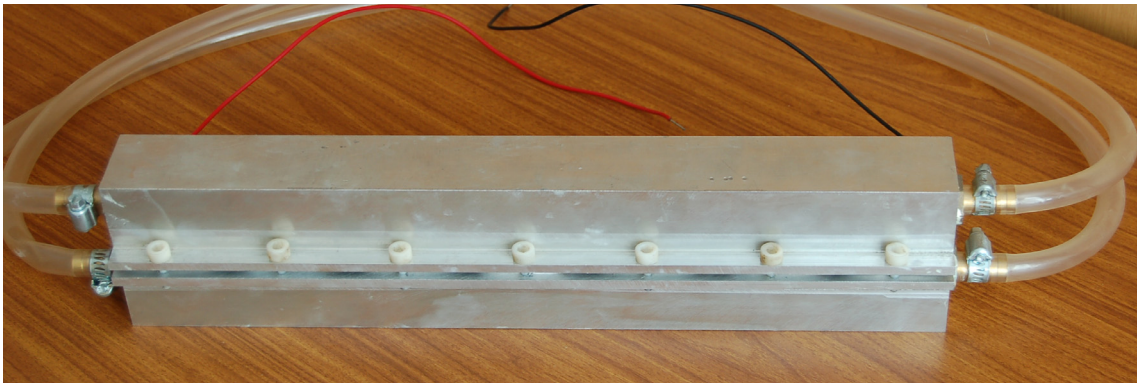

Fig. 6. External view of a thermoelectric heat exchange apparatus with thermal bridges.

Electrically connected in series, TEM and thermal bridges are fixed between the two pipes through thermally conductive paste KPT.

To exclude heat exchange with the environment, the entire structure is placed into a foam package. Mounted on the lateral faces along the length of the pipes are copper-constantan thermocouples $t_1 - t_{10}$ the reference junctions of which are thermally stabilized at 0°C in a Dewar flask.

Experimental curves of temperatures distribution along the length were obtained by measurement of temperatures at different points of heat exchange apparatus:

– for different factors of filling with semiconductor modules,

– for different currents flowing through thermoelement,

– for different materials of thermal bridges.

All the experiments were carried out at given constant temperatures and flow rates of cold and heat carriers at structure inlets. For this purpose, only semiconductor TEM in the amount of 10 were placed at first in the heat exchange apparatus (100% filling with TEM, filling factor $\xi = 1$).

Ultra thermostats were used to maintain the assigned flow rates and temperatures of cold and heat carriers at the inlets. On stabilizing the mode of ultra thermostats (in 15 – 20 minutes), a program of cyclic polling of thermocouples was run on the measuring system with subsequent output of temperature values to PC. At the same time, the heat exchange apparatus was connected to direct current source by the measuring instrument of which the necessary value of supply current was established.

Filling factor was varied as follows. After device assembly, part of TEM were disconnected, the remaining modules were moved apart and uniformly distributed along the length of the pipe, between the TEM thermal bridges were installed made of suitable material (copper, aluminum, steel), the total area of which was equal to the total area of modules removed. For this purpose, thermal bridges of different sizes were manufactured. Thus, for instance, to obtain 80% of filling ($\xi = 0.8$), two modules of 10 were removed, to be replaced by two thermal bridges, each of which is equal to 1/4 of module area.

Based on the test bench, a series of experiments was carried out giving an idea of practical applicability of the elaborated mathematical model of thermoelectric heat exchange apparatus with thermal bridges.

The basic task when performing the experimental investigations of the prototype of heat exchange apparatus was to determine the dependence of temperature at the above control points on thermoelement supply current, filling factor and thermal bridge material.

Fig. 7 presents the results of experimental investigations (points) of heat exchange apparatus under steady-state operating modes with different TEM filling factors and, for comparison, the results of theoretical calculations (solid line). The calculations employed passport data on thermophysical properties of semiconductor substance and characteristics of TEM used in the structure, the geometric parameters of legs, and the values of contact electric and thermal resistances. The heat capacities of the pipes in the calculations were disregarded. Comparison with the results shows an agreement between the calculated and experimental data. Maximum quantitative discrepancies between the theoretical calculations and the experimental results not exceeding 12% were observed in the initial section of the pipelines, which can be considered satisfactory. From the figure it follows that as filling factor increases, temperature distribution curves change more drastically, i.e. heat exchange apparatus operates more efficiently.

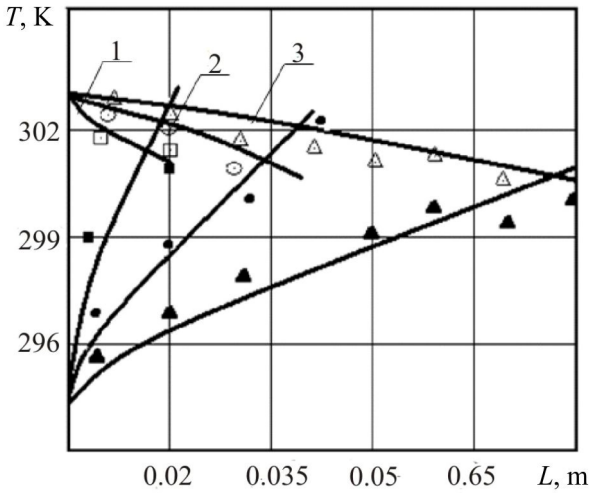

Fig. 7. Experimental and theoretical dependences of heat carrier temperatures at heat exchanger outlet on length at different filling factors (1 – ξ = 1.0; 2 – ξ = 0.5; 3 – ξ = 0.2; TEM supply current 1.8 A).

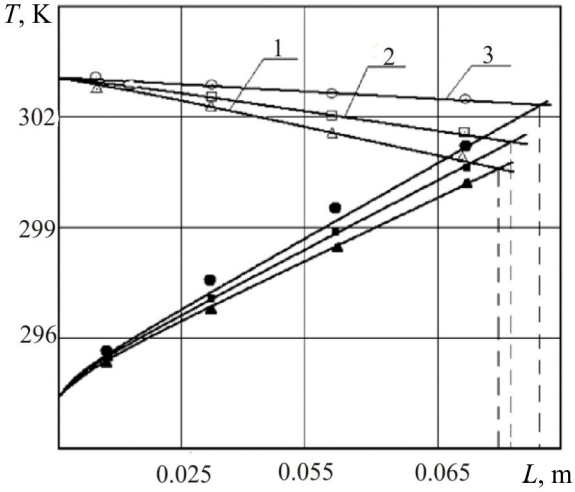

Fig. 8. Experimental and theoretical dependences of heat carrier temperatures at heat exchanger outlet on length for thermal bridges of different materials (1 – copper, 2 – aluminum, 3 – steel; TEM supply current 1.8 A)

Fig. 8 shows the curves of temperature distribution along the length of heat exchange apparatus with filling coefficient ξ = 0.2 for thermal bridges made of different materials: copper, aluminum and steel. From the represented data it follows that the operating efficiency of heat exchange apparatus does not essentially depend on thermal bridge material, as confirmed by the results of numerical experiment. However, the use of copper thermal bridges is more efficient, which is due to a higher thermal conductivity of this material.

Fig. 9 shows a dependence of thermopile length with device operation in the intensification mode on supply current at filling factor ξ = 0.5 for thermal bridges made of copper. As is obvious, increase in supply current reduces the area of heat exchanger where thermopile works in the mode of heat exchange intensification. For instance, with current increase by 0.5 A for given conditions the above length is reduced by 1.8 cm.

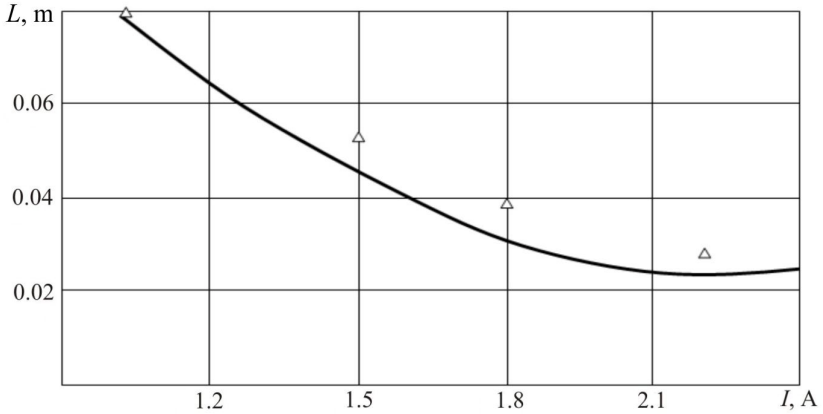

Fig. 9. Dependence of thermopile ultimate length in heat exchange apparatus on supply current (ξ = 0.5, thermal bridge material – copper).

Fig. 10 shows experimental time dependences of temperature variation at a point 1.5 cm distant from heat exchanger inlet. The represented data suggest the onset of stabilization in about 27 minutes after thermopile switching.

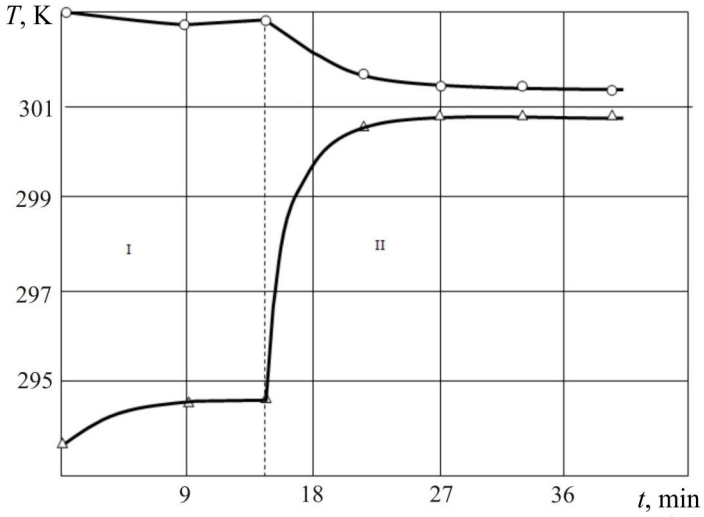

Fig. 10. Dependence of heat carrier temperatures on time without (area I) and with switched thermopile (area II) (ξ = 0.8, L = 0.015 m; I = 1.8 A, thermal bridge material – copper).

On the whole, the results of experimental investigations prove the validity of the elaborated mathematical model.

Conclusions

1. On the basis of investigations performed, the following conclusions can be made:
2. Based on the results of the survey of methods for heat exchange intensification, as well as the structures of heat exchangers it is shown that for the intensification of heat exchange between two heat carrier flows it is advisable to use thermoelectric power converters.
3. A new concept of creating thermoelectric recuperative-type heat exchangers consisting in combination of heat transfer through highly thermally conductive material (thermal bridge) heat exchange intensification with the use of thermopiles.
4. A mathematical model is developed for the calculation of thermal mode of thermoelectric recuperative-type heat exchangers combined with thermal bridges of various configurations.
5. The basic characteristics of thermoelectric heat exchanger with thermal bridges have been calculated, including temperature variation of heat carriers depending on filling factor, thermopile supply current, as well as the length of heat exchange apparatus.
6. The adequacy of the elaborated mathematical model has been proved experimentally; comparison of the experimental and calculated data has shown that their discrepancy has not exceeded the permissible values.

References

1. K.F.Karimov, Performance Evaluation of Heat Exchangers for Refrigerating Machines, *Herald of International Academy of Refrigeration* **4**, 14 – 16 (2006).
2. L.I.Anatychuk, *Thermoelectricity. Vol. 2. Thermoelectric Power Converters* (Kyiv-Chernivtsi: Institute of Thermoelectricity, 2003).
3. T.A.Ismailov, *Thermoelectric Semiconductor Devices and Heat Transfer Intensifiers* (Saint-Petersburg: Polytekhnika, 2005).

Submitted 15.06.2015.

Sh. A. Yusufov

Sh. A. Yusufov, M. A. Khazamova

Federal State Budgetary Educational Institution of Higher Professional Education "Dagestan State Technical University", 70, Imam Shamil avenue, Makhachkala, 367015, Russia

M. A. Khazamova

THERMOELECTRIC SYSTEM OF CONTRAST THERMAL EFFECT ON THE REFLEXOGENIC ZONES OF HUMAN FOOT

The paper deals with a thermoelectric system for contrast thermal effect on the reflexogenic zones of human organism, in particular, for local effect on the lower surface of human foot. The results of its mathematical simulation and prototype full-scale test are presented. Experimental plots of temperature variation at different system points are given.

Key words: reflexogenic zone, thermoelectric system, thermopile, thermal effect, temperature field, mathematical model, prototype, experiment.

Introduction

In modern medical practice increasing acceptance is gained by the methods based on the use of various physical factors (heat, electromagnetic radiation, low-potential electric effect, etc). The advantage of these methods over pharmacotherapy in medical rehabilitation, treatment and health improvement lies in the fact that they stimulate own resources of the organism, that is, sanogenesis processes, actually have no contraindications and do not result in any considerable complications when administered.

The methods using physical factors also include local thermal effect on the biological tissues that has certain specific features. Unique therapeutic properties of heat and cold are physiologically and immunologically substantiated when affecting human organism and its individual organs and areas, in particular, low-conductivity reflexogenic zones. One of the areas of medicine where exposure to heat is efficient is physiotherapy, especially with regard to locomotor apparatus treatment.

Currently known methods of exposure to heat (contrast baths, whirlpool baths, paraffin and ozokeritotherapy, etc.) have various shortcomings [1], such as low efficiency, procedure discomfort, impossibility of contrast combined exposure to several physical factors. Under these conditions, it is efficient to use as a source of cold and heat the thermoelectric power converters offering high reliability, environmental friendliness, and noise-free operation, possibility of quick transition from cooling to heating mode and vice versa.

At the Research Institute of Semiconductor Thermoelectric Instruments and Devices of Federal State Budgetary Educational Institution of Higher Professional Education "Dagestan State Technical University" a semiconductor thermoelectric (TE) device has been developed for carrying out physiotherapeutic thermal procedures related to effect on the reflexogenic zones of human foot [3, 4]. The device design is shown in Fig. 1, and its appearance – in Fig. 2. the device comprises a thermopile 1 the first junctions of which are in thermal contact with the lower surface of human foot 2 through bath 3 made of highly thermally conductive material having on its bottom metal balls 4, also made of

high thermal conductivity materials. Heat removal from the second junctions of thermopile 1 is done by liquid heat exchanger 5. The operating modes of thermopile 1 are controlled by programmable supply unit.

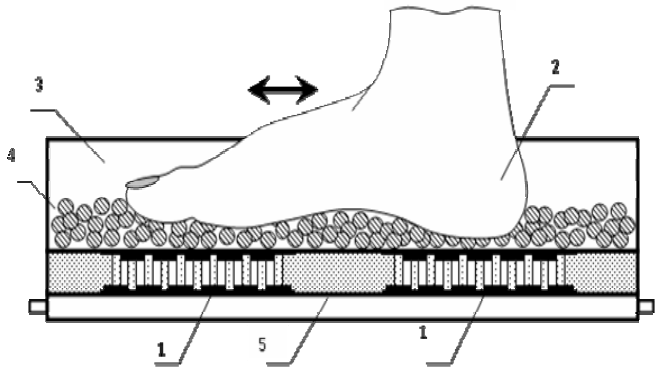

Fig. 1. Design of thermoelectric device for carrying out physiotherapeutic procedures.

Fig. 2. Appearance of thermoelectric device for carrying out physiotherapeutic procedures.

The purpose of this work is theoretical and experimental investigation of the above described design with a view to optimize its characteristics.

Mathematical simulation of thermoelectric system for contrast thermal effect on the reflexogenic zones of human foot

In the analysis of operation of thermoelectric systems used for cryothermoapplication, i.e. the use of local thermal effect, it is very important to know not only the steady-state characteristics of device, but also the peculiarities of transient processes of device-target object system. It is due to the necessity of evaluation of such parameter of thermoelectric device operation as the time to reach given operating mode, as well as determination of the dynamic characteristics of device.

To evaluate said parameters, a quasi-stationary model of transient process of device for thermal effect on human foot was created which considers a thermoelectric device as a single combination of elements – heat exchangers, thermopile, and thermal insulation assuring temperature reduction of biological object within required time to required value.

We now consider a thermal model of system under study which is shown in Fig. 3.

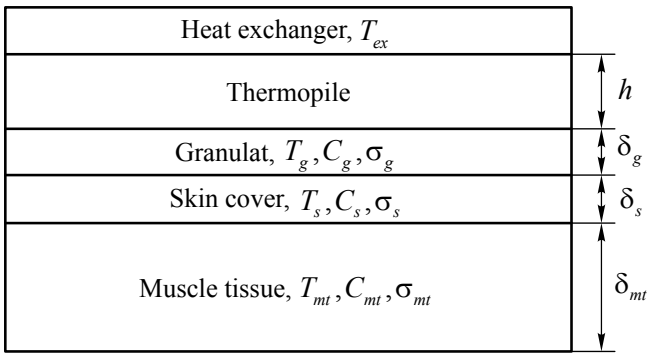

Fig. 3. Thermal model of thermoelectric system.

In this system, a thermopile through heat exchanger of heat capacity C_g and thermal

conductivity σ_g with its first (internal) junction is connected to target object more simply represented as a two-layer structure consisting of skin cover and muscle tissue of heat capacity C_g, C_{mt} and thermal conductivity σ_s, σ_{mt}, respectively. The temperature of external thermopile junction via air or liquid heat exchanger is maintained at certain time-invariant value T_{ex}. Current of constant density *j* flows through the thermopile. Moreover, it is supposed that heat exchange between tissue and blood occurs at any point of biological object under study and is characterized by specific power of volumetric heat sources P_s and P_{mt} for skin cover and muscle tissue, respectively.

Mathematical realization of the model is determined by a system of the following differential equations [2]:

$$\left.\begin{aligned} \frac{dT_g}{d\tau} &= \frac{1}{C_g}\left[\sigma_g\left(T_s - T_g\right) + \left[qejT_g + \frac{1}{2}j^2\rho h + \frac{\lambda}{h}\left(T_{ex} - T_g\right)\right] + \sigma_g\left(T_{amb} - T_g\right)\right] \\ \frac{dT_s}{d\tau} &= \frac{1}{C_s}\left[\sigma_g\left(T_g - T_s\right) + \sigma_s\left(T_{mt} - T_s\right) + P_s\right] \\ \frac{dT_{mt}}{d\tau} &= \frac{1}{C_{mt}}\left[\sigma_s\left(T_s - T_{mt}\right) + P_{mt}\right] \end{aligned}\right\} \quad (1)$$

where T_g is temperature of heat exchanger which is in thermal contact with the biological object; T_s is skin cover temperature; $q = -1$ at thermopile operation in target object cooling mode, $q = 1$ at thermopile operation in target object heating mode; *e* is the Seebeck coefficient of thermoelements in a thermopile; ρ is thermopile electric resistivity; *h* is the height of thermoelements in a thermopile; λ is thermal conductivity of thermopile material; T_{amb} is ambient temperature; T_{mt} is temperature of muscle tissue.

The initial conditions are assigned on the assumption that at initial time instant a TE device is in thermodynamic equilibrium with the environment and the temperature of all system points is equal to ambient temperature, and the temperature of target object is 309 K.

The solution of system (1) was done numerically in MATHCAD applied program package with the use of the Runge-Kutta fourth-order method. Calculation was done with the following input data: $e = 350 \cdot 10^{-6}$ V/K; $h = 0.002$ m; $\lambda = 3$ W/m·K; $\rho = 0.0001$ Ohm·m; $C_g = 380$ J/kg·K; $C_s = 3600$ J/kg·K; $C_{mt} = 3458$ J/kg·K. In so doing, thermal conductivities were determined by the formulae:

$$\sigma_g = \frac{\lambda_g \cdot S}{\delta_g}, \quad (2a)$$

$$\sigma_s = \frac{\lambda_s \cdot S}{\delta_s}, \quad (2b)$$

$$\sigma_{mt} = \frac{\lambda_{mt} \cdot S}{\delta_{mt}}, \quad (2c)$$

where λ_g, λ_s, λ_{mt} is thermal conductivity of heat exchanger, skin cover and muscle tissue, respectively; *S* is the area of contact surface between TE device for cryothermoapplication and biological target object; σ_g, σ_s, σ_{mt} is the thickness of heat exchanger, skin cover and muscle tissue layer, respectively. The numerical values of original quantities in expressions (2) were assumed to be as follows: $\lambda_g = 200$ W/m·K; $\lambda_s = 0.389$ W/m·K; $\lambda_{mt} = 0.2$ W/m·K; $S = 0.015$ m^2; $\delta_g = 0.02$ m; $\delta_s = 0.002$ m; $\delta_{mt} = 0.03$ m.

Figs. 4 – 5 show the results of calculation of thermal field of device-target object system as a function of time at $T_{amb} = T_{ex} = 293$ K for the case of thermopile operation in cooling mode (Fig. 4) and heating mode (Fig. 5) of biological object. Time variation of heat exchanger temperature on thermopile internal junction, skin cover and muscle tissue temperature has been analyzed. As it follows from the represented data, the dependences are of monotonous nature – decreasing at thermopile operation in cooling mode and increasing when using thermopile in biological object heating mode.

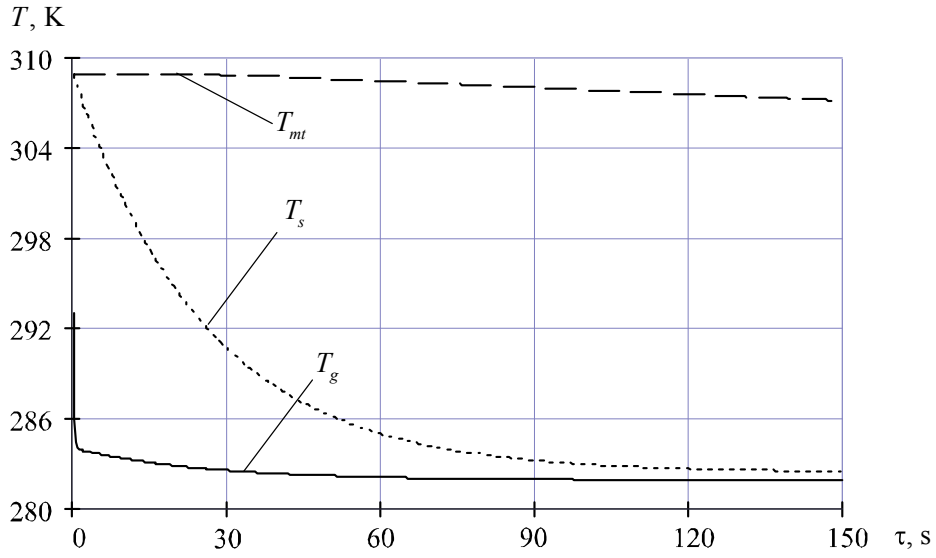

Fig. 4. Time history of granulate temperature on the internal junction of thermopile, skin cover and muscle tissue in cooling mode.

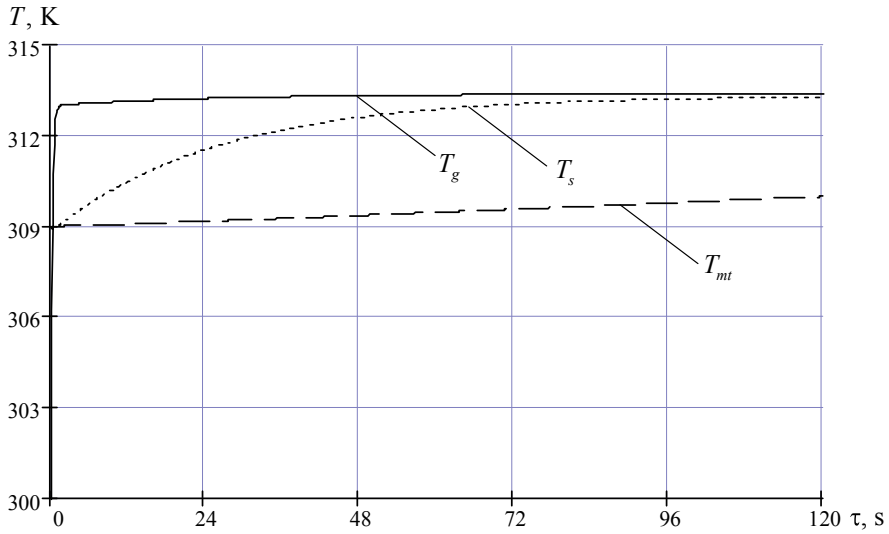

Fig. 5. Time history of granulate temperature on the internal junction of thermopile, skin cover and muscle tissue in heating mode.

According to the plots, the temperature of heat exchanger and skin cover is rather quickly stabilized (in case of cooling, the time to reach the steady-state of heat exchanger and skin cover temperature is 93 and 120 s, respectively, and in case of heating – 72 and 96 s), which is due to low heat capacity and high thermal conductivity of heat exchanger, as well as small thickness of skin cover. Assuming that exactly skin cover is rich in thermal receptors and is a direct object of

cryothermoapplication, this fact indicates to apparent advantages of TE device use which are primarily due to fast response of thermal effect.

Fig. 6 shows the plots of time variation of skin cover temperature for different values of thermopile supply current I ($j = \frac{I}{S}$). The data are given for the case of local cooling and heating of target object. According to these dependences, the duration of temperature stabilization of skin cover in the considered current range is constant and makes about 120 s. In Fig. 6, a dependence of skin cover cooling on supply current value can be traced. From the plots describing time variation of skin cover temperature it follows that with a change of current force from 0 to optimal value whereby there is maximum temperature reduction on thermopile cold junction (in the present case 2 A), the ratio of temperature variation to current force variation is reduced.

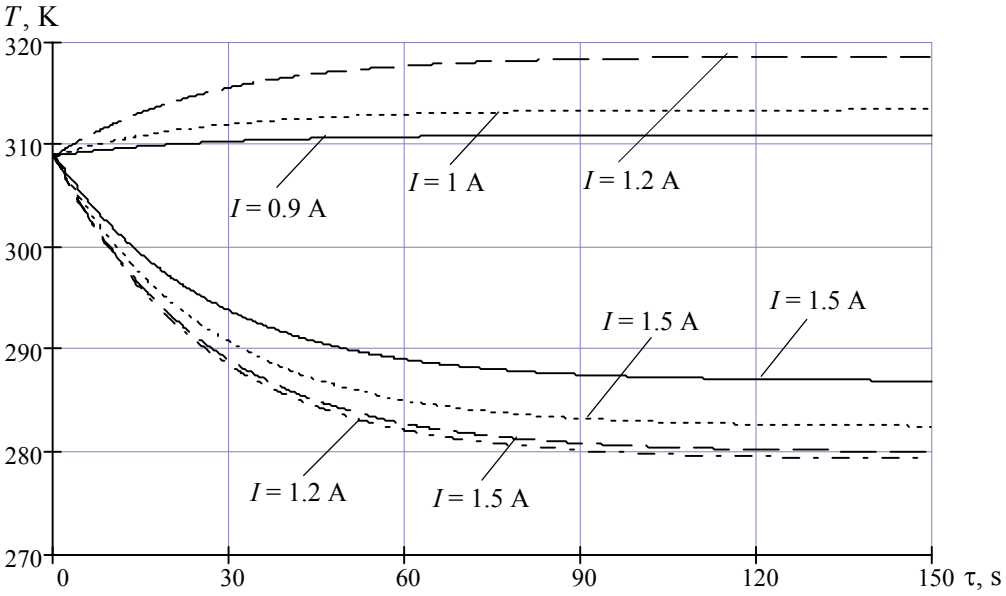

Fig. 6. Time history of skin cover temperature at different supply currents of thermopile operated in cooling mode.

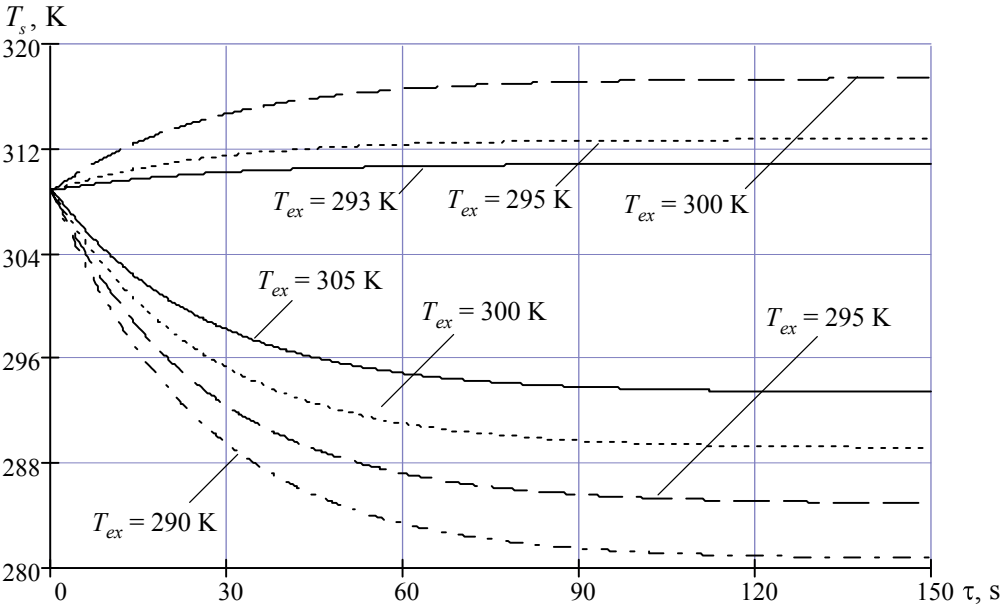

Fig. 7. Time history of skin cover temperature at different values of T_{ex}.

Thus, for the above case (upon reaching of steady-state) with increasing supply current from 0.5 A to 1 A, the temperature of skin cover is reduced from 286.5 K to 282.5 K, increase of current strength from 1 A to 1.5 A reduces the temperature from 282.5 K to 280 K, and increase of supply current from 1.5 A to 2 A reduces the temperature to 279.5 K. Further increase in current strength leads to prevailing of the Joule heat over the Peltier heat, increasing the temperature of target object. Thus, at fixed temperature T_{ex} of TE device the ultimate temperature reduction of biological object is limited by the value of thermopile supply current optimal for this thermopile type. A deeper temperature reduction of target object can be obtained by reducing the value of T_{ex}. This is illustrated in Fig. 6, showing time variation of skin cover temperature for different values of T_{ex} in cooling and heating modes of TE device (supply current – 0.9 A). From the analysis of data shown in Fig. 6 and Fig. 7 it follows that for the reduction of skin cover temperature, for instance, to 280 K at a temperature T_{ex} = 290 K, one needs 0.6 A less than at stabilization of T_{ex} on the level of 293 K. At the same tine, reduction of temperature of external junction (T_{ex}) requires increase in thermopile supply current with operation of the latter in the mode of biological object heating to obtain the same temperature of skin cover. However, it should be noted here that the required increase of thermopile supply current is insignificant. In so doing, a gain in electric energy consumption at TE device operation in cooling mode is vastly superior to its loss at TE device operation on biological object heating mode.

Experimental investigations of thermoelectric system for local freezing of larynx tissues.

In order to verify the results of mathematical simulation, a prototype of this thermoelectric system was subject to full-scale test. The object of experimental investigations was a prototype for effect on human foot in the form of a case comprising a thermopile made of standard unified thermoelectric modules (TEM), brought by the junctions into a thermal contact with the case base in the form of a copper plate that can be filled with copper granulate. The opposite thermopile junctions were in a thermal contact with liquid heat exchanger intended for heat pick-up.

In the course of the experiment, the prototype was placed into thermally insulated climatic chamber that has a thermostated work volume 120 l. The chamber provides for temperature upkeep from 283 to 343 K to accuracy of 1°C and with a relative humidity from 30% to 98%. Given temperature and relative humidity in the chamber is regulated by control unit connected with temperature and humidity sensor whose readings are registered on a digital display.

As thermopiles, standard unified TEM of ICE-71 type were used, produced by Engineering and Production Firm “Kryotherm” and connected in parallel. The TEM were powered from electric energy source. The flow rate of liquid in a heat exchanger was regulated by a controller. The measurements were conducted with the use of ammeter and voltmeter built into electric energy source, liquid flow rate sensor in liquid flow rate controller and a multi-channel meter IRTM 2402/ M3 connected to PC.

During the experiment, the thermopile voltage and current, ambient temperature and the temperatures at different points of the prototype were determined. Temperature measurements were performed by copper-constantan thermocouples the reference junctions of which were arranged in a Dewar vessel, and the signal was read by IRTM 2402/M3 meter.

Thermocouples were located on the reference and operating junctions of TEM, at heat exchanger inlet-outlet, on the surface of plate (edge and centre), in the ambient, on granulate layers (using the latter in the process of experiment), as well directly on the biological object (in this case human foot).

The measurements were performed for the case of device idle operation (without thermal load), under thermal load, with and without granulate in device (measurements were performed with the use of granulate of various diameters, from 4 mm to 10 mm, with increment 2 mm). The experiment was carried out with direct thermal effect on human foot the temperature of which was controlled by thermocouples placed on the sole.

Figs. 8 – 9 represent time dependences of plate temperature and sole temperature at different currents in heating mode (Fig. 8) and cooling mode (Fig. 9).

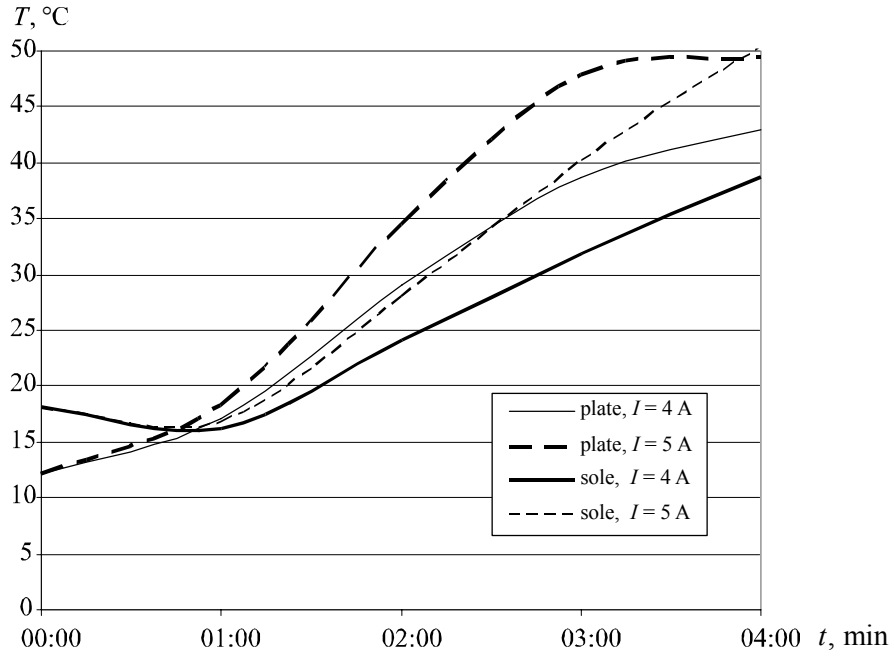

Fig. 8. Time history of temperature on the plate and foot at different supply currents of thermopile operated in heating mode.

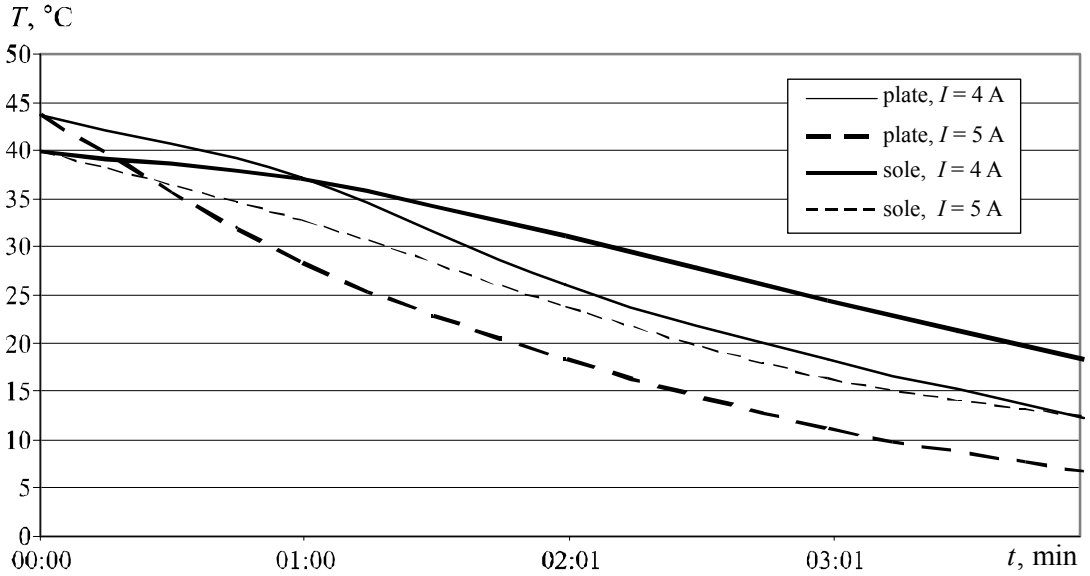

Fig. 9. Time history of temperature on the plate and foot at different supply currents of thermopile operated in cooling mode.

Investigation of these dependences shows that plate temperature grows with increasing thermopile supply current, whereas on the sole one can observe processes of thermal regulation of

living systems. At first instant of exposure to heat the sole temperature is drastically increased which is due to vasoconstriction, the second phase is accompanied by vasodilatation, afflux of blood to effecting zones and, as a result, insignificant temperature reduction. Then, thermoregulation mechanisms are involved, and temperature is gradually equalized depending on the effecting mode. It is noteworthy that plate temperature reaches the required value, namely 42 – 450°C in heating mode and 10 – 120°C in cooling mode within 3-5 minutes.

Apart from that, during our experimental investigations the following dependences were obtained: temperature variation of the operating and reference junctions of TEM versus supply current value, temperature at different plane points versus current, the curves of heating and cooling time in the range of temperatures from 10°C to 45°C versus supply current, as well as transient characteristics of device.

Fig. 10 shows transient characteristics, since this device is intended for operation in a dynamic mode, providing for alternative exposure to heat and cold.

Analysis of the dependences has shown that total time of one cycle with supply current 5 A is about 6 – 7 min, heating mode being assured in 2 – 3 min and cooling mode – in 3 – 5 min.

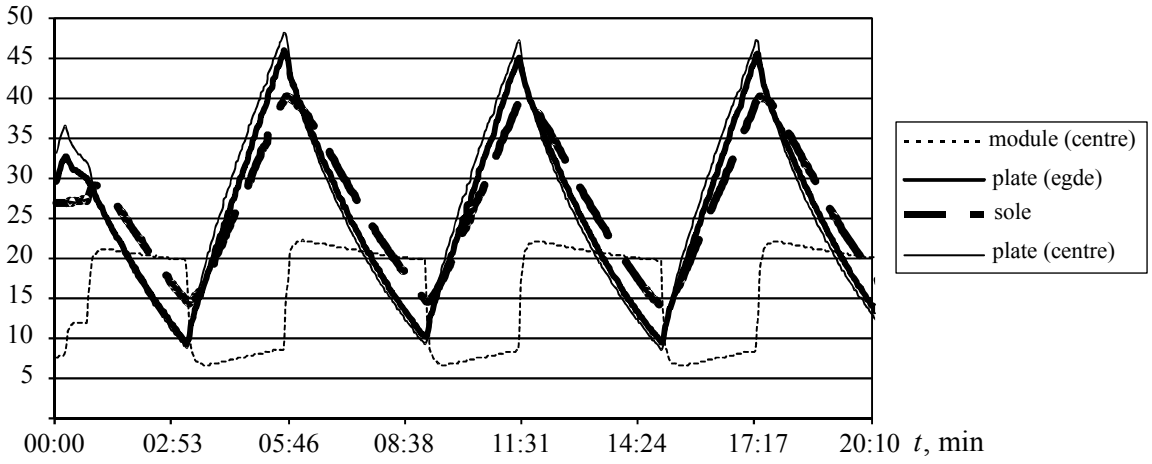

Fig. 10. Dependence of T in a dynamic mode at supply current I = 5 A.

The results obtained define the acceptable accuracy of system mathematical model. Maximum discrepancy between the calculated and experimental data does not exceed $7 – 7.5^0$C. The greatest deviation of calculated data is mainly observed during the interval related to time necessary for device to reach the mode, which is due to environmental influence and non-perfect thermal insulation of "device-target object" system, as well as certain spread in parameters of TEM and measuring instruments.

Conclusions

On the basis of investigations performed, the following conclusions can be made:

1. A thermoelectric device for contrast thermal effect on the reflexogenic zones of human foot, composed of a thermopile, a bath filled with granules/granulate and heat exchanger, has been developed
2. A quasi-stationary mathematical model of the system under steady-state conditions has been created.
3. An experimental bench and measurement procedure for prototype full-scale test have been developed.

4. The results of experimental research on device prototype have shown satisfactory repeatability of calculated and experimental data.

References

1. V.T. Olefirenko, *Heat-Water Therapy* (Moscow: Meditsina Publ., 1986), 288p.
2. V.D. Molostov, *Acupuncture: Practical Guide* (Rostov/Don, 2000), 480p.
3. *Patent RF № 2245693*, Semiconductor Thermoelectric Device for a Local Thermal Effect on Human Foot / T.A,Ismailov, G.I.Aminov, O.V.Yevdulov, M.A. Khazamova //Bulletin of Inventions № 4, 2002.
4. *Patent RF № 2245694*, Semiconductor Thermoelectric Device for a Local Thermal Effect on Human Foot / T.A.Ismailov, G.I.Aminov, A.Zarat, O.V.Yevdulov, M.A.Khazamova // Bulletin of Inventions № 4, 2002.
5. T.A. Ismailov, O.V. Yevdulov, and M.A. Khazamova, Mathematical Model of Semiconductor Thermoelectric Device for Thermal Effect on Human Foot, *Izvestiya Vuzov: Instrument Engineering* **47**(7), 43 – 50 (2004).

Submitted 17.06.2015

NEWS

L. P. Bulat[1], M. I. Fedorov[2]

[1]ITMO University, Kronverkskii ave 49,
Saint Petersburg, 197101, Russia;
[2]Ioffe Physical-Technical Institute,
26 Politekhnicheskaya,
St Petersburg 194021, Russia

L. P. Bulat

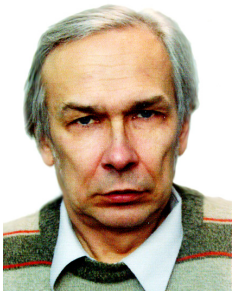

M. I. Fedorov

INTERNATIONAL LABORATORY "DIRECT ENERGY CONVERSION AND NANOENGINEERING OF THERMOELECTRIC STRUCTURES"

In 2013 the Government of the Russian Federation developed and approved a plan of measures on the development of the Russian universities and improving their competitiveness among leading world scientific-educational centres. As a result of implementation of this plan, by 2010 at least five Russian universities are to be inside the top hundred of leading world higher educational institutions.

Saint-Petersburg National Research University of Information Technologies, Mechanics and Optics (ITMO University) [1] was selected on a competitive basis to join a group of 15 leading Russian universities that are supported by the government for the implementation of the program of improving their international competitiveness.

In conformity with the "roadmap", a number of international laboratories have been organized at the ITMO University. In particular, we initiated creation of the International Laboratory "Direct Energy Conversion and Nanoengineering of Thermoelectric Structures" [2]. The Laboratory was opened on September 10, 2013 on the basis of the Electrical and Electronic Engineering Chair, ITMO University and Physics of Thermoelements Laboratory, Ioffe Physical-Technical Institute.

The Laboratory is headed by L.P.Bulat, D.Sc. in Physics and Mathematics, Head of the Electrical and Electronic Engineering Chair, ITMO University; M.I.Fedorov, D.Sc.,Head of the Physics of Thermoelements Laboratory, Ioffe Physical-Technical Institute and Dr. Gerald Jeffrey Snyder, Head of the Caltech thermoelectrics group [3].

More than 20 well-known foreign scientists and company leaders are Associate Members of the Laboratory [4]. Involved in the work are students studying at the ITMO University according to master's program 141200.68.04 "Thermoelectric energy conversion", as well as postgraduate students.

International Laboratory "Direct Energy Conversion and Nanoengineering of Thermoelectric Structures" actively cooperates with the following Russian organizations: "GIREDMET" JSC, the National University of Science and Technology "MISiS", Technological Institute for Superhard and Novel carbon Materials (FSBI TISNUM), KRYOTHERM Scientific Production Company, etc.

The main line of research in the Laboratory is creation of high-performance thermoelectric materials, including those based on nanostructures, and development on their basis of a new generation of ecologically clean coolers and generators.

The applications of developed thermoelectrics include:

1. Ecologically clean solid-state cooling – the best technical solution for problems of temperature reduction and thermal management of the components of microelectronics, optoelectronics and lighting technology, cooling of medico-biological objects, laboratory devices and

scientific equipment.

2. Thermoelectric generation of electric energy from low-grade heat sources makes it possible to use waste heat from transport units and energy plants, to provide power supply to telecommunication systems, space stations and to use the thermal part of solar radiation spectrum.

The Laboratory is interested in participating in various international scientific or educational programs or projects, in creating joint educational programs in master and postgraduate courses with leading world universities, in attracting Russian and foreign master and postgraduate students, young scientists to the work in the Laboratory.

International Laboratory "Direct Energy Conversion and Nanoengineering of Thermoelectric Structures" is ready to cooperate with all interested colleagues in the pursuance of research works and organization of teaching process for master and postgraduate students.

1. http://en.ifmo.ru/
2. http://irc.ifmo.ru/en/87791/history/main_info.htm
3. http://thermoelectrics.caltech.edu/
4. http://www.its.org/content/laboratory-direct-energy-conversion-and-nano-engineering-thermoelectric-structures

L. P. Bulat[1], M. I. Fedorov[2], A. V. Novotelnova[1]

[1]ITMO University, Kronverkskii ave 49, Saint Petersburg, 197101, Russia;
[2]Ioffe Physical-Technical Institute, 26 Politekhnicheskaya, St Petersburg 194021, Russia

MASTER'S PROGRAM "THERMOELECTRIC ENERGY CONVERSION" AT ITMO UNIVERSITY

In September 2013 at Saint-Petersburg National Research University of Information Technologies, Mechanics and Optics (ITMO University), for the first time in the Russian Federation, training of masters started in the program 141200.68.04 "Thermoelectric energy conversion".

ITMO University is one of the oldest educational institutions in Russia. 2010 marked 110 years since the date of adoption of the decision by the State Council of Russian Empire "On the foundation of a Mechanics, Optics and Watchmaking Department in the Prince Nicholas Vocational School". The University is a successor of Leningrad Institute of Fine mechanics and Optics (LIFMO). In 2009, based on the results of competitive selection by the Ministry of Education and Science of the Russian Federation, the university gained the status of "national research university".

ITMO University is one of 15 leading Russian universities. Students take training at 18 departments, institutes and academies. Full-time department trains bachelors in 31 majors and 94 specialties, and correspondence department – in 27 majors. 190 master's programs in 32 majors are implemented at ITMO University.

Master's program "Thermoelectric energy conversion" has been organized and supervised by the Electrical and Electronic Engineering Chair together with the Physics of Thermoelements Laboratory, Ioffe Physical-Technical Institute. Most qualified instructors, including those from Ioffe Physical-Technical Institute, have been involved in training of master students.

Master's course can be entered by persons with bachelor's or specialist degrees.

Total duration of teaching is 2 years (4 terms), that is, 104 weeks, 120 ECTS (European Credit Transfer and Accumulation System), including:

- theoretical classes, including examinations - 60 ECTS;
- practice - 12 ECTS or 432 hours;
- research work - 24 ECTS or 864 hours;
- doing master's degree - 14 ECTS or 504 hours;
- State Final Examination - 2 weeks (10 ECTS).

The curriculum is oriented at research and developments in the area of thermoelectric coolers and generators, thermoelectric materials, including their nanostructuring and properties measurement. The curriculum includes the following majors and elective courses:

- Requirements to thermoelectrics and their classification.
- Methods for the production of thermoelectrics.
- Thermoelectric nanostructures.
- Methods for measurement of thermal conductivity.
- Methods for measurement of electric conductivity and the Seebeck coefficient.
- Direct energy conversion and renewable energy sources.
- Solid-state cooling methods.

- Simulation of temperature and electric fields in thermoelectric systems.
- Thermoelectric cooling modules and systems and their manufacturing technique.
- Calculation principles of thermoelectric coolers.
- Thermoelectric generator modules and systems, low-grade heat recovery.
- Calculation principles of thermoelectric generators.
- Computational fluid dynamics, heat-mass exchange and computer engineering.
- Special chapters of thermodynamics of low-temperature systems.
- Development prospects and applications of low-temperature systems and plants.
- Philosophy and methodology of scientific cognition.
- Business foreign language.
- Practical course of professionally-oriented translation.

Master's students use the unique and expensive equipment of the ITMO University and of the Physics of Thermoelements Laboratory, Ioffe Physical-Technical Institute. These are various benches for measurement of thermoelectric parameters by different methods in the temperature range of (80 –1300) K; technological equipment, including that for production of the bulk nanothermoelectrics; structural test facilities.

Master's students receive work experience in the Physics of Thermoelements Laboratory, Ioffe Physical-Technical Institute, carry out scientific investigations in the International scientific laboratory of direct energy conversion and nanoengineering of thermoelectric structures.

During the period of studies master's students can undergo training in one of the universities of Europe.

We are interested in cooperation with leading foreign universities in the area of training masters and PhDs in thermoelectricity, in particular, in creation of joint master's and postgraduate programs.

Substantial aid in the development of curriculum and work programs of master's program "Thermoelectric energy conversion" has been rendered by Department of Thermoelectricity and Physical Metrology of Chernivtsi National University (Ukraine) and Institute of Thermoelectricity of the National Academy of Sciences and Ministry of Education and Science of Ukraine. We express deep appreciation to members of Department of Thermoelectricity and Physical Metrology of Chernivtsi State University and personally to Professor Lukyan Anatychuk.

ARTICLE PREPARATION RULES

The article shall conform to the journal profile. The article content shall be legible, concise and have no repetitions.

The article shall be submitted to the editorial board in electronic version.

The text shall be typed in text editor not lower than MS Word 6.0/7.0.

Page setup: "mirror margins"- top margin – 2.5 cm, bottom margin – 2.0 cm, inside – 2.0 cm, outside– 3.0 cm, from the edge to page header – 1.27 cm, page footer – 1.27 cm.

Graphic materials, pictures shall be submitted in color or, as an exception, black and white, in .opj or .cdr formats, .jpg or .tif formats being also permissible. According to author's choice, the tables and partially the text can be also in color.

The article shall be submitted in English on A4 paper sheets; the number of pages shall not exceed 12. By agreement with the editorial board, the number of pages can be increased.

To accelerate publication of the article, please adhere to the following rules:

- the authors' initials and names are arranged in the centre of the first page at the distance of 1 cm from the page header, font Times New Roman, size 12 pt, line spacing 1.2;
- the name of organization, address (street, city, postal code, country) – indent 1 cm below the authors' initials and names, font Times New Roman, size 11 pt, line spacing 1.2, center alignment;
- the title of the article is arranged 1 cm below the name of organization, in capital letters, semi-bold, font New Roman, size 12 pt, line spacing 1.2, center alignment. The title of the article shall be concrete and possibly concise;
- the abstract is arranged 1 cm below the title of the article, font Times New Roman, size 10 pt, in italics, line spacing 1.2 ,center alignment;
- key words are arranged below the abstract, font Times New Roman, size 10 pt, line spacing 1.2, justified alignment. The title "Key words" – font Times New Roman, size 10 pt, semi-bold;
- the main text of the article is arranged 1 cm below the abstract, indent 1 cm, font Times New Roman. size 11 pt, line spacing 1.2, justified alignment;
- formulae are typed in formula editor, fonts Symbol, Times New Roman. Font size is "normal" – 12 pt, "large index" – 7 pt, "small index" – 5 pt, "large symbol" – 18 pt, "small symbol" – 12 pt). The formula is arranged in the text, centre aligned and shall not occupy more than 5/6 of the line width, formulae are numbered in round brackets right;
- dimensions of all quantities used in the article are represented in the International System of Units (SI) with the explication of the symbols employed;
- figures are arranged in the text. The figures and pictures shall be clear and contrast; the plot axes – parallel to sheet edges, thus eliminating possible displacement of angles in scaling;
- tables are arranged in the text. The width of the table shall be 1 cm less than the line width. Above the table its ordinary number is indicated, right alignment. Continuous table numbering throughout the text. The title of the table is arranged below its number, center alignment;
- references should appear at the end of the manuscript. References within the text should be enclosed in square brackets. References should be numbered in order of first appearance in the text. Examples of various reference types are given below.

– L.I. Anatychuk, *Thermoelements and Thermoelectric Devices: Handbook* (Kyiv: Naukova Dumka, 1979), p.766. (Book)
– T.M. Tritt, Thermoelectric Phenomena, Materials, and Applications, *Annual Review of Materials Research* **41**, 433 (2011). (Journal paper)
– U. Ghoshal, *Proceedings of the XXI International Conference on Thermoelectrics* (N.Y., USA, 2002), p. 540. (Proceedings Conference)

The article should be supplemented by:

• letter from the organization where the work was performed or from the authors of the work applying for the publication of the article;

• information on the author (authors): last name and initials; full name and postal address of the institution where the author works; academic degree; position; telephone number; E-mail;

• author's (authors') photo in color or, as an exception, in black and white. With the number of authors more than two their photos are not given;

• author's application to the following effect:

We, the undersigned authors, … transfer to the founders and editors of "Journal of Thermoelectricity" the right to publish the article…in Ukrainian, Russian and English. This is to confirm that the present publication does not violate the copyright of other persons or organizations.

Date Signatures